Leverage the Energy of EM Propagation in RF/Microwave Designs p34

Ultra-Small Antennas Thanks to CRLH Transmission Lines/SIRs p42

Ka-band Systems Progress Quickly Despite Lingering Issues p82

Microwaves & RF®

YOUR TRUSTED ENGINEERING RESOURCE FOR OVER 50 YEARS

MARCH 2018 mwrf.com

OTA BROADCAST TV GETS A REMAKE

ATSC 3.0 isn't a tweak: It's a complete transformation for over-the-air TV p72

$10.00

Amplifiers – Solid State
Attenuators – Variable/ Programmable
Couplers (Quadrature, 180° & Directional)
Detectors – RF/Microwave
DLVAs, ERDLVAs & SDLVAs
DTOs, VCOs, PLO, DROs, & Frequency Synthesizers
Filters & Switched Filter Banks
Form, Fit, Functional Products & Services
Frequency Discriminators & IFMs
Integrated MIC/MMIC Assemblies (IMAs)
IQ Vector Modulators
Limiters – RF/Microwave
Log Amplifiers
Millimeter Wave Components (Up to 50 GHz)
Miscellaneous Products
Monopulse Comparators
Multifunction Integrated Assemblies (MIAs)
Phase Shifters & Bi-Phase Modulators
Power Dividers/Combiners (Passive & Active)
Pulse Modulators (SPST)
Rack & Chassis Mount Products
Receiver Front Ends & Transceivers
SDLVAs, ERDLVAs & DLVAs
Single Side Band Modulators
SMT & QFN Products
Switch Matrices
Switched Filter Banks
Switches – Solid State
Systems – Fly Eye Radars
Threshold Detectors
USB Products

Planar Monolithics Industries, Inc.

Industry Leader in DLVAs, ERDLVAs & SDLVAs

PMI offers a variety of SDLVA's over the DC to 40 GHz frequency range with high dynamic range, along with excellent temperature stability. Log Amplifiers provide a limited RF output or CW Immunity, if required. PMI offers many standard models with various options that are available at http://www.pmi-rf.com/Products/SDLVA/features.htm

Model SDLVA-0R5G18G-50R-30DBM:
http://www.pmi-rf.com/Products/SDLVA/SDLVA-0R5G18G-50R-30DBM.htm

Package Size: 3.2" x 1.8" x 0.4"
DC Voltage: +12 to +15 V @ 189 mA, -12 to -15 V @ 95 mA
Connectors: SMA Female

Model SDLVA-18G40G-65-CD-292FF-A15:
http://www.pmi-rf.com/Products/dlva/PLVA-500M18G-50.htm

Package Size: 2.2" x 1.5" x 0.4"
DC Voltage: +12 V @ 310 mA -12 V @ 150 mA
Connectors: 2.92mm Female

Specification	SDLVA-0R5G18G-50R-30DBM	SDLVA-18G40G-65-CD-292FF-A15
Frequency Range	0.5 to 18.0 GHz	18.0 to 40.0 GHz
Flatness	±2.0 dB Typ Measured ±1.0 dB	±2.5 dB Max @ 25 ºC Measured ±2.10 dB
VSWR	2.5:1 Max - Measured 2.47:1	2.5:1 Max - Measured 2.34:1
TSS	-71 dBm Min - Measured -72 dBm	-67 dBm @ 25 ºC - Measured -68 dBm
Logging Range	-70 dBm to 0 dBm	-63 dBm to +2 dBm
Log Slope	25 mV/dB (±10%) Measured 24.03 mV/dB	25 mV/dB Nom - Measured 24.4 mV/dB
Log Linearity	±1.5 dB (-20 °C to +85 °C) Max Measured ±0.75 dB	±1.5 dB @ 25 ºC Measured +1.27 dB, -1.48 dB
Video Output Range	0 VDC to 2.2 VDC into a 50 Ω Load Measured 325 mV to 2.1 VDC	0 to 2.5 V (50 Ω minimum load)

Model SDLVA-218-60-70MV-CW:
http://www.pmi-rf.com/Products/SDLVA/SDLVA-218-60-70MV-CW.htm

Package Size: 3.5" x 2.5" x 0.5"
DC Voltage: +15 VDC @ 320 mA, -15 VDC @ 10 mA
Connectors: 2.92mm Female

Model SDLVA-50M18G-70:
www.pmi-rf.com/Products/SDLVA/SDLVA-50M18G-70.htm

Package Size: 2.30" x 2.20" x 0.40"
DC Voltage: +12 to +15 V @ 134 mA, -12 to -15 V @ 111 mA
Connectors: SMA Female

Specification	SDLVA-218-60-70MV-CW	SDLVA-50M18G-70
Frequency Range	2.0 to 18.0 GHz (CW Immune)	0.05 to 18.0 GHz (CW Immune)
Flatness	±2.0 dB Typ - Measured ±1.9 dB	±2.0 dB Max - Measured ±1.4 dB
VSWR	1.5:1 Max - Measured 1.18:1	2.0:1 Max - Measured 1.74:1
TSS	-66 dBm for 10 MHz Video Bandwidth Measured -66 dBm	-70 dBm Typ - Measured -72 dBm
Logging Range	-60 dBm to 0 dBm	-70 dBm to 0 dBm Min
Log Slope	70 mV/dB Nom - Measured 70 mV/dB into a 75 Ω Load	25 mV/dB (±5%) @ 50 Ω Load Measured 25.43 mV/dB
Log Linearity	±0.5 dB - Measured +0.4 / -0.35 dB	±1.75 dB (-65 to 0 dBm) Max Measured ±0.88 dB

West Coast Operation:
4921 Robert J. Mathews Pkwy, Suite 1
El Dorado Hills, CA 95762 USA
Tel: 916-542-1401, Fax: 916-265-2597

East Coast Operation:
7311-F Grove Road
Frederick, MD 21704 USA
Tel: 301-662-5019, Fax: 301-662-1731

sales@pmi-rf.com • www.pmi-rf.com
ISO9001-2008 REGISTERED

HIGH POWER

5 - 500 WATTS PRODUCTS

POWER DIVIDERS RoHS

Model #	Frequency (MHz)	Insertion Loss (dB) [Typ./Max.] ◊	Amplitude Unbalance (dB) [Typ./Max.]	Phase Unbalance (Deg.) [Typ./Max.]	Isolation (dB) [Typ./Min.]	VSWR (Typ.)	Input Power (Watts) [Max.] ◦	Package
2-WAY								
CSBK260S	20 - 600	0.28 / 0.4	0.05 / 0.4	0.8 / 3.0	25 / 20	1.15:1	50	377
DSK-729S	800 - 2200	0.5 / 0.8	0.05 / 0.4	1 / 2	25 / 20	1.3:1	10	215
DSK-H3N	800 - 2400	0.5 / 0.8	0.25 / 0.5	1 / 4	23 / 18	1.5:1	30	220
P2D100800	1000 - 8000	0.6 / 1.1	0.05 / 0.2	1 / 2	28 / 22	1.2:1	2	329
DSK100800	1000 - 8000	0.6 / 1.1	0.05 / 0.2	1 / 2	28 / 22	1.2:1	20	330
DHK-H1N	1700 - 2200	0.3 / 0.4	0.1 / 0.3	1 / 3	20 / 18	1.3:1	100	220
P2D180900L	1800 - 9000	0.4 / 0.8	0.05 / 0.2	1 / 2	27 / 23	1.2:1	2	331
DSK180900	1800 - 9000	0.4 / 0.8	0.05 / 0.2	1 / 2	27 / 23	1.2:1	20	330
3-WAY								
S3D1723	1700 - 2300	0.2 / 0.35	0.3 / 0.6	2 / 3	22 / 16	1.3:1	5	316
4-WAY								
CSDK3100S	30 - 1000	0.7 / 1.1	0.05 / 0.2	0.3 / 2.0	28 / 20	1.15:1	5	169S

◦ With matched operating conditions

HYBRIDS RoHS

Model #	Frequency (MHz)	Insertion Loss (dB) [Typ./Max.] ◊	Amplitude Unbalance (dB) [Typ./Max.]	Phase Unbalance (Deg.) [Typ./Max.]	Isolation (dB) [Typ./Min.]	VSWR (Typ.)	Input Power (Watts) [Max.]	Package
90°								
DQS-30-90	30 - 90	0.3 / 0.6	0.8 / 1.2	1 / 3	23 / 18	1.35:1	25	102SLF
DQS-3-11-10	30 - 110	0.5 / 0.8	0.6 / 0.9	1 / 3	30 / 20	1.30:1	10	102SLF
DQS-30-450	30 - 450	1.2 / 1.7	1 / 1.5	4 / 6	23 / 18	1.40:1	5	102SLF
DQS-118-174	118 - 174	0.3 / 0.6	0.4 / 1	1 / 3	23 / 18	1.35:1	25	102SLF
DQK80300	800 - 3000	0.2 / 0.4	0.5 / 0.8	2 / 5	20 / 18	1.30:1	40	113LF
MSQ80300	800 - 3000	0.2 / 0.4	0.5 / 0.8	2 / 5	20 / 18	1.30:1	40	325
DQK100800	1000 - 8000	0.8 / 1.6	1 / 1.6	1 / 4	22 / 20	1.20:1	40	326
MSQ100800	1000 - 8000	0.8 / 1.6	1 / 1.6	1 / 4	22 / 20	1.20:1	40	346
MSQ-8012	800 - 1200	0.2 / 0.3	0.2 / 0.4	2 / 3	22 / 18	1.20:1	50	226
180° (4-PORTS)								
DJS-345	30 - 450	0.75 / 1.2	0.3 / 0.8	2.5 / 4	23 / 18	1.25:1	5	301LF-1

◊ In excess of theoretical coupling loss of 3.0 dB

COUPLERS RoHS

Model #	Frequency (MHz)	Coupling (dB) [Nom]	Coupling Flatness (dB)	Mainline Loss (dB) [Typ./Max.]	Directivity (dB) [Typ./Min.]	Input Power (Watts) [Max.] ◦	Package
KFK-10-1200	10 - 1200	40 ±1.0	±1.5	0.4 / 0.5	22 / 14	150	376
KDS-30-30	30 - 512	27.5 ±0.8	±0.75	0.2 / 0.28	23 / 15	50	255 *
KBS-10-225	225 - 400	10.5 ±1.0	±0.5	0.6 / 0.7	25 / 18	50	255 *
KDS-20-225	225 - 400	20 ±1.0	±0.5	0.2 / 0.4	25 / 18	50	255 *
KBK-10-225N	225 - 400	10.5 ±1.0	±0.5	0.6 / 0.7	25 / 18	50	110N *
KDK-20-225N	225 - 400	20 ±1.0	±0.5	0.2 / 0.4	25 / 18	50	110N *
KEK-704H	850 - 960	30 ±0.75	±0.25	0.08 / 0.2	38 / 30	500	207
SCS100800-10	1000 - 8000	10.5 ±1.5	±2.0	1.2 / 1.8	8 / 5	25	361
KBK100800-10	1000 - 8000	10.5 ±1.5	±2.0	1.2 / 1.8	8 / 5	25	322
SCS100800-16	1000 - 7800	16.8 ±1.5	±2.8	0.7 / 1.0	14 / 5	25	321
KDK100800-16	1000 - 7800	16.8 ±1.5	±2.8	0.7 / 1.0	14 / 5	25	322
SCS100800-20	1000 - 7800	20.5 ±2.0	±2.0	0.45 / 0.75	12 / 5	25	321
KDK100800-20	1000 - 7800	20.5 ±2.0	±2.0	0.45 / 0.75	14 / 5	25	322
KEK-1317	13000 - 17000	30 ±1.0	±0.5	0.4 / 0.6	30 / 15	30	387

* Add suffix - LF to the part number for RoHS compliant version.
◦ With matched operating conditions

Unless noted, products are RoHS compliant.

SYNERGY® MICROWAVE CORPORATION

Phone: (973) 881-8800 | Fax: (973) 881-8361
E-mail: sales@synergymwave.com
Web: WWW.SYNERGYMWAVE.COM
Mail: 201 McLean Boulevard, Paterson, NJ 07504

March 2018 VOLUME 57, ISSUE 3 Microwaves&RF

IN THIS ISSUE

FEATURES

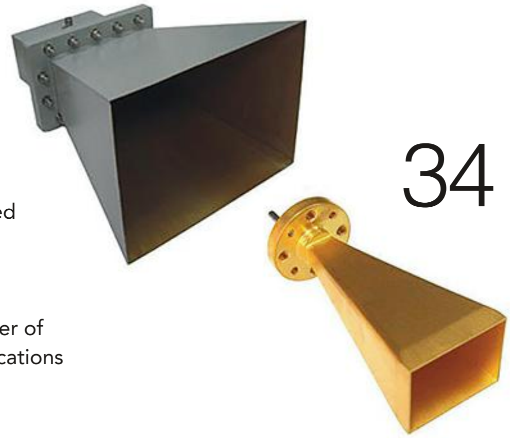

34

38

72

80

PRODUCTS & TECHNOLOGY

NEWS & COLUMNS

defense electronics

Starts on page **49**

JOIN US ONLINE

follow us @MicrowavesRF

become a fan at facebook.com/microwavesRF

3H Communication Systems

3H offers innovative, high quality and cost effective RF / Microwave Filter solutions ranging from DC to 50 GHz backed by our 5 year warranty nd manufactured in our ISO 9001 facilities.

3H Nano-Filters
smallest custom filter on the market today!

FEATURED RF FILTER SOLUTIONS:

DEFENSE | TELECOM | SECURITY | TRANSPORTATION | AEROSPACE | MEDICAL

Passive Intermodulation Filters
for Distributed Antenna Systems

Nano Filters
Down to 0.059" profiles

Ceramic Filter
reduced footprints & low profiles

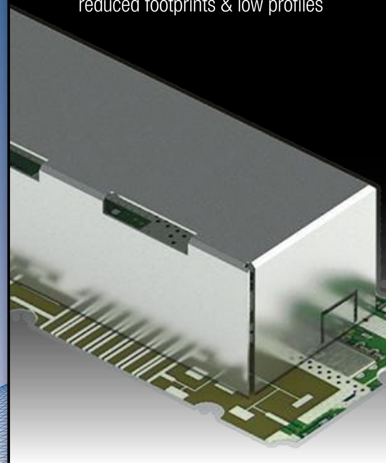

Cavity Filters
multiplexers and multi-functions assemblies

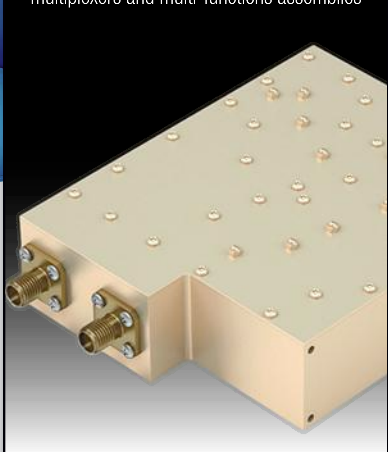

Switch Filter Banks
ranging from 40 MHz to 18 GHz

Duplexers
for Distributed Antenna Systems

CONTACT US TO DISCUSS YOUR APPLICATION

3H COMMUNICATION SYSTEMS

www.3HCommunicationSystems.com | Telephone: +1 949 529 1583

New! Compact 2-kW CW PA

The THEIA-H is the industry's smallest, lightest, best-performing 2-kW amplifier covering 1.5 to 30 MHz.

The new THEIA-H from Delta-Sigma, Inc. is our latest achievement in delivering high power and superb performance in a small package. Measuring only 4U high including the power supply and weighing only 57 lb., it delivers 2 kW CW from 1.5 to 30 MHz with 57% AC-to-RF efficiency. The THEIA-H is extremely rugged and designed for military communication systems including QPSK, GMSK and OFDM, meteor scatter, and airborne platforms to 30,000 ft., as well as test systems and HF radar.

The amplifier has the high linearity required for digital modulation, a linearity-controlled loop for less than 0.5 dB compression at rated power, a hot-swappable amplifier module that weighs only 29 lb., and total weight of 57 lb. Extensive protection circuits are included and full control and monitoring are available via RS-232, RS-485, or Ethernet. **Can be upgraded to operate up to 45 MHz.

Frequency range (MHz)	1.5 to 30
RF output, CW (kW)	1.8, 2 typical
THD, 5 to 90% modulation (%)	<5
Gain (dB)	54
AC-to-RF efficiency at rated power (%)	57
Noise floor in transmit-disable mode (dBm/Hz)	-173
Harmonic suppression (dBc)	-10 second order -28 third order -60 with filter
Spurious rejection (dBc)	<-70
Third-order IMD (dBm)	+75
Input/output return loss (dB)	22/16
Phase flatness (±2 MHz BW) (deg)	<1
Maximum duty cycle (%)	100
Maximum VSWR	2:1, 30:1 with foldback
TX/RX isolation (option)(dB)	60
RX/TX switching time (option)(μs)	5, 2 typical
Prime power (VAC)	85 to 265
Control/Monitoring	RS-232 or RS-485, Ethernet
Altitude (ft.)	30,000
Dimensions (in. HWD)	7x19x20. Amplifier 5.25 H , power supply 1.25 H
Weight (lb.)	Amplifier (29), total (57)
Protection	Thermal overload, over/under voltage, temperature, fan
Monitoring	Forward/reflected power, gain, temperature, hours of operation, fan status, filter selection, BIT status, others

PLEASE CONTACT US FOR ADDITIONAL INFORMATION

(951) 343-4005 | www.111rfpower.com

ΔΣ DELTA SIGMA Inc.

ON MICROWAVES&RF.COM

Satellites Provide Distant Connections

The growing number of artificial satellites—notably those with low earth orbits—is a sign of the essential roles that they will play in many emerging communications applications, including IoT, 5G, and connected cars.

http://www.mwrf.com/systems/satellites-provide-distant-connections

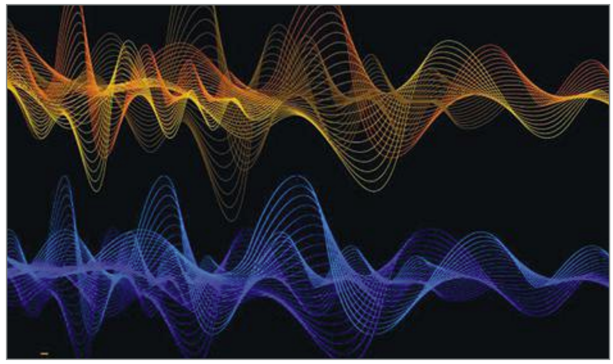

Comparing Narrowband and Wideband Channels

Narrowband and wideband communications channels make use of available bandwidth in different ways—so employ them according to the requirements of a particular application.

http://www.mwrf.com/systems/comparing-narrowband-and-wideband-channels

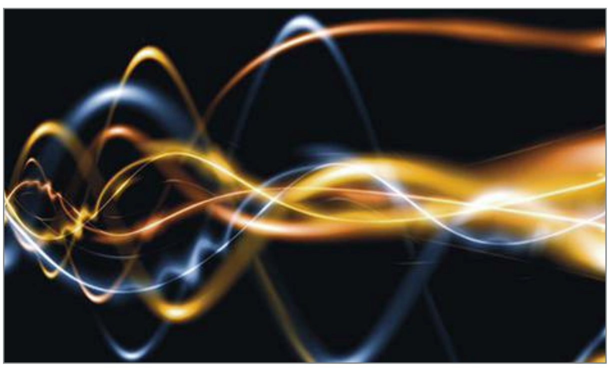

Reducing Time-Delay Interference in Mission-Critical Situations

While time-delay interference (TDI) is a necessary evil when it comes to public safety communications, its effects can be reduced by utilizing several best practices. This article first explains what TDI is before presenting some approaches that can help to overcome it.

http://www.mwrf.com/systems/reducing-time-delay-interference-mission-critical-situations

Get Your Hands Dirty with These VNA Tools

Traditionally built in the form of a large box that combines both measurement and display capabilities, the vector network analyzer is in the process of being redefined. While traditional VNAs are not likely to disappear anytime soon, some of today's VNAs are being built in smaller portable sizes.

http://www.mwrf.com/test-measurement/get-your-hands-dirty-these-vna-tools

twitter.com/MicrowavesRF facebook.com/microwavesrf

Editorial

CHRIS DeMARTINO | Technical Editor
chris.demartino@informa.com

Don't Overlook These Events Before IMS

As the time for this year's International Microwave Symposium (IMS) draws near, several shows leading up to it may also pique your interest.

As most reading this already know, the IEEE International Microwave Symposium (IMS) is the flagship event of the RF/microwave industry each year. This year's version, which will take place in Philadelphia this June, promises to be no different. However, before IMS gets underway, several events scheduled for the month of April may be worthy of your attention.

For one, those in the Long Island area may want to check out the Long Island RF/Microwave Symposium & Exhibits on Thursday, April 5th. It will take place at the Radisson Hotel in Hauppauge, N.Y. from noon to 8 p.m.

The show will consist of an exhibition and several technical lectures. Registered attendees will receive admission to the exhibit floor, technical lectures, and complimentary networking lunch and dinner. The first 200 registered attendees will also receive a complimentary swag bag that contains gifts from the exhibitors.

Another event to take note of is the 2018 IEEE Wireless and Microwave Technology Conference (WAMICON 2018), which will convene April 9th and 10th at the Sheraton Sand Key in Clearwater Beach, Fla. The central theme is "mm-Waves and Internet of Things (IoT) for Commercial and Defense." Among the highlights of WAMICON 2018 are two plenary presentations and a workshop on additive manufacturing. There's a session on RF/microwave education titled "RF/Microwave Education: Where are we headed?" Also on tap are a poster session and a young professionals workshop.

Not to be outdone, the fifth annual Brooklyn 5G Summit will take place April 24th-27th at the NYU Tandon School of Engineering in Brooklyn, N.Y. Its focus is "overall 5G system design across the entire spectrum range, progress in 5G channel modeling, and 5G regulatory aspects." In addition, the 5G Summit will examine "concrete use cases for 5G in the evolving IoT space." Several keynotes and panel sessions, in addition to exhibits, are among the highlights. Exhibiting companies include Keysight Technologies, National Instruments, and Rohde & Schwarz.

While the industry prepares for IMS in June, these events in the interim during April have lots to offer. And then before you know it, IMS will be right around the corner! mw

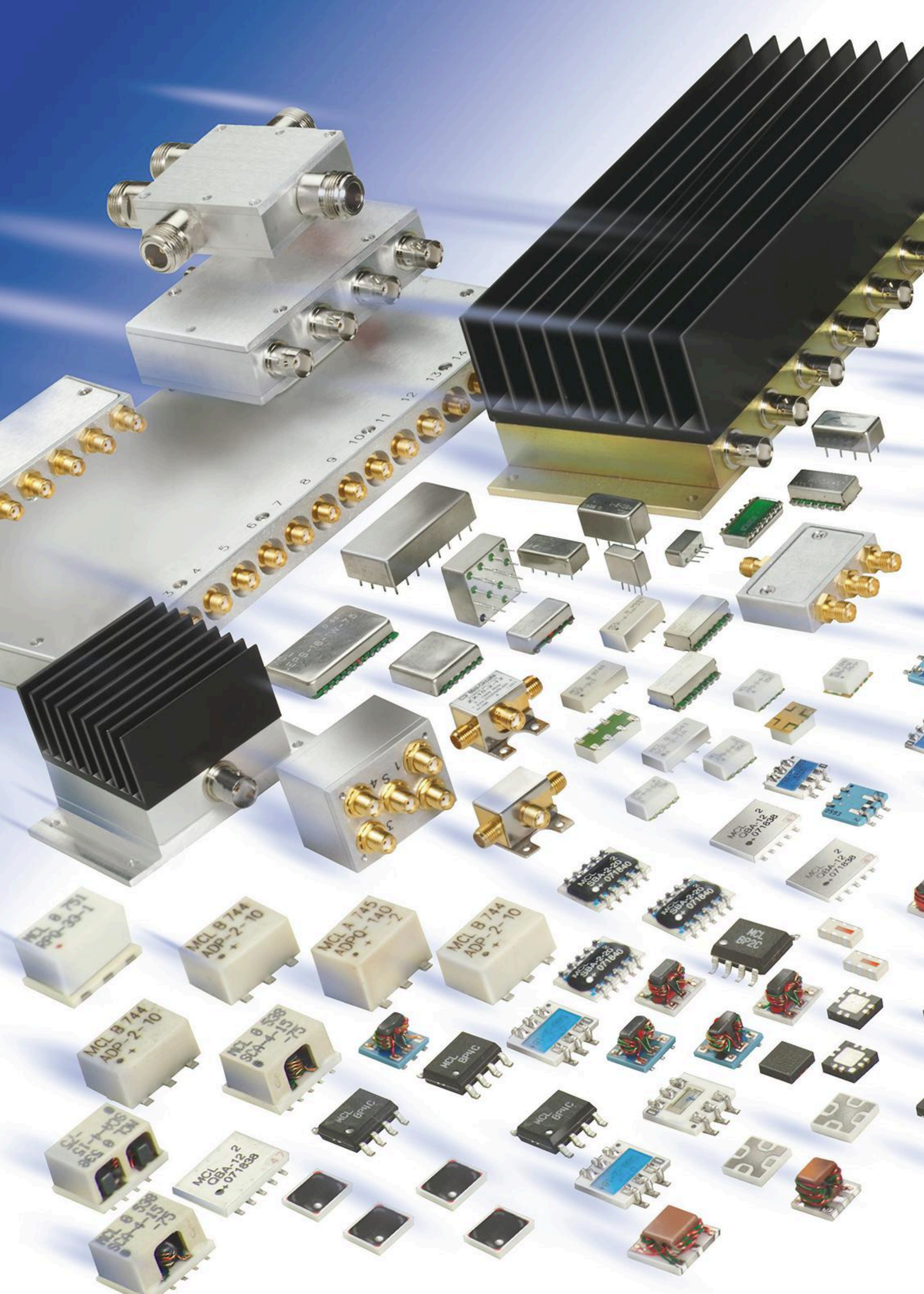
MCL B 744
ADP-2-10
MCL QBA-12
071638
MCL SBA-2-20
071840
MCL BP2C
MCL BPNC

Microwaves&RF **MARCH 2018**

INFORMA MEDIA INC.

1166 AVENUE OF THE AMERICAS, 10TH FLOOR
NEW YORK, NY 10036 **T** | 212.204.4200

informa

Electronic Design | Machine Design | Microwaves & RF | Source ESB | Hydraulics & Pneumatics | Global Purchasing | Distribution Resource | Power Electronics | Defense Electronics

News

An Obstacle Course Ahead
for 5G Technology

In December, the 3GPP published the first draft of the 5G New Radio standard. It is an important first step toward 5G communications, but not all carrier equipment following the standard will automatically and consistently link to all smartphones and other devices. It's not that easy.

This is where test equipment companies can flex their muscles. Austin, Texas-based National Instruments recently collaborated with Samsung on interoperability testing, which is critical piece of preparation for 5G. The firm developed test equipment that can be programmed to act like smartphones or other devices and used to test Samsung's commercial 5G base stations.

"With any new standard, there are lots of questions," said James Kimery, director of wireless research and software-defined radio marketing for National Instruments. "An engineering team takes a 2,500-page document, implements it, and connects to a network first try? That will never happen."

The wireless industry is going to expunge ambiguous language and other errors from the standard – the Non-Standalone 5G standard, not Standalone 5G – over the next two years. But mistakes could be missed without systems from the likes of National Instruments, Keysight and Rohde & Schwarz to check out commercial base stations.

National Instruments showed Samsung's 28 GHz base station communicating over the air with its test equipment at Mobile World Congress last month. The device links to the base station and then validates that the downlink functionality and performance are in line with the 3GPP standard. Samsung's hardware uses a MIMO configuration with two transmit and two receive antennas.

Any changes to the standard would probably affect how devices connect to a network, Kimery said. The physical layer of the standard is probably finished, and that explains why companies like Intel, Qualcomm, Qorvo and Skyworks Solutions have already announced 5G modems and other components for phones.

National Instruments also recently released a 5G reference test solution by updating the software that runs in its PXIe-5840 vector signal transceiver. The VST system provides 1 GHz of instantaneous bandwidth for testing power amplifiers and other parts operating in sub-6 GHz spectrum, the same range of frequencies used in 3G and 4G networks.

Jason White, director of RF wireless test for National Instruments, said that the PXI-based system would help customers make quicker, more precise measurements. Before the 5G standard was published, many companies were guessing how 5G would work. And they had to generate custom waveforms based on these guesses to test 5G parts.

Qorvo used National Instruments' system to test its first front-end module for 5G smartphones, which combines a power amp and low noise amplifier operating at 3.4 GHz into a single package. The companies collaborated on a test demonstration at the Global TD-LTE Initiative Workshop last month.

The biggest challenge for hardware vendors is to balance the wide bandwidth and high efficiency requirements of 5G, White said. There are also test and measurement challenges "because if you are designing a part with 100 MHz of bandwidth, you need a test system with three to five times the bandwidth to test pre-distortion conditions, which is how you measure linearity," he added.

5G technology will use both low and high frequencies. The 28-GHz spectrum has rarely been used before for communications, so it will have greater capacity than lower bands. But these millimeter waves have more limited uses because they can be blocked by buildings and absorbed by air over long distances.

That has upended how the engineers go about testing, White said. Instead of using emulators to digitally simulate how millimeter waves will propagate through an environment, companies are going right to expensive, over the air tests. It is not clear that an inexpensive emulator for millimeter waves can be built. The technology used to steer them around obstacles is just too complex.

National Instruments says that it has taken steps to lower the cost of testing, but many other challenges stand in the path of widespread 5G. It is significantly more complex than 4G technology, and the switchover to the new standard will not happen overnight in 2020 (when most wireless carriers want to roll out service).

"With every wireless standard, the whole specification doesn't get implemented on the first try. There is probably not one base station in the world that is compliant with the latest LTE release. I just don't believe it," Kimery, the wireless research director for National Instruments, said.

"But we're going to make it work," Kimery said. "And when I say we, I mean the collective industry." ■

BROADCOM RECOILS After Qualcomm Raises Offer for NXP

BROADCOM RATCHETED DOWN its $121 billion offer for Qualcomm, which recently raised its $47 billion offer for NXP Semiconductors, putting another twist into Broadcom's attempt to become the third largest chip supplier in the world. Broadcom said Wednesday that it is now willing to pay around $116 billion for Qualcomm.

Broadcom is offering $79 per share for Qualcomm, down from $82 per share. The $79 per share offer only returns to the previous level if Qualcomm cannot complete the NXP deal. The company also said that it would still include an $8 billion breakup fee to calm Qualcomm's nerves about a Broadcom deal being blocked by regulators.

The announcement came a day after Qualcomm offered to pay $54.5 billion instead of $47 billion for NXP. The acquisition has been the subject of skepticism from NXP shareholders and harsh scrutiny from antitrust agencies around the world. Industry analysts viewed the offer as a severe blow to Broadcom's chances to take over Qualcomm.

(Continued on page 22)

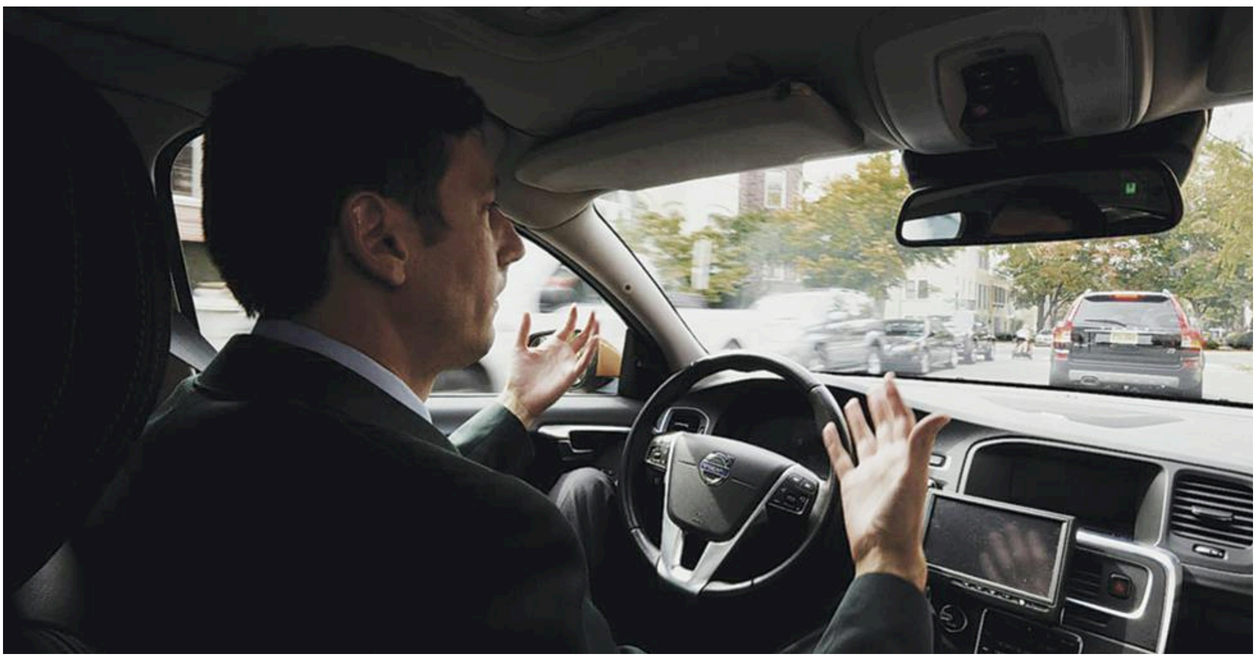

STMICROELECTRONICS BROADENS Bet on Power Amplifiers

THE SUN IS SETTING slowly on laterally diffused metal oxide semiconductors, which are still widely used in power amplifiers embedded in cellular base stations. Even though gallium nitride is prying into its market share, LDMOS is still cherished for its high voltages, high efficiency and relatively low cost.

That is the reason why STMicroelectronics recently agreed to license it from Innogration Technology, a chip supplier based in Suzhou, China. The agreement gives it the right to manufacture products for markets ranging from the industrial to medical to aerospace to wireless infrastructure. The terms were not disclosed.

STMicroelectronics has been striking deals to expand into RF power amplifiers. The company has agreed to manufacture GaN layered on thin slabs of silicon as a second source for Macom Technology Solutions. It is staying out of the market for telecom equipment but targeting applications like industrial heating and spark plugs.

Over the next decade, these applications could add hundreds of millions of dollars to the market for power amplifiers. Major LDMOS suppliers like Ampleon, NXP Semiconductors and Infineon are putting out chips based on gallium nitride that can be used in next generation base stations as well as ones that can concentrate radio waves into beams hot enough to cook food and power light bulbs.

In 2015, LDMOS represented half of the $1.5 billion market for power amplifiers used in applications that exceed three watts, excluding smartphones, according to market research firm Yole Developpment. The RF power semiconductor market is forecast to grow to $2.6 billion over the next four years, but the market share of LDMOS technology is expected to fall to 25% over the same span.

Industry analysts say that the technology is losing its luster to gallium nitride technology, which can handle higher voltages and hotter temperatures and could be used in a new generation of 5G equipment. In 2022, these gallium nitride power amplifiers will have 40% market share, according to Yole Developpment. An estimated 35% of the market that year will be sales of chips based on gallium arsenide, or GaAs.

Many companies have been clawing and scratching to plunder part of the market for gallium nitride. Infineon, for instance, was unable to complete its acquisition of Wolfspeed, Cree's power and radio frequency division, for $850 million. The company also stumbled into a lawsuit with Macom, which accused it of infringing upon several key patents for gallium nitride. ■

More than the Industry's Widest Variety of MMIC Components

FREE Modelithics Simulation Models

MMIC Amplifiers

MMIC Mixers

MMIC Multipliers

MMIC Splitter/Combiners

MMIC Transformers

MMIC Couplers

MMIC Attenuators

MMIC Filters

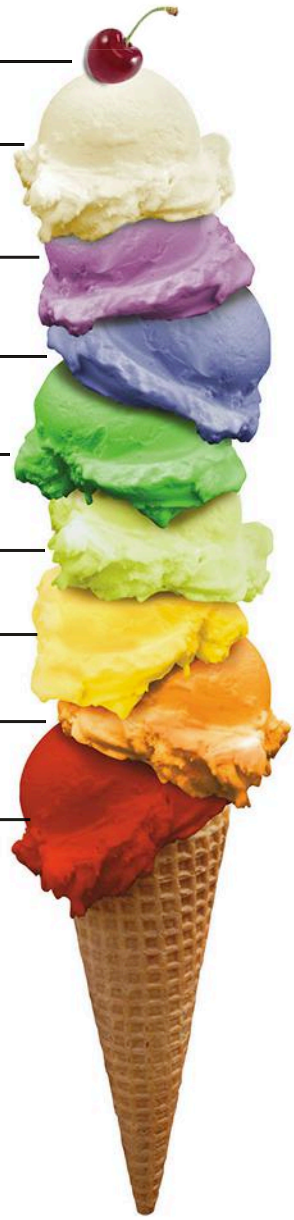

Mini-Circuits

The other guy

Make the Smart Choice…

Our promise to you goes beyond selection alone. Sure, Mini-Circuits MMIC products give you over 200 unique models from DC to 40 GHz to choose from, but when you choose Mini-Circuits, you're choosing more than the right component for your system. You're choosing all the advantages of 31 years of in-house, state-of-the-art design experience, absolute commitment to excellence in quality, reliable product supply through the lifetime of your system, and assurance of fast, easy, engineer-to-engineer application support whenever you need it. Our MMIC products don't just give you more choice. They give you peace of mind that you're making the smart choice.

Make the smart choice. Visit minicircuits.com today.

Modelithics®
Vendor Partner
"FREE High Accuracy RF Simulation Models!"
https://www.modelithics.com/MVP/MiniCircuits

Mini-Circuits®

www.minicircuits.com P.O. Box 350166, Brooklyn, NY 11235-0003 (718) 934-4500 sales@minicircuits.com 551Rev C

(Continued from page 19)

On Wednesday, Qualcomm said in a statement that "Broadcom's reduced proposal has made an inadequate offer even worse despite the clear increase in value to Qualcomm stockholders from providing certainty around the NXP acquisition." Broadcom has previously said that $82 per share was its "best and final" offer.

This is the second time that Broadcom has amended its offer since it originally pledged to pay around $105 billion for Qualcomm, which has been battered in recent years by legal battles with Apple and regulators threatening to hurt licensing business. Hock Tan, Broadcom's chief executive, has argued that he can smooth out these wrinkles.

Qualcomm's board unanimously rejected the $105 billion bid. In response, Broadcom sparked a hostile takeover of Qualcomm's board. Broadcom's next move was to raise its bid to $121 billion, which was rejected last week after the board of both companies met. If Qualcomm had taken the deal, it would not have been allowed to sweeten the NXP deal.

The advisory firm Institutional Shareholder Services recommended in a recent report that Qualcomm shareholders vote for four of the directors that Broadcom nominated for election at Qualcomm's investor meeting next month. That would fall short of the number that Broadcom needs to push through a hostile takeover, but it could prompt more negotiation.

Broadcom said in a statement that Qualcomm should have followed the advisory firm's advice. "Instead Qualcomm's board acted against the best interests of its stockholders by unilaterally transferring excessive value to NXP's activist stockholders," the company said.

"Broadcom has refused and continues to refuse to engage with Qualcomm on price," Qualcomm riposted in its Wednesday statement. Qualcomm has argued that all of Broadcom's bid ignores the growth potential of markets for 5G wireless technology, the Internet of Things, and automotive – markets that both Qualcomm and NXP are chasing. ■

IN REVERSAL, WOLFSPEED BUYS Infineon's Radio Frequency Power Business

LAST YEAR, INFINEON agreed to pay $850 million for Cree's power and radio frequency business unit, Wolfspeed. But American officials refused to approve the deal and, after weakly toying with fixes and compromises, Infineon waved the white flag and pulled out of the deal.

Now both companies have hammered out a deal in the opposite direction, following Cree's vow to aggressively invest in its Wolfspeed business through the end of the decade.

On Tuesday, Wolfspeed said that it had acquired Infineon's radio frequency power business for about $430 million, bolstering its catalog of power amplifiers used in wireless infrastructure and radar. That includes chips manufactured with gallium nitride layered onto silicon carbide to handle the wider bandwidths and higher frequencies of 5G.

"The acquisition strengthens Wolfspeed's leadership position in RF GaN-on-SiC technologies, as well as provides access to additional markets, customers and packaging expertise," said Cree's chief executive Gregg Lowe in a statement. The deal "positions Wolfspeed to enable faster 4G networks and the revolutionary transition to 5G."

The deal encompasses Infineon's factory for LDMOS and GaN technologies located in Morgan Hill, California. The facility also includes packaging and test operations. Wolfspeed will also take on around 260 employees from the Neubiberg, Germany-based Infineon, including more than 70 engineers.

For Wolfspeed, which generated $221 million of revenue last year and has shipped more than 15 million devices since Cree began targeting compound semiconductors at applications other than lighting, Infineon's business is expected to add $115 million to its balance sheet in the first twelve months after the acquisition. ■

Si CMOS TRANSMITTER Tackles 90 to 105 GHz

The race to develop millimeter-wave devices for short-range wireless communications applications typically starts with an advanced semiconductor process based on compounds such as gallium arsenide (GaAs) or gallium nitride (GaN). But a growing number of investigators are finding that a lower-cost silicon semiconductor process, complementary metal oxide semiconductor (CMOS) technology, is quite capable of generating millimeter-wave signals. While many of the advances in Si CMOS are motivated by the needs of the cellular communications industry, many other industries can benefit from progress in this low-cost silicon transistor technology, including for gas sensors and medical analysis.

To explore the possibilities of Si CMOS technology at higher frequencies, researchers from the Jet Propulsion Laboratory of the California Institute of Technology (Pasadena) and the University of California at Los Angeles developed a CMOS transmitter for a sub-Doppler spectroscopy system. The fundamental frequencies produced by the CMOS transmitter are generated by delta-sigma fractional synthesis. A 48-MHz reference frequency is used for the synthesizer, with a 10-MHz atomic clock as the frequency standard. The synthesized output signals from the CMOS source range from 46 to 53 MHz.

These signals are then fed to a custom CMOS multiplier integrated circuit (IC), where the 1,920th harmonic is used to lock a 90-to-105-GHz voltage-controlled oscillator (VCO) in a type 2 phase-locked-loop (PLL) frequency synthesizer architecture. The VCO output is then boosted by means of a four-stage transformer-coupled power amplifier (PA) before being wire-bonded to WR10 rectangular waveguide for transfer to millimeter-wave components, such as the W-band pyramidal horn antenna used with the gas spectroscopy system.

For gas spectroscopy applications (and many communications applications), modulation is required, and this CMOS-based millimeter-wave source is capable of producing amplitude modulation (AM) by means of a digital pulse generator designed into the transmitter IC. In addition, by introducing a time-varying sinusoidal signal to the 48-MHz reference signal, it is possible to generate frequency modulation (FM).

Admittedly, this millimeter-wave source delivers extremely low output power levels with such large multiplication factors, since the reference source itself is only provided a few milliwatts of power. But the CMOS millimeter-wave source achieves low phase noise in a region of −125 dBc/Hz offset 20 kHz from the carrier, measured at the 1,920th harmonic. The experimental approach more than hints that silicon CMOS may still have some ways to go in terms of output signal frequency, if strategies can be developed to increase the amplitude of the output signals without seriously degrading the phase-noise performance.

See "Sub-Doppler Spectroscopy With a CMOS Transmitter," *IEEE Transactions on Terahertz Science and Technology*, Vol. 8, No. 1, January 2018, p. 121.

CORRECTING FOR THE LOSS of Phased-Array Antenna Elements

PHASED-ARRAY ANTENNAS have become almost essential parts of modern aerospace and defense radar systems. The multiple elements combine for high-speed and effective beamforming and beam diversity, allowing a radar system to receive and transmit advanced waveforms under a variety of operating conditions. Unfortunately, those antenna array elements can fail, resulting in some amount of degradation in the antenna pattern and the radar system performance.

Researchers at KIIT University (BhuBaneswar, India) and the Indian Institute of Technology (Roorkee, India) explored the use of two algorithms—the particle swarm optimization (PSO) and the bacteria foraging optimization (BSO) algorithms—to analyze the effects of failed antenna array elements on the overall performance of the antenna. The simplest form of analysis is an assumption in the loss of amplitude from the failed element, but without affecting the amplitude contributions of the other antenna elements. As the researchers explain, the argument for replacing the failed or partially radiating antenna element is not valid in all cases.

In some cases, the original beam pattern can be resynthesized by recalculating the excitations of the remaining working antenna elements. Newer active phased-array antennas include remote control of antenna element excitations, allowing for retuning of the remaining elements for desirable antenna beamforming. By applying the BSO and PSO algorithms and amplitude-only method, the experimenters developed a relatively simple technique for reconstructing a desired antenna pattern when one or more antenna elements failed partially or fully.

They examined the sidelobe levels (SLLs) of different phased-array antenna designs, using three different experimental cases: restoration of the single null in a failed array, restoration of a double null in a failed array, and restoration of the broad/sector null in a failed array. The researchers found the PSO approach to perform considerably better than the BSP technique when correcting for the failure of antenna elements in phased arrays.

See "Antenna Array Failure Correction," *IEEE Antennas & Propagation Magazine*, December 2017, p. 106.

JEFFREY KAHLER | Technical Director, Nuhertz Technologies
ALAN M. EGGER | Marketing Manager, Nuhertz Technologies
www.nuhertz.com

Filters that Use Resonators with DMS Can Produce Optimal Results

Designing distributed filters that incorporate resonators with defected microstrip structures (DMSs) can help combat spurious passbands. This article explains how such filters can be efficiently designed with software tools.

Nuhertz Technologies recently introduced a feature in its FilterSolutions program to support the design of filters utilizing defected microstrip structures (DMSs). When used with AWR's Microwave Office, this new modeling capability makes it possible for engineers to achieve accurate synthesis of stripline, microstrip, or suspended substrate filter designs when using these resonators. FilterSolutions not only enables the design of these distributed-element filters, but the software can also synthesize the design of lumped-element, active, and digital filters.

This article presents an example of a hairpin resonator microstrip bandpass filter. In this example, we will look at a filter with unmodified resonators. We will then modify the resonators to produce a T-shaped notch "defect" in the conductors.

Figure 1 shows the hairpin example, which illustrates the inherent problem of distributed designs concerning frequencies much greater than the design passband frequency. With a design frequency of 1 GHz, we see other spurious passbands at 2 GHz and then again at 3 GHz. If we were to extend the frequency range being examined, we would continue to see spurious passbands at every multiple of the 1-GHz design frequency. Although the natural parasitic effects will suppress the passbands at some point, the lower-frequency parasitic passbands would likely be a design problem.

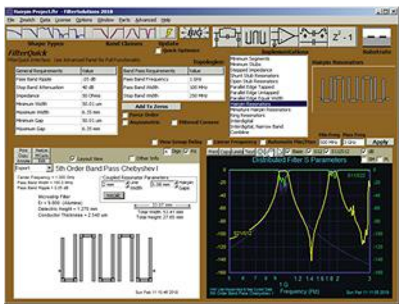

1. The spurious passbands can be seen in this FilterSolutions design interface.

Our thanks to National Instruments' AWR *(www.awrcorp.com)* design group for the use of its Microwave Office and AXIEM software tools in the AWR Design Environment, as will be noted.

A major advantage when using DMSs in filter designs is that it can minimize spurious passbands, or modes, in the frequency response. Such designs are often useful in wideband applications that require suppression of frequencies much higher than the passband.

The DMS resonators form a notch inside the resonators of the main filter that is tuned to a spurious frequency, thereby suppressing the spur. Any spurious frequency may be targeted by the DMS notch filter. FilterSolutions provides automated tuning for the first spurious mode. The parasitic issues are handled by adding transmission zeros to the legs of the inductor sections.

Figure 2 shows the layout of a coupled resonator section in the AWR Microwave Office program. Here, we see an example that has two embedded DMS resonators tuned to the first spurious frequency.

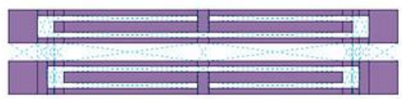

2. Shown are DMS notch resonators embedded inside a coupled resonator section.

After designing the network in FilterSolutions, the filter can be exported to Microwave Office by using the "AWR Export Selections" control panel in FilterSolutions. "Use DMS Resonators" is selected in the dialog box *(Fig. 3)*.

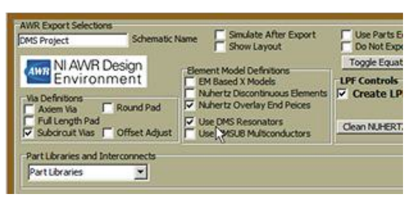

3. Designers can select "Use DMS Resonators" from the FilterSolutions "AWR Export Selections" control panel.

The use of DMS resonators in filters can be contrasted with the use of defected ground structures (DGSs). These structures are also well-known and well-documented as a means for saving space and minimizing spurious responses.

Spurious frequency suppression is best handled with fine tuning in a good optimizer. A DMS will contribute its own parasitics to the circuit. Therefore, the coupling between the transmission line resonators needs to be optimized along with the other optimization targets, taking these parasitic responses into account.

FilterSolutions utilizes NI AWR software to further analyze and optimize the synthesized design for rigorous circuit simulation, electromagnetic (EM) analysis, and optimization. We have used Microwave Office for circuit simulation and then the AXIEM 3D planar simulator, another important tool in the AWR Design Environment.

SIMULATION IN MICROWAVE OFFICE

The design can be exported to Microwave Office for initial circuit simulation and optimization. *Figure 4* shows the initial DMS layout and simulation results. We can see that the first spurious frequency response has been attenuated. In addition, the DMS parasitic effects have slightly altered the design passband. We can then use the optimization capabilities of the program to increase the spurious suppression and minimize the parasitic effects on the passband.

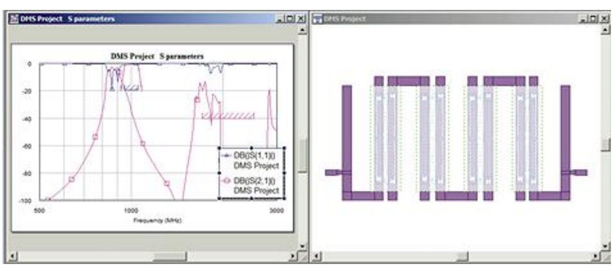

4. Shown are the initial DMS layout and simulation results.

After using Microwave Office with its efficient optimization capabilities, we can see that the circuit response has greatly improved *(Fig. 5)*. The suppressed first spurious frequency and main passband are now mostly within the S11 and S21 optimization goals.

EM ANALYSIS IN THE AWR AXIEM PROGRAM

To ensure full design accuracy, the DMS filter will be electromagnetically optimized using AWR's AXIEM. This EM solver offers the speed to support extraction optimization.

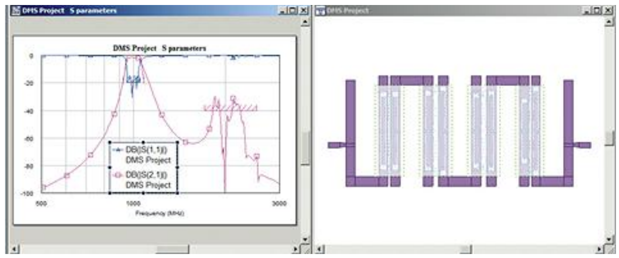

5. The filter was optimized in Microwave Office to obtain the DMS layout shown. The simulation results are also provided.

Figure 6 shows the results.

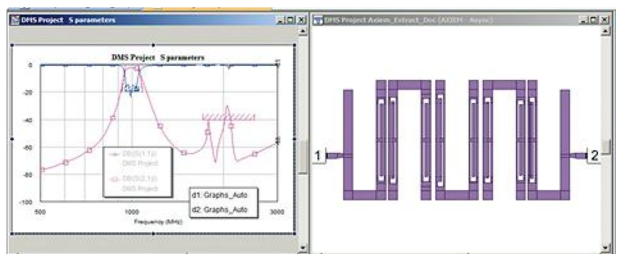

6. This figure depicts the DMS layout and response after optimization with AWR's AXIEM.

Aside from solving spurious response issues, the resulting filter design may also yield other advantages for circuit production. The design may help reduce the filter's overall size by removing otherwise needed circuitry required to limit spurious effects, thereby lowering overall product costs.

OTHER DMS DESIGNS AND COMPARISON TO DEFECTED GROUND STRUCTURE DESIGNS

The use of DMS resonators in filters can be contrasted with the use of defected ground structures (DGSs). These structures are also well-known and well-documented as a means for saving space and minimizing spurious responses. However, a major disadvantage when using a DGS is it creates a notch in the ground plane that leads to EM radiation. Thus, an elaborate and carefully constructed enclosure would be required to defeat the generated EM interference. The radiation would also likely add size and cost to the circuit.

Discover the Power of Real-Time Spectrum Analysis

Capture
Transient & short duration signals confidently

Identify
Errors in power, frequency and time

Isolate
Signals of interest

Analyze
RF signals & the devices that control them

Spectrum Monitoring

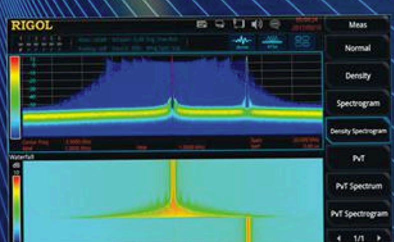

RF Device Characterization

NEW RSA5000 Series

Real-Time Spectrum Analyzers

Combining a High Performance Swept Spectrum Analyzer with Superior Real-Time Analysis

- 3.2 and 6.5GHz models • 1ms Sweep
- 1Hz RBW • 40MHz Real-Time Bandwidth
- 7.45 µsec 100% POI • Powerful Triggering
- 7 Visualization Modes

RIGOL
Innovation or nothing

Discover the Power of Real-Time @ www.RigolNA.com/Real-Time

In the case of a DMS-based design, we can create a circuit in planar microstrip without requiring additional via lines to ground as compared to using conventional lumped-element resonators. In the 1-GHz filter example designed for this paper, the conductors of the DMS resonator sections are notched in a T-shaped configuration *(Fig. 7)*.

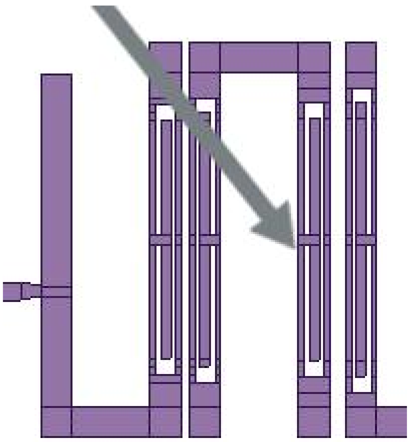

7. Illustrated here is a close-up view of the resonators that shows the notches.

A review of recent literature includes T-shaped notches (like our example), but also more complex spiral,[1] and G-Shaped[2] notched resonators, as well as arrays of DMS resonators (ADMS).[3] These resonator structures are footnoted and shown in *Figures 8, 9, and 10*, respectively.

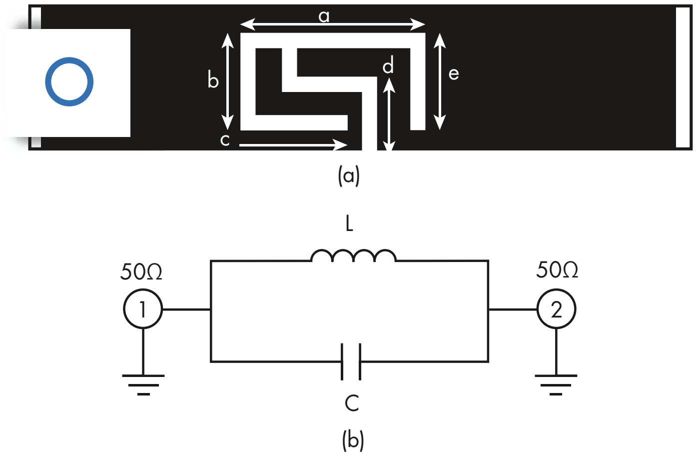

8. Shown is a spiral DMS resonator. *(Source: Parui, Choudhury, Murmu, and Das[1])*

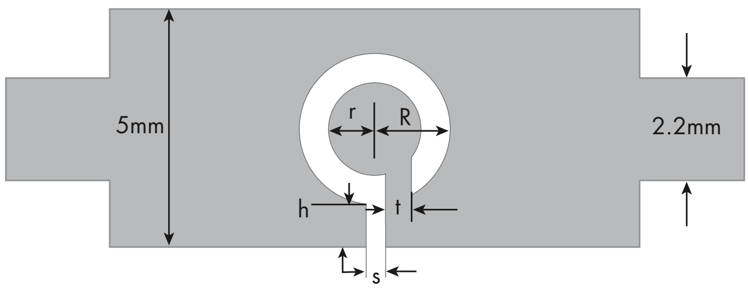

(a)

9. Another type of resonator structure is the G-Shaped DMS resonator. *(Source: Wang and Chen[4])*

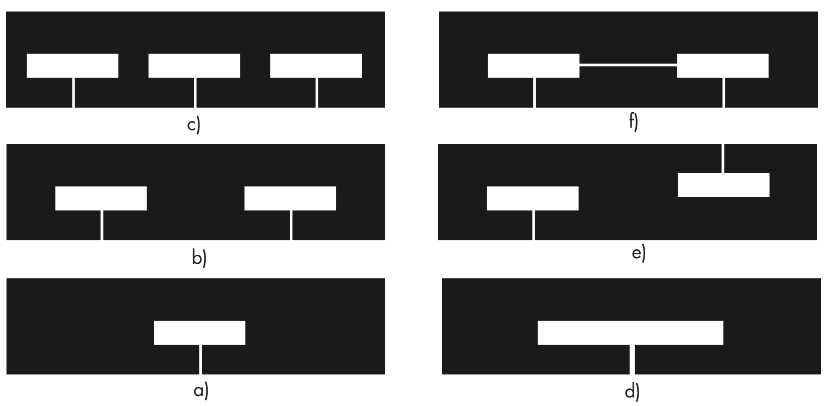

10. Array defected microstrip structures are illustrated here. *(Source: Kazerooni and Cheldavi[5])*

SUMMARY

The DMS resonator used in certain classes of distributed element filters can reduce filter complexity by working on the parasitic issues that arise and are seen in EM post-processing. The resultant distributed planar resonator filter can help to realize spurious-free wideband designs with commensurate size and cost advantages. mw

REFERENCES

1. Parui, S., Choudhury, S., Murmu, A., and Das, S., "Bandstop Filtering Characteristics of a New Spiral Defected Microstrip Structure (DMS)," *International Journal of Computer Applications,* August 3, 2015.
2. Wang. J., Ning, H. Xiong, Q., and Mao, L. "A Compact Shape Narrow-Band Bandstop Filter Using Spiral–Shaped Defected Microstrip Structure," *RadioEngineering,* Volume 23, no. 1, April 2014, pp. 209-213.
3. Subhashini, M., "Defected Microstrip Structure Based Bandpass Filter," *Indian Journal of Electronics and Electrical Engineering (IEEE)*, Volume 1, no. 1, pp. 1-6, March 28, 2013.
4. Wang, W., and Chen, Z., "Compact Lowpass Filter with Wide Stopband Using G-shaped Defected Microstrip Structure," *Advanced Material Engineering-Proceedings of the 2015 International Conference,* World Scientific Publishing Company, Ltd, Page 84, 2015.
5. Kazerooni, M. and Cheldavi, A., "Simulation, Analysis, Design and Applications of Array Defected Microstrip Structure (ADMS) Filters Using Rigorously Coupled Multi-Strip (RCMS) Method,"*Progress in Electromagnetic Research"* PIER 63, pp. 193-207.

Ultra high bandwidth Payload & RF Multipath Link Emulator

Just released ...

Sophisticated high bandwidth (up to 600MHz) emulation of physical layer RF link effects channel modeling (delay, Doppler, AWGN, Multipath) and hardware in the loop impairments modeling (programmable Group delay, Phase noise, gain/compression distortion and non-linearity AM/AM, AM/PM simulation etc.

Comprehensive range of instruments from 72 MHz to 600 MHz bandwidth with a wide RF frequency tuning range.

Contact dBm for specifications, pricing information and demonstration/evaluation units.

- **RF physical layer Link emulation**
- **Point to Point UHF/VHF radio testing**
- **Real time control for Arial Vehicle (UAV) testing**
- **Payload and ground station emulation**
- **Multipath, 12 paths @ 600MHz BW**

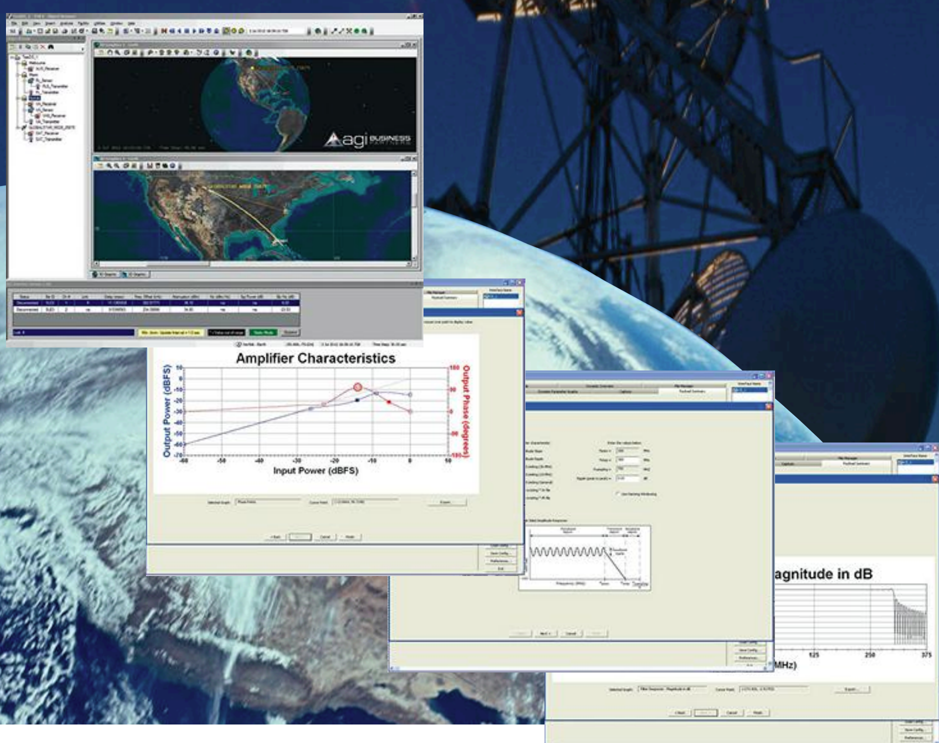

dBm

RF Test Equipment for Wireless Communications

email: info@dbmcorp.com

dBm Corp, Inc

32A Spruce Street ◆ Oakland, NJ 07436

Tel (201) 677-0008 ◆ Fax (201) 677-9444

www.dbmcorp.com

JACK BROWNE | Technical Contributor

Pursuing the Paths of EM Propagation

Propagation of electromagnetic (EM) energy, which involves a number of different paths from start to finish, makes possible many of the applications for RF/microwave signals.

High-frequency electronic platforms, such as RF/microwave communications and radar systems, often rely on the propagation of electromagnetic (EM) energy from one location to another, as well as back and forth between two locations. James Clerk Maxwell is credited with a unified theory that explains the propagation behavior of EM energy. Maxwell noted the EM nature of light, and that light and EM energy will travel through a vacuum with the same speed, c, known as the speed of light (186,000 miles/s). EM energy will propagate through other media, but at speeds less than c.

RF/microwave systems depend on the propagation of EM energy or waves through certain materials to connect transmitters with communications receivers and the reflection from certain materials for radar systems to "illuminate" a target with EM energy. Understanding some of the basic propagation effects for EM waves can help when designing and planning for many high-frequency systems, even to the extent of preventing EM interference (EMI) from disrupting the proper operation of a nearby RF/microwave system. Reviewing the basics of EM propagation may help.

A QUICK PRIMER ON EM PROPAGATION

EM propagation through space usually begins and ends with some form of antenna. Many different types of antennas are used at RF/microwave frequencies, from simple dipoles to more complex arrays with multiple antenna elements. However, the principles of operation are the same: to radiate EM energy during transmission and collect the energy from propagating EM waves and convert to voltage during reception.

Transmit antennas are often referred to as point sources of EM radiation, with the energy spreading out in all directions from the point source. When measured at a considerable distance from the point source, the radiated energy will appear to have the same power level or amplitude at all measurement points along an apparent plane that is perpendicular to the direction of travel for the radiated energy.

Radio waves travel from one ground-based antenna to another with the velocity of light, another form of EM radiation. A radio wave consists of magnetic (H) and electric (E) or electrostatic fields at right angles to each other and at right angles to the direction of travel. One-half of the energy of the propagating radio wave is in the form of electrostatic energy, while the other half of the wave's energy is in magnetic energy form. The radio wave carries energy as voltage from one location to another, with antennas serving as the means of transmission and reception for that energy.

The direction of the electrostatic-flux lines is called the direction of polarization of a radio wave. When the electrostatic lines of flux are vertical, the waves have vertical polarization; when the lines of flux are horizontal, it is horizontal polarization. These are both forms of linear polarization. EM waves can also propagate in a kind of cork-screw-shaped motion known as circular polarization. If the E field is rotating

1. One of the more popular antenna formats for satcom and terrestrial LOS communications links is the parabolic or dish antenna. *(Courtesy of RadioWaves)* in a clockwise motion relative to the direction of propagation, it is called right-handed circular polarization (RHCP). If the rotation of the E field is counterclockwise relative to the direction of propagation, it is referred to as left-handed circular polarization (LHCP).

As it propagates through space, EM energy can be visualized as a plane wave traveling in a single direction, such as from a transmit antenna to a receive antenna, rather than as energy spreading out in all directions. Ideally, such a plane wave would travel from transmit antenna to receive antenna with no loss in energy. But EM plane waves often come into contact with media other than the air through which they typically propagate. When that happens, the EM energy in the plane wave may propagate into (and through) the new medium, if it is a conductor, or bounce off another medium, if it is a reflector, as in a pulsed radar signal.

Communications signals, for example, typically propagate in many directions outward from a transmit antenna, whether it is an omnidirectional or directional antenna. Signals that follow a line-of-sight (LOS) path from the transmit to the receive antenna will also be joined at the receiver by EM energy from signals that have reflected from other media, such as buildings, with resultant slight delays or shifts in phase of these reflected signals.

Such reflections in EM propagation lead to what is known as multipath propagation, which can cause distortion at the receiver when the delays or phase shifts are significant. However, multipath propagation can also be put to good use, in the form of multiple-input, multiple-output (MIMO) antennas designed to take advantage of the multiple propagation paths to increase the effective data rate of a communications link.

Depending on frequency and such factors as antenna types and positions, radio waves are affected by the surface of the Earth and the atmosphere. Lower-frequency EM radiation, such as VHF and UHF radio waves, with longer wavelengths, tend to propagate along the Earth's surface in a mode known as ground-wave propagation. Higher-frequency signals, with shorter wavelengths, will propagate as LOS signals or as skywaves that have traveled through the troposphere (which contains the air and clouds around the Earth) and have been reflected by the atmospheric layer above that, the ionosphere.

Propagation through the troposphere and in turn reflecting from the ionosphere as skywaves results in some EM energy loss. However, it also enables longer propagating distances for radio waves at some frequencies.

ANALYZING ANTENNAS

Efficient EM propagation relies heavily on the performance of the point source antenna. Many different types of antennas are used with radio waves at different frequencies. The simplest antenna is the dipole antenna, which is essentially a section of straight wire. It's a configuration often used as a building block for other antenna types, When a voltage is applied to the wire, current flows through it and electrical charges collect at either end of the wire. It is referred to as a dipole because a balanced set of positive and negative charges collect at either end.

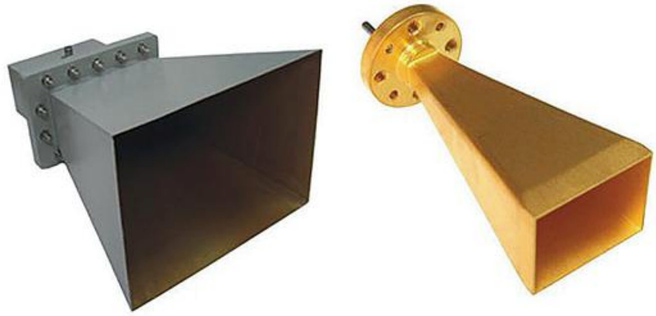

2. Horn antennas are very directional in nature, with physical dimensions a function of the wavelength/frequency of the signals to be handled. The standard gain horn on the left measures 384 × 284 × 360 mm for use from 0.96 to 1.45 GHz, while the horn on the right is a mere 21.4 × 16.6 × 51.0 mm for frequencies from 90 to 140 GHz. *(Courtesy of Gapwaves)*

When a voltage at some resonating or alternating frequency is applied to the dipole, its electric moment oscillates, resulting in oscillation of its positive and negative charges and oscillation of its electric current. The oscillating current creates the E and H fields which give rise to the outwardly propagating EM wave. The E field is oriented along the axis of the antenna and the H field is perpendicular to both the E field and the direction of propagation. This orientation of the fields is also the polarization of the antenna.

The physical size of a dipole antenna determines its operating frequency. A standard dipole has a total length equal to one-half wavelength of the operating frequency. Each side of the dipole structure is equal to one-quarter wavelength of the operating frequency, with each side of the antenna fed 180 deg. out of phase from the other side of the antenna.

The omnidirectional behavior of dipole antennas makes them well-suited for EM waves with dominant LOS and ground-wave characteristics. But many applications, e.g., satcom systems, operate with EM propagation that is more directional in nature, through the use of space waves. This requires antennas that are more directional in nature, such as the apparently ever-present parabolic reflector or "dish" antenna (*Fig. 1*).

The antennas, which are also commonly used in terrestrial point-to-point communications systems that rely on LOS EM propagation, can be designed with single or multiple polarization modes, with sizes that vary according to wavelength and frequency. Similarly, horn antennas (*Fig. 2*) are quite directional in nature, operating with fairly narrow beam widths, depending on frequency, to transmit and receive in LOS mode.

Understanding some of the basic propagation effects for EM waves can help when designing and planning for many high-frequency systems, even to the extent of preventing EM interference (EMI) from disrupting the proper operation of a nearby RF/microwave system.

SENDING MILLIMETER WAVES

As the frequencies of EM waves increase, the distances traveled by those radio waves decrease as they lose EM energy due to propagation and attenuation of the Earth and the atmosphere. Very low frequencies, such as the bandwidths used for amplitude-modulated (AM) broadcast radios, achieve long distances due to ground-wave propagation and minimal atmospheric losses. Satellite communications (satcom) systems *(see "Satellites Provide Distant Connections" on mwrf.com)* take advantage of orbiting satellites and directional antennas to bypass the losses of ground-wave propagation and achieve relatively low-loss EM propagation through the atmosphere.

With the coming of fifth-generation (5G) wireless communications networks and their multiple-frequency-band configurations that incorporate microwave and millimeter-wave frequencies, various EM propagation modes will be employed by these systems, along with the different types of antennas that will be needed for those propagation modes. As the frequencies used in 5G systems extend to 28 GHz and beyond, EM propagation at these higher frequencies will be more directional and LOS in nature over shorter distances to conserve as much EM energy (and the data it carries) as possible.

In keeping with the relationship of wavelength and antenna size, some of the newer companies working on antennas for the millimeter-wave portions of 5G systems are at the chip and PCB level for their designs, including Gapwaves (*www.gapwaves.com*) with its phased-array antennas and beamforming techniques for millimeter-wave frequencies in 5G systems (*Fig. 3*). The company's PCB antennas include high-gain models with an effective isotropic radiated power (EIRP) level of +65 dBm at 28 GHz.

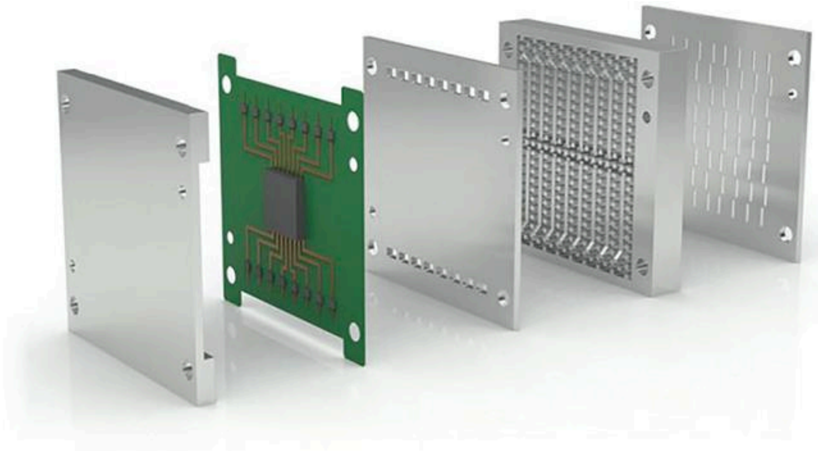

3. This miniature PCB-based phased-array antenna makes use of beamforming techniques for handling EM waves at 28 GHz. *(Courtesy of Gapwaves)*

Anokiwave has shown tremendous innovation in its lines of active antenna integrated circuits (ICs) for millimeter-wave frequencies through 80 GHz. For example, the AWMF-0129 is a 28-GHz 5G active antenna design kit that includes a 64-element phased-array antenna assembled on a PCB with the company's active antenna ICs. It operates from 27.5 to 30.0 GHz with linear polarization and has programmable beam widths, with independent phase and gain control in both transmit and receive operating modes. Its low-power, compact design is very much a sign of things to come for ubiquitous EM propagation at millimeter-wave frequencies as part of shorter-distance data links in 5G wireless networks. mw

CHRIS DEMARTINO | Technology Editor

NI Answers the Call for Flexibility with Automated Test Software

The latest release of the LabVIEW NXG software provides test engineers with a new feature that allows them to configure test system hardware in less time. On top of that, the new release also enables users to build web-based user interfaces (UIs) based on standard web technologies.

There is no question that National Instruments' (NI; *www.ni.com*) LabVIEW software has a long and distinguished history. Last year, NI made major headlines by introducing LabVIEW NXG, which the company describes as the next generation of LabVIEW. NI is continuing its momentum with its recent announcement of a new release of LabVIEW NXG. NI asserts that this new version introduces key functionality for engineers involved with automated test-and-measurement systems.

ENHANCING THE AUTOMATED TEST WORKFLOW

So what are the enhancements that this new version of LabVIEW NXG offers? And what prompted NI to provide them in the first place? "The technologies that are embedded inside of test-and-measurement equipment are accelerating in performance at exponential rates," explained David Hall, senior product marketing manager for RF and communications at NI. "Our approach for serving that capability to customers is through a flexible software-centric approach."

BUILDING AN AUTOMATED TEST SYSTEM WORKFLOW

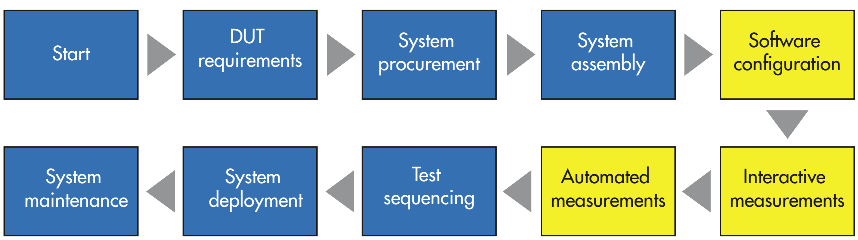

1. This figure illustrates an automated test system workflow. The yellow blocks represent the areas that NI is aiming to boost.

Let's first take a look at the role of a typical test engineer. "When we look at how customers use our software to build an automated test system, there are probably a number of different steps that they go through that historically have all been pretty discrete," said Hall. "A test engineer typically gets a spec sheet, a measurement list, or a test plan to start with. This documentation tells the engineer what results are needed for which set of measurements at which set of frequencies or under what operating conditions.

"What a test engineer is responsible for is to translate that set of requirements into a test system," he continued. "That starts with procuring hardware, assembling that hardware, and starting to develop the code for each individual test module for each individual test. The process also involves troubleshooting and making sure measurements are accurate through an interactive measurement experience, eventually automating those measurements, and then reporting the results."

Figure 1 shows an automated test system workflow. NI's goal is to essentially simplify the middle sections of this workflow *(shown in yellow in Fig. 1)*. "In each of those areas, the way in which we are attempting to help those engineers is to effectively reduce the time it takes to do those tasks," Hall noted, referring to those middle sections.

Let's look at just how NI intends to accomplish these goals. Anyone who has spent time in a test lab knows that a test bench typically consists of a number of different test instruments that are often manufactured by different vendors. These instruments are also likely to vary in age. Given these dissimilarities, Hall noted, it can be a challenge to get all of the instruments in a test bench to work together.

"In a typical test bench that many of our customers might start with," he said, "there is a challenge from an automation perspective—the automation technologies for some of the instruments might be different. There are challenges with synchronization—the way that you synchronize them may all be different. There are issues with programming, particularly because the driver software for each of these instruments is often very different. That creates a level of complexity that test engineers typically have to wade through by themselves."

To overcome these challenges, NI is offering a new feature in LabVIEW NXG called SystemDesigner *(Fig. 2)*. "SystemDesigner is a diagram that allows engineers to configure the hardware they have present in their test system," explained Hall. "That includes a combination of PXI hardware or other NI hardware, as well as other third-party instruments."

3. The LabVIEW NXG Web Module enables users to create UIs that can run in modern web browsers without plug-ins or installers.

2. SystemDesigner helps users check a system's configuration as its being built, thus simplifying the process of building test systems.

Let's explain a little of what SystemDesigner can offer. For one, when using NI hardware in a test system, SystemDesigner allows engineers to see specific details concerning that hardware. This information can include connector pinouts, the manual for the specific instrument, and more.

SystemDesigner also supports third-party instruments in a test system. "SystemDesigner can connect engineers to the driver software for third-party instruments—in part because many of those drivers are hosted on ni.com," Hall said. "From the SystemDesigner view, you can find out which drivers you need to control hardware and install and manage the driver installation from within the LabVIEW environment. That actually can save a lot of time, as it's often difficult to find the most appropriate version of the driver—particularly if you're using instruments from multiple vendors."

SystemDesigner lets users operate in either Live or Design mode. "When you're in Live mode, the software goes out and looks to see what instruments are connected," said Hall. "When you're in Design mode, you can configure a hypothetical system that you want to put together. So you can configure a SystemDesigner view before you actually procure your instruments. That helps you to identify which instruments you need and what software you're going to need before you physically have those instruments."

A WEB-BASED APPROACH

SystemDesigner is not the only new feature offered in the latest release of LabVIEW NXG. The other new aspect involves today's web technologies. "The other set of challenges we're attempting to solve with the latest iteration of NXG involves serving data through the right mechanisms—particularly using web technologies," Hall explained. "When talking with many of our customers, we get a tremendous amount of feedback concerning their desire for doing remote configurations, remotely operating instruments, potentially real-time monitoring measurements, and having the capability to view data offline."

As an example, remote operation and monitoring is clearly a necessity if a test system is located in a dangerous environment—one obviously wouldn't want to be physically present with that test system. Some of today's web technologies have made remote operation and monitoring much easier through a web-based approach.

"The use of web technologies could be pretty useful, particularly when you want your test system configured in a closed environment where you don't want physical access," Hall said. "There a number of web technologies that engineers could use themselves to enable remote data access, but it's honestly pretty complicated. Only a pretty small group of individuals have the knowledge set that a typical test engineer is required to have. If you were to add detailed knowledge of web programming tools and client/server communications, you further limit your pool of individuals. The result is you either have to go and learn a whole bunch of new technology, or you have to outsource some aspects of that project."

So just what is NI hoping to achieve? Hall explained: "What we're attempting to do with LabVIEW NXG is abstract some of the difficulty and make it really accessible to create polished, professional web user interfaces (UIs) within the LabVIEW environment. And we're doing that through some pretty standard technologies like HTML and JavaScript. We're doing it in a way such that the users themselves can actually host the UI on local servers."

Let's now talk about the new LabVIEW NXG Web Module, which is the actual product that NI now offers that makes what was just said a reality *(Fig. 3)*. The LabVIEW NXG Web Module, which works within the LabVIEW NXG environment, lets users create web-based UIs to remotely control and monitor test-and-measurement systems.

WebVIs lie at the heart of the LabVIEW NXG Web Module. WebVIs are essentially LabVIEW VIs that allow users to build UIs via drag-and-drop widgets. WebVIs are based on standard web technologies, such as HTML, CSS, and JavaScript, meaning UIs that are created can be viewed in any modern web browser.

In addition, LabVIEW actually scripts HTML, CSS, and JavaScript as a UI is being created. This generated code can be accessed at any time, allowing engineers to customize the code to meet their specific needs.

To summarize, this latest release of LabVIEW NXG offers new capabilities that are sure to be highly beneficial for engineers involved with automated test-and-measurement systems. SystemDesigner is sure to save test engineers a great deal of time, while the web-based capabilities add a new dimension to developing automated test-and-measurement systems. Test engineers all over are sure to take advantage of these latest tools. mw

MAHMOUD A. ABDALLA | Department of Electronic Engineering, Military Technical College, Cairo, Egypt; maaabdalla@ieee.org | Department of Computer and Electrical Engineering, University of Waterloo, Waterloo, Canada; mahmoud.a.abdalla@uwaterloo.ca

SAMEER KUMAR SHARMA | Student Member, IEEE; sharma.sameer16@gmail.com

ZHIRUN HU | School of Electrical Engineering, University of Manchester, Manchester, UK; z.hu@manchester.ac.uk

CRLH TLs and SIRs Lead to the Incredibly Shrinking Antenna

The use of CRLH transmission lines and stepped impedance resonators (SIRs) on low-cost circuit materials delivers highly selective single- and dual-band antennas a fraction the size of conventional components.

Practical use of realizable circuit structures such as stepped impedance resonators (SIRs) and various forms of transmission lines (TLs) can lead to highly selective, yet also quite small, single- and dual-band antennas. Analysis of antenna designs based on SIRs and composite right/left-handed (CRLH) transmission lines can show how to cover several frequency bands while also miniaturizing the antenna designs, for both quarter-wavelength and half-wavelength antenna configurations.

To demonstrate the approach, quarter- and half-wavelength antennas were designed with a common band centered at 4.5 GHz and an impedance bandwidth ($|S_{11}| < -10$ dB) of 500 MHz, and with the half-wavelength antenna also handling a second frequency band centered at 1.8 GHz. For a fair comparison of the two configurations, the size of both antennas is the same (26×21.3 mm^2).

LEVERAGING METAMATERIALS

Metamaterials have sparked a great deal of interest among high-frequency designers and researchers in recent years. Metamaterials are characterized by having both negative permittivity and permeability.[1,2]

Metamaterial structures such as split-ring resonators (SRRs) and complementary SRRs (CSRRs) have been loaded on monopole antennas to effectively reduce the electrical size and increase the number of frequency bands.[3-6]

Nonresonant and wideband metamaterials have been realized by using a TL that is periodically loaded with series capacitors and shunt inductors, along with conventional TL elements. Such a circuit structure is referred to as a composite right/left-handed (CRLH) TL.[7,8] CRLH TLs exhibit a progressive phase shift that can be completely controlled by the loading/parasitic elements' values in a nonlinear frequency dependence such that both can be used to adjust arbitrary frequency bands.

Several compact single-, dual-, and multi-band antenna designs presented in literature involve use of CRLH TL,[9-15] modified versions of CRLH TLs,[16-18] and loading monopole/dipole antenna structures with CRLH cells.[19-21] Extremely compact antennas have also been employed in multiple-input, multiple-output (MIMO) applications.2[2,23] However, designing small antennas with simple independent design procedures is an ongoing high-frequency design need that has not been covered completely in the literature.

IMPACT OF RESONANCE

The performance of many different antennas depends highly on the effect of its resonators or, in general, some form of resonance. These resonant effects are employed in many ways, for example, to form the fundamental operating frequency/band or to provide high isolation for other frequencies. Regardless of the design approach, most antennas face a common challenge, which is the presence of spurious frequencies due to various modes and resonances.

A simple solution is to use filters before or after the antenna block, depending on whether signal information is transmit-

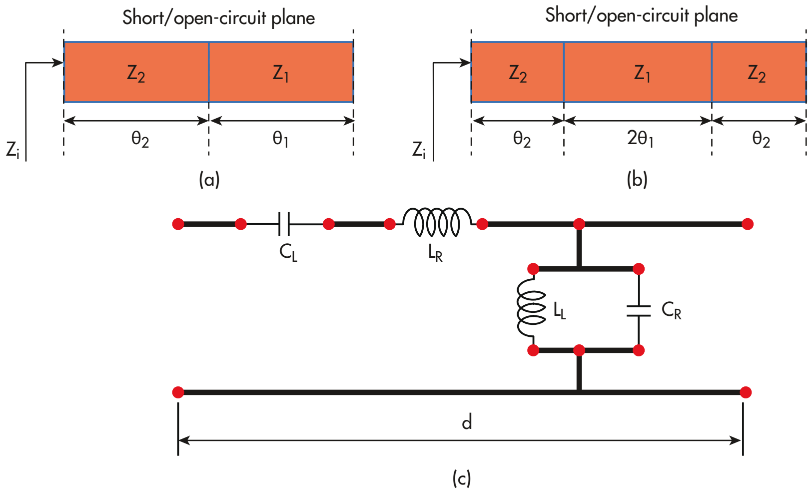

1. The schematic diagrams show a quarter-wave SIR (a) and a half-wave SIR (b), while the equivalent circuit shows a CRLH cell (c).

ted or received.[24] However, this strategy results in a larger overall structural size. Another solution can be the use of SIRs, which inherently block spurious bands and provide better isolation. Approaches for CRLH-based SIR filters are presented in refs.[25-29]. Some attempts for high-selectivity metamaterial-based SIR antennas are also suggested in refs.[30-34]

To show the effectiveness of metamaterials in antenna design, notably the use of SIRs and CRLH transmission lines, $\lambda/4$ and $\lambda/2$ short-circuited metamaterial SIR transmission lines were explored for application in antenna design as their fundamental element. The $\lambda/4$-based antenna has a single-band response at 4.5 GHz while the $\lambda/2$-wavelength antenna offers the 4.5-GHz band as well as an additional band at 1.8 GHz for the same geometrical size, with sharper cutoff characteristics.

The antennas are built on low-cost FR-4 substrate material with relative permittivity of 4.3, thickness of 1.6 mm, and loss tangent ($\tan \delta$) of 0.02. To generate an omnidirectional pattern, the proposed metamaterial SIR antennas were designed in coplanar waveguide (CPW) configurations. The commercial computer-aided-engineering (CAE) circuit design software CST Microwave Studio from Computer Simulation Technology *(www.cst.com)* helped in the design process.

The SIR can be realized by cascading transmission lines with different characteristic impedances and electrical lengths. The schematic for quarter-wavelength SIR and half-wavelength SIR are shown in *Figs. 1a and 1b*, respectively. The term Z_i refers to the characteristic impedance, while θ_i is the electrical length of each transmission line. The resonators can be open or short circuit in configuration. As a result, four possible configurations are available to achieve minimum or maximum impedance. In all configurations, the target resonant condition for employing these structures as antennas requires achieving zero input admittance ($Y_i = 0$).

For a short-circuit, quarter-wavelength SIR antenna, the input impedance can be expressed as Eq. 1:

$$Z_{inQ} = (jZ_2)[(Z_2\tan\theta_2 + Z_1/\tan\theta_1)/(Z_2 - Z_1\tan\theta_2/\tan\theta_1)] \quad (1)$$

The input impedance for a short-circuit $\lambda_g/2$ CRLH SIR can be extracted mathematically by means of Eq. 2:

$$Z_{inH} = Z_{2(}j[Z_2\tan(\theta_2) + Z_1\tan(2\theta_1)] + jZ_2\tan(\theta_{2)}[Z_1 - Z_2\tan(2\theta_1)\tan(\theta_2)]/Z_2[Z_1 - Z_2\tan(2\theta_1)\tan(\theta_2)] - Z_1\tan(\theta_2)[Z_2\tan(\theta_2) + Z_1\tan(2\theta_1)]\,) \quad (2)$$

The resonant conditions for quarter-wavelength and half-wavelength short-circuit SIR antennas can be achieved when the input impedance is infinite (zero input admittance), as shown by Eqs. 3 and 4:

$$Z_2 = Z_1\tan(\theta_2) / \tan(\theta_1) \quad (3)$$

$$Z_2[Z_1 - Z_2\tan(2\theta_1)\tan(\theta_2)] = Z_1\tan(\theta_2)[Z_2\tan(\theta_2) + Z_1\tan(2\theta_1)] \quad (4)$$

When designing the SIR using CRLH TLs, the parameters expressed as Eqs. 5 and 6 are used for the SIRs:

$$Z_i = \{[L_{Li}(\omega^2L_{Ri}C_{Li} - 1)] / [C_{Li}(\omega^2L_{Li}L_{Ri} - 1)]\}^{0.5} \quad (5)$$

$$\theta_i = \omega(L_{Ri}C_{Ri})^{0.5}\{[1 - 1/(\omega^2C_{Li}L_{Ri})][1 - 1/(\omega^2C_{Ri}L_{Li})]\}^{0.5} \quad (6)$$

From Eqs. 5 and 6, and by substitution of Eqs. 3 and 4, it is possible to confirm that the resonant condition has a higher-order degree of freedom for the half-wavelength case compared to the quarter-wavelength case. Thus, more bands and highly selective antennas can be realized using half-wavelength CRLH SIR antenna for short-circuit termination.

DOUBLING UP

The earlier conclusions can be reinforced through the introduction of two CRLH SIR antennas, a quarter-wavelength and a half-wavelength antenna. *Fig. 2* shows a planar 2D layout of the quarter-wavelength antenna. The antenna is formed with two cascaded CRLH cells after the equivalent circuit of *Fig. 1c*. The first cell is designed using an 11-finger interdigital capacitor and low-value meandered-line inductor. The second cell is realized with a series gap capacitor and high-value meandered-line inductor. *Fig. 2* provides details of the antenna's dimensions. The antenna

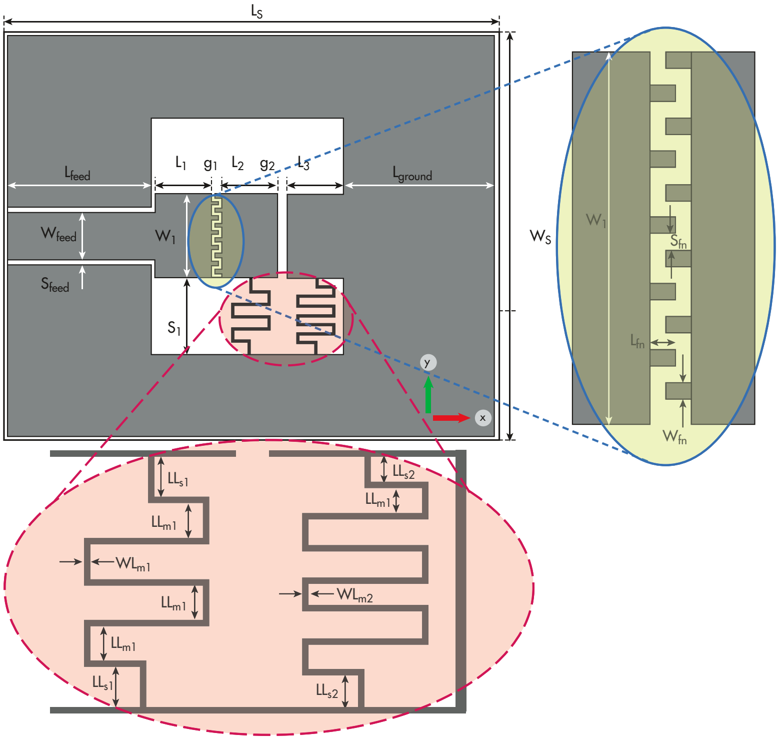

2. This 2D layout shows a CPW short-circuit, half-wavelength (λ/2) CRLH SIR antenna, with L_s = 26 mm; W_s = 21.3 mm; $L_1 = L_2 = L_3 = L_4$ = 3 mm; $g_1 = g_2 = g_3$ = 0.5 mm; L_{feed} = 7.7 mm, W_{feed} = 2.5 mm; S_{feed} = 0.2 mm; S_1 = 4 mm; W_1 = 4.6 mm; L_{ground} = 8.1 mm; L_{L1} = 0.4 mm; L_{Lm2} = 4 mm; L_{L2}=0.65 mm; L_{Lm2} = 0.55 mm; $W_{Lm1} = W_{Lm2}$ = 0.1 mm.

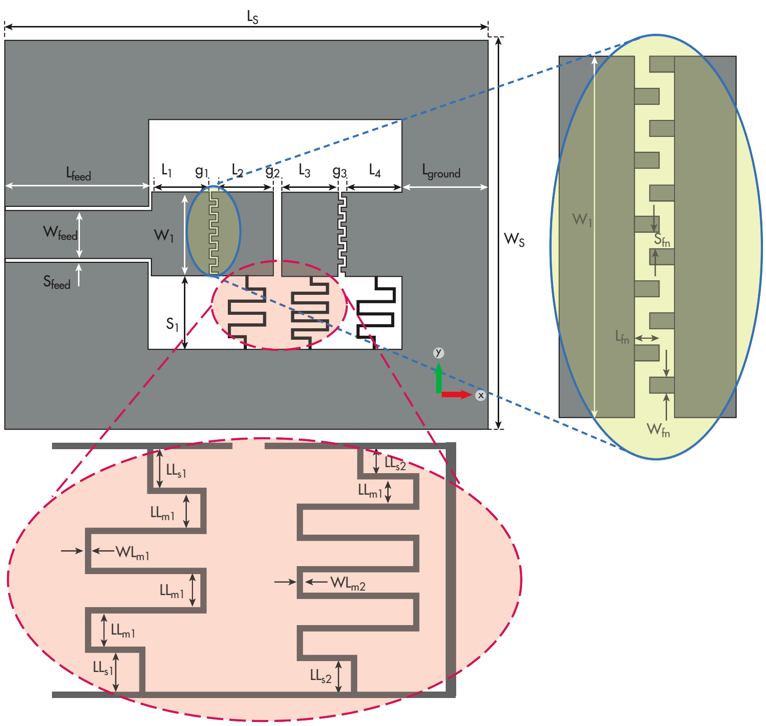

3. This 2D layout shows a CPW short-circuit half-wavelength (λ/2) CRLH SIR antenna with L_s=26 mm; W_s=21.3 mm; $L_1 = L_2 = L_3 = L_4$ = 3 mm; $g_1 = g_2 = g_3$ = 0.5 mm; L_{feed}= 7.7 mm; W_{feed} = 2.5 mm, S_{feed} = 0.2 mm; S_1 = 4 mm; W_1 = 4.6 mm; L_{ground} = 4.6 mm; L_{L1}=0.4 mm; L_{Lm2}= 0.5 = 4 mm; L_{L2} = 0.65 mm; L_{Lm2} = 0.55 mm; $W_{Lm1} = W_{Lm2}$ = 0.1 mm.

measures just 26 × 21.3 mm^2, or only about 30% the size of a conventional patch antenna.

The modification that was added to the quarter-wavelength configuration is to realize the resonator as a half-wavelength configuration *(shown earlier in Fig. 1b)*. The antenna with the modification (as a half-wavelength antennas) is shown in *Fig. 3*. As can be seen, the antenna consists of three cascaded CRLH TLs. The first and third TLs are identical, with somewhat different TL used between them. The first and third TLs are realized using an interdigital capacitor and low-value meandering-line inductor. The middle TL is realized using an air-gap capacitor. This means that the outer TLs have higher C_L and lower L_L values, which yields smaller characteristic impedance and nearly equivalent electrical length as can be concluded from Eqs. 5 and 6. In a similar fashion to the short-circuit load, the antenna has a 50-Ω feedline and connected to the short-circuit load. Fig. 2 provides further details of the dimensions for the different components of the antennas.

The simulated reflection coefficients of the proposed antennas (quarter- and half-wavelength SIR antennas) are shown in Fig. 3. It can be clearly seen that the λg/4 quarter-wavelength antenna has a single resonance at 4.6 GHz for which the reflection coefficient is −20 dB with an impedance bandwidth ($|S_{11}| < -10$ dB) of 0.6 GHz (from 4.4 to 5 GHz).

The half-wavelength CRLH SIR antenna has two resonances, at 1.8 and 4.5 GHz. At both frequencies, the reflection coefficient is closer to −15 dB. However, the first band is very selective (a sharper cutoff) at 1.8 GHz, whereas the second band has a comparatively flatter slope. The proposed half-wavelength antenna design is only 5% and 29% the size of two separate conventional patch antennas used to handle 1.8 and 4.5 GHz separately.

Phone: (973) 881-8800 | Fax: (973) 881-8361
E-mail: sales@synergymwave.com
Web: WWW.SYNERGYMWAVE.COM
Mail: 201 McLean Boulevard, Paterson, NJ 07504

WHAT ABOUT THE RADIATION?

The radiation properties of the quarter-wavelength CRLH SIR antenna were investigated by plotting the simulated three-dimensional (3D) gain radiation pattern at 4.6 GHz *(Fig. 4)*. The quarter-wavelength SIR antenna has a typical omnidirectional pattern with a realized gain of 2.169 dB and good radiation efficiency of 77.5% *(Fig. 5)*. The maximum radiation directivity occurs along the Z-direction (the broadside of the antenna geometry) and has null radiation along the C direction (the feeding direction).

The simulated 3D radiation patterns of the half-wavelength CRLH SIR antenna are plotted in *Figs. 6a and 6b* for the two resonant frequencies at 1.8 and 4.6 GHz, respectively. The half-wavelength antenna design exhibits similar high-directivity properties at both frequencies, in the manner of the quarter-wavelength antenna at its single frequency. The maximum directivity occurs in the broadside direction (Z-direction). The antenna has different radiation efficiencies at the two frequencies: 72% at 4.5 GHz and 1% at 1.8 GHz. The low efficiency at the lower frequency (1.8 GHz) can be attributed to the small physical size of the antenna for that wavelength.

Small antennas can be designed using CRLH SIR technology, as has been shown for two different configurations. These two antennas are quarter-wavelength and half-wavelength CRLH SIR antennas with only one cell, each a fraction the size of a conventional printed antenna. In the case of the half-wavelength antenna, the proposed design approach can result in antennas as small as only 5% the size of a conventional printed antenna. mw

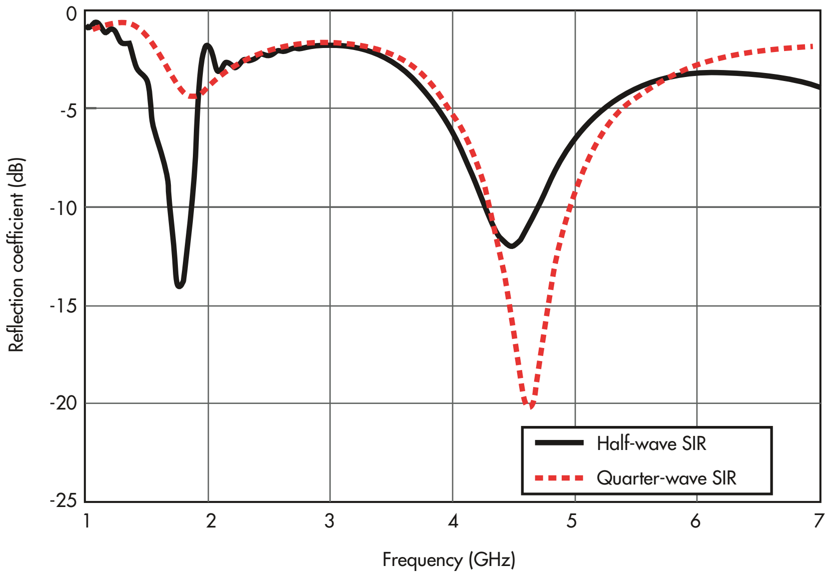

4. A commercial simulation program produced this simulated reflection coefficients for the quarter- and half-wave SIR antennas.

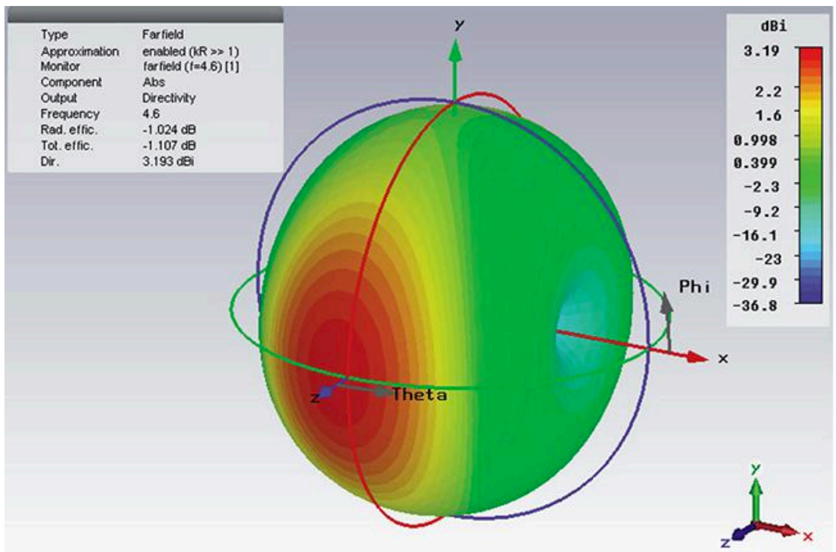

5. This simulation shows the 3D directive gain radiation pattern at 4.6 GHz.

REFERENCES

1. Nader Engheta, and Richard W. Ziolkowski, Eds., *Metamaterials: Physics and Engineering Explorations,* Wiley, New York, 2006.

2. Ricardo Marqués, Ferran Martín, and Mario Sorolla, *Metamaterials with Negative Parameters: Theory, Design, and Microwave Applications,* Vol. 183, Wiley, New York, 2011.

3. Meng Li, Xian Qi Lin, Jessie Yao Chin, Ruopeng Liu, and Tie Jun Cui, "A Novel Miniaturized Printed Planar Antenna Using Split-Ring Resonator," *IEEE Antennas and Wireless Propagation Letters,* Vol. 7, 2008, pp. 629-631.

4. Li-Ming Si, Weiren Zhu, and Hou-Jun Sun, "A Compact, Planar, and CPW-Fed Metamaterial-Inspired Dual-Band Antenna," *IEEE Antennas and Wireless Propagation Letters*, Vol. 12, 2013, pp. 305-308.

5. S. K. Sharma and R. K. Chaudhary, "Dual-band Metamaterial-inspired Antenna for Mobile Applications," *Microwave and Optical Technology Letters,* Vol. 57, No. 6, 2015, pp. 1444-1447.

6. Walaa Wahba, Mahmoud Abdalla, Ahmed Mohamed, and Abdelmegeed Allam, "A Uni-Planar Microstrip CSRR metamaterial Antenna," 2014 IEEE AP-S International Antenna and Propagation Symposium Digest, Memphis, TN, July 6-11, 2014, pp.545-546.

7. C. Caloz and T. Itoh, *Electromagnetic Metamaterials Transmission Line Theory and Microwave Applications,* Wiley, Paramus, NJ, 2006.

8. G. V. Eleftheriades and K. G. Balmain, *Negative Refractive Metamaterials,* Wiley, Paramus, NJ, 2005.

9. Cheng-Jung Lee, Wei Huang, A. Gummalla, and M. Achour, "Small Antennas based on CRLH Structures: Concept, Design, and Applications," IEEE Antennas and Propagation Magazine, Vol. 53, No. 2, 2011, pp. 10-25.

10. R. W. Ziolkowski, P. Jin, and C. Lin, "Metamaterial-Inspired Engineering of Antennas," IEEE Proceedings, Vol. 99, No. 10, 2011, pp. 1720-1731.

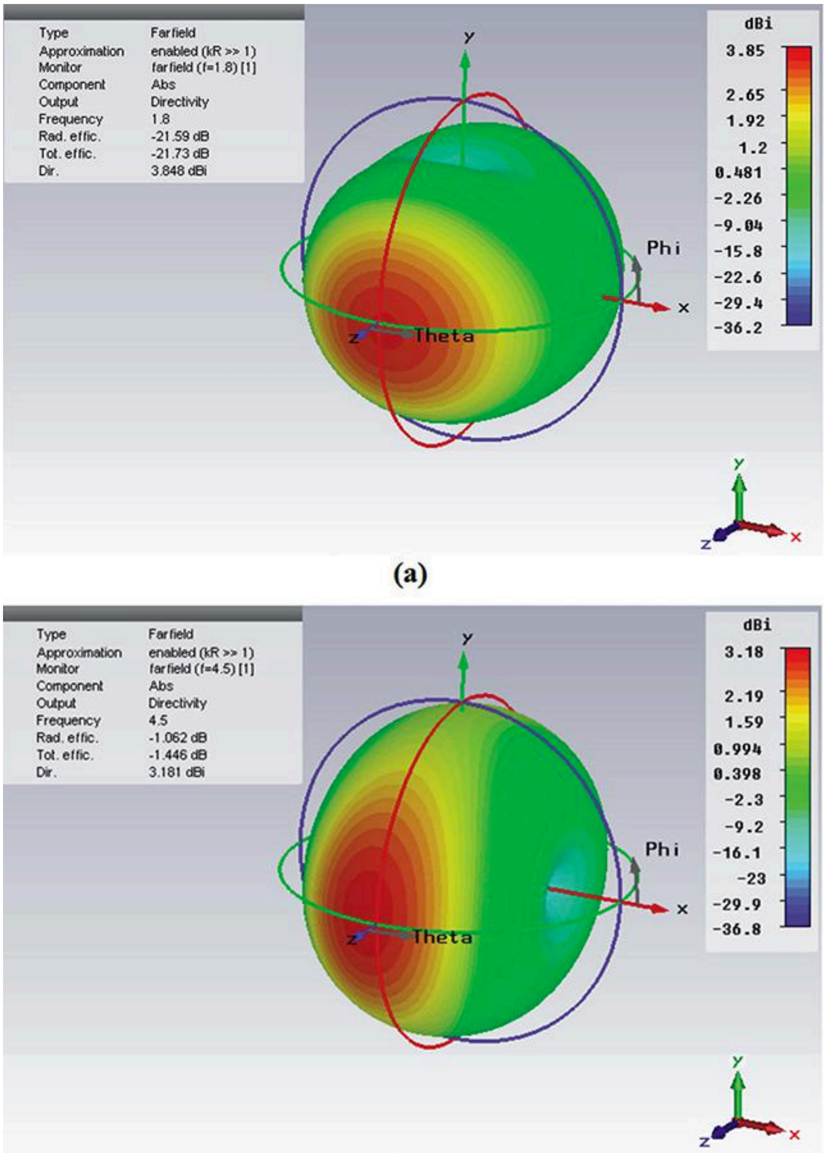

6. This simulation shows the 3D directive gain radiation pattern at 1.8 GHz (a) and 4.5 GHz (b).

11. M. Abdalla and Z. Hu, "Compact and Tunable Metamaterial Antenna for Multi-band Wireless Communication applications," 2011 IEEE AP-S International Antenna and Propagation Symposium Digest, July 2011, pp. 2951-2953.

12. S. K. Sharma, and R.K. Chaudhary, "A Compact Zeroth-order Resonating Wideband Antenna with Dual-band Characteristics," *IEEE Antennas and Wireless Propagation Letters*, Vol. 14, 2015, pp.1670-1672.

13. Mahmoud A. Abdalla, Walaa W. Wahba, and Abdelmegid M. Allam, "Asymmetric dual-band integrated compact CRLH SIW array antenna," *Journal of Electromagnetic Waves and Applications,* Vol. 31, No. 3, 2017, pp. 284-296.

14. Li, Long, Zhen Jia, Feifei Huo, and Weiqiang Han, "A novel compact multiband antenna employing dual-band CRLH-TL for smart mobile phone application," *IEEE Antennas and Wireless Propagation Letters,* Vol. 12, 2013, pp. 1688-1691.

15. Jeong Keun Ji, Gi Ho Kim, and Won Mo Seong, "Bandwidth enhancement of metamaterial antennas based on composite right/left-handed transmission line," *IEEE Antennas and Wireless Propagation Letters,* Vol. 9, 2010, pp. 36-39.

16. Mahmoud A. Abdalla and Mohamed I. Abdelnaser, "A Compact Dual Band D-CRLH Antenna with Radiation Pattern Directional Characteristics," 2016 IEEE AP-S International Antenna and Propagation Symposium Digest, 2016, Portorreco, pp. 277-278.

17. Mohammad Bemani, Saeid Nikmehr, and Mahdi Fozi, "A Dual-Band Feed Network for Series-Fed Antenna Arrays Using Extended Composite Right/Left-Handed Transmission Lines," *IEEE Transactions on Antennas and Propagation*, Vol. 65, No. 1, 2017, pp. 178-189.

18. M. A. Abdalla and Z. Hu, "A Compact Dual Band Meta-material Antenna for Wireless Applications," 2012 Loughborough Antennas & Propagation Conference, Loughborough, UK, pp. 1-4, 2012.

19. J. Zhu and G.V. Eleftheriades, "Dual-band metamaterial-inspired small monopole antenna for WiFi applications," *Electronics Letters,* Vol. 45, No. 22, 2009, pp. 1104-1106.

20. M. A. Abdalla, U. Abdelnaby, and A. A. Mitkees, "Compact and Triple Band Meta-material Antenna for All WiMAX Applications," 2012 International Symposium on Antennas and Propagation (ISAP), 2012, pp. 1176 – 1179.

21. S. Jamilan, M. A. Antoniades, J. Nourinia, and M. N. Azarmanesh, "A compact multiband printed dipole antenna loaded with two unequal parallel NRI-TL metamaterial unit cells," *IEEE Transactions on Antennas and Propagation,* Vol. 63, No. 9, 2015, pp. 4244-4250.

22. Ahmed A. Ibrahim and Mahmoud A. Abdalla, "CRLH MIMO Antenna with Reversal Configuration," *AEÜ- International Journal of Electronics and Communications,* Vol. 70, No. 7, pp. 1134-1141,2016.

23. Mahmoud A. Abdalla and Ahmed A. Ibrahim, "Design and Performance Evaluation of Metamaterial Inspired MIMO Antennas for Wireless Applications," *Wireless Personal Communication*, 2016, pp. 1-17.

24. C. A. Balanis, *Antenna Theory and Design*, Wiley, Paramus, NJ, 2005.

25. S. Karimian, M. A. Abdalla, and Z. Hu, "Left-handed Stepped Impedance Resonator for WLAN Applications," 2009 3rd International Congress on Advanced Electromagnetic Material in Microwave and Optics, London, UK, August 30 to September 4, 2009, pp. 1-4.

26. S. Karimian, M. Abdalla, and Z. Hu, "Compact Half-wavelength Metamaterial Stepped Impedance Resonator (SIR)," 2011 IEEE AP-S International Antenna and Propagation Symposium Digest, July 3-8, 2011, Spokane, WA, pp. 1054-1057.

27. S. Karimian, M. Abdalla, and Z. Hu, "Tunable Metamaterial Ferrite Stepped Impedance Resonator (SIR)," 2010 PIERS, 27th Progress in Electromagnetics Research Symposium, March 2010, Xi'an, China, pp 165-168.

28. Paris Vélez, Miguel Durán-Sindreu, Armando Fernández-Prieto, Jordi Bonache, Francisco Medina, and Ferran Martın, "A Compact Dual-Band Differential Power Splitter With Common-Mode Suppression and Filtering Capability Based on Differential-Mode Composite Right/Left-Handed Transmission-Line Metamaterials," *IEEE Antennas and Wireless Propagation Letters,* Vol. 13, 2014, pp. 536-539.

29. Mahmoud A. Abdalla and Ahmed A. Ibrahim, "Metamaterials Sculpt UWB Bandpass Filter," *Microwaves and RF,* Vol. 56, No. 3, March 2017, pp. 1-4.

30. Mahmoud. A. Abdalla, Aliaa A. Awad, and Khaled M. Hassan, "Wide Band High Selective Compact Metamaterial Antenna for 2 GHz Wireless Applications," 2014 Loughborough Antennas & Propagation Conference, November 10-11, 2014, Loughborough, UK, pp. 350-354.

31. M. A. Abdalla, S. Karimian, and Z. Hu, "Dual Band Spurious-Free SIR Metamaterial Antenna," 2014 IEEE AP-S International Antenna and Propagation Symposium Digest, July 2014, pp. 1005-1006.

32. Mahmoud Abdalla, Mohamed Abo El-Dahab, and Mohamed GHouz, "SIR Double Periodic CRLH Loaded Dipole Antenna," 2015 IEEE AP-S International Antenna and Propagation Symposium Digest, July 2015, Vancouver, Canada, pp. 832-833.

33. Y. Kushiyama, T. Arima, and T. Uno, "Differential-Type CRLH Leaky-Wave Antenna Using Stepped Impedance Resonators," *IEEE Antennas and Wireless Propagation Letters,* Vol. 15, 2016, pp. 321-324.

34. S. K. Sharma, M. A. Abdalla, and R. K. Chaudhary, "An Electrically Small SICRR Metamaterial-inspired Dual-band Antenna for WLAN and WiMAX applications," *Microwave and Optical Technology Letters*, Vol. 59, No. 3, 2017, pp. 573-578.

ULTRA-REL™

CERAMIC MMIC AMPLIFIERS

10 MHz to 7 GHz

Low NF from 0.5 dB   *High IP3 up to +42 dBm*   *Low DC current 65 mA*   *from* $7.45 *ea. (qty 20)*

When failure is not an option! Our CMA family of ceramic MMIC amplifiers is expanding to meet your needs for more critical applications. Designed into a nitrogen-filled, hermetic LTCC package just 0.045" high, these rugged models have been qualified and are capable of meeting MIL standards for a whole battery of harsh environmental conditions:

Qualified for: *(see website for complete list and details)*

Gross and Fine Leak	*HTOL (1700 hours @ +105°C)*
Mechanical Shock	*Steam Aging*
Vibration	*Solder Heat Resistance*
Acceleration	*Autoclave*
PIND	*And More!*

**Gross leak only*

Robust performance across wide bandwidths makes them ideal for military and defense applications, hi-rel instrumentation, and anywhere long-term reliability adds bottom-line value. Go to minicircuits.com for all the details today, and have them in your hands as soon as tomorrow!

Electrical Specifications *(-55 to +105°C)*

3 x 3 x 1.14 mm

Model	Freq. (GHz)	Gain (dB)	P_{OUT} (dBm)	IP3 (dBm)	NF (dB)	DC (V)	Price $ ea. (qty 20)
CMA-81+	DC-6	10	19.5	38	7.5	5	8.95
CMA-82+	DC-7	15	20	42	6.8	5	8.95
CMA-84+	DC-7	24	21	38	5.5	5	8.95
CMA-62+	0.01-6	15	19	33	5	5	7.45
CMA-63+	0.01-6	20	18	32	4	5	7.45
CMA-545+	0.05-6	15	20	37	1	3	7.45
CMA-5043+	0.05-4	18	20	33	0.8	5	7.45
CMA-545G1+	0.4-2.2	32	23	36	0.9	5	7.95
CMA-162LN+	0.7-1.6	23	19	30	0.5	4	7.45
CMA-252LN+	1.5-2.5	17	18	30	1	4	7.45

RoHS compliant

Mini-Circuits®

www.minicircuits.com P.O. Box 350166, Brooklyn, NY 11235-0003 (718) 934-4500 sales@minicircuits.com

defense electronics

A Special Section to INFORMA'S DESIGN ENGINEERING & SOURCING GROUP MARCH 2018

JACK BROWNE | Technical Contributor

COMSAT Teams with Iridium for Secure DoD Satcom Service

The launch of the satellites for the next-generation Iridium system, Iridium NEXT, and its broadband L-band capabilities, has made it possible for partners such as COMSAT to provide high-speed, global, and secure communications services. *(Courtesy of The Maritime Executive)*

SATELLITE COMMUNICATIONS (satcom) networks offer communications services that are potentially global in nature, among users on land, at sea, and in the air. And now, with the joint efforts of satcom providers COMSAT and Iridium and its Iridium Certus system (based on the second-generation Iridium NEXT satellite constellation), U. S. Department of Defense (DoD) users can benefit with global communications that are secure and reliable. A long-term agreement between COMSAT and Iridium will result in the availability of secure satcom connectivity for mobile voice and data users to the U.S. DoD by the middle of 2018.

COMSAT *(www.comsat.com)* has long provided secure satellite solutions to government, military, and maritime users, and this agreement will allow the company to bring its full suite of value-added services to the Iridium *(www.iridium.com)* Certus program *(see figure)*. The teaming will enable COMSAT to leverage the benefits of the Iridium network, including global, on-the-move L-band wireless connectivity, to provide services that meet the Communications Security (ComSec) requirements for the DoD, such as real-time statistics on use, telematics data, voice calling, personnel tracking, and real-time environmental assessments.

(Continued on page 52)

Mercury's Memory Devices Bound for Airborne System

MERCURY SYSTEMS *(www.mrcy.com)* has received a $3.2 million follow-on order from a leading defense contractor for its BuiltSECURE ruggedized memory devices, which are being integrated into an advanced airborne military computing system. As with the follow-on business for multichip modules from a leading defense contractor *(see "Mercury Systems Supplies MCMs for Airborne EW System" on mwrf.com)*, this order was booked in the company's fiscal 2018 second quarter and is expected to ship over the next several quarters.

This secure solid-state device (SSD) is an example of the type of high-speed memory component that will be integrated into an advanced airborne military computing system. *(Courtesy of Mercury Systems)*

(Continued on page 52)

Electronic Weapons Systems Begin to See the Light

LASER WEAPONS have long been part of science-fiction movies, telling imaginative tales of humans battling with alien species in outer space. But right back here on Earth, in the here and now, laser weapons are not only being designed, developed, and tested—they are being used effectively on the battlefield to show just what this form of electromagnetic (EM) energy can do in some military applications.

The U.S. Navy's well-publicized demonstrations in the Persian Gulf, starting in 2014 with the AN/SEQ-3 laser weapon system (also known as the XN-1 laser weapon system, or LaWS) aboard the USS Ponce, presented some of the possibilities for laser weapons for disabling smaller moving targets, such as missiles and armed unmanned aerial vehicles (UAVs). That laser system combined the outputs of a half-dozen fiber laser sources to produce an optical beam with 30-kW power, enough power to destroy an incoming missile or drone from a distance with great precision.

The U.S. Navy's enthusiasm for developing higher-power LaWS equipment is one sign of the success of those early demonstrations from the USS Ponce. Many military commanders are intrigued by the possibilities of a "rechargeable" weapons system that does not rely on reloading with a substance such as gunpowder, even though the technology is still in its earlier stages and may require some time before the seas, let alone the skies, are filled with laser beams like something in a scene from a sci-fi film. But a number of major contractors, including Lockheed Martin, Northrop Grumman, and Raytheon Co. are working to overcome the current limitations of these optical weapons, especially in terms of size, weight, and power (SWaP).

The major defense contractors are well aware of the challenges and are making major strides in bringing this technology to the everyday battlefield. Those science-fiction battle scenes may not be as far-fetched as they originally appeared on screen! de

Jack Browne, Technical Contributor

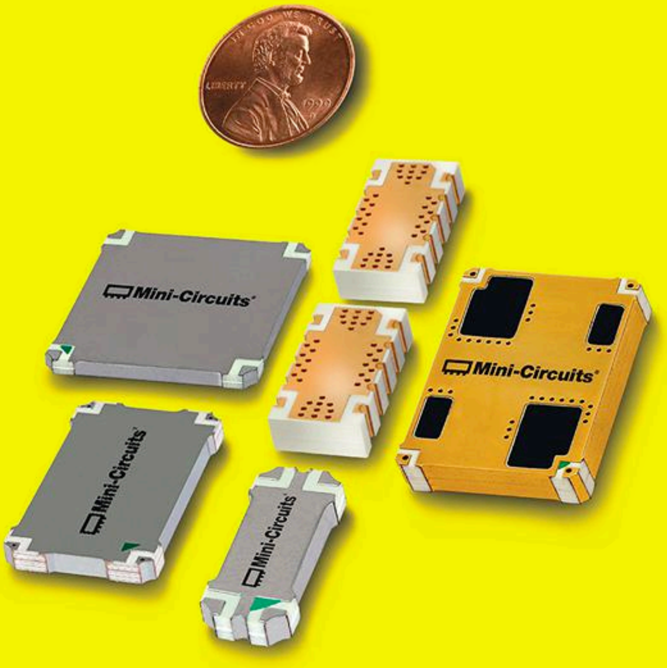
Mini-Circuits

COMSAT Teams with Iridium for Secure DoD Satcom Service

(Continued from page 49)

The Iridium Certus terminals are smaller than traditional satcom terminals, and the multiple-function satellite system will enable users to debut at transfer speeds of 352 kb/s, with upgrades available to 704 kb/s. "This is a new generation of technology that will keep users connected on-the-move, combining the robustness and reliability of the Iridium network with the value-added services and years of experience provided by COMSAT," says David Greenhill, president of COMSAT. "U.S. government users will experience a new level of mission-critical mobile capabilities thanks to this partnership. We're excited to bring this new service to them."

The Iridium network is designed to provide high-performance, secure communications no matter the operating conditions. It will allow government and military users to establish reliable communications anywhere on the globe in a cost-effective and secure manner, with connections to command and control centers in the U.S., even in Arctic and Antarctic regions.

"Iridium and the DoD have maintained a longstanding and collaborative partnership through our Enhanced Mobile Satellite Services (EMSS) contract, and we believe Iridium Certus complements this perfectly by bringing never-before-possible, mission-critical broadband capabilities to the warfighter," says Matt Desch, CEO, Iridium. "We're excited to partner with COMSAT, who brings innovation and a broad portfolio of capabilities to the table, and we look forward to working together for many years to come." de

Mercury's Memory Devices Bound for Airborne System

(Continued from page 49)

"Receiving this BuiltSECURE memory order from a prominent defense prime contract reaffirms Memory's leadership role in the design and manufacturing of commercial microelectronics in a highly secure and trusted environment," says Iain Mackie, vice president and general manager of Mercury's Microelectronics Secure Solutions group. "We are honored to provide long-term supply continuity of high-speed, SWaP-optimized memory devices enabling the success of our military forces in the harshest operating environments," adds Mackie. The hardware is manufactured in Mercury's Advanced Microelectronics Center (AMC), a secure Defense Microelectronics Activity (DMEA) trusted facility in Phoenix, Ariz. ■

Smart Mount Brings Satcom to ARC-210 Radios

ROCKWELL COLLINS *(www.rockwellcollins.com)* has developed a smart mount that will give ARC-210 networked communications airborne radio users added satellite communications (satcom) capabilities via the Iridium satellite network. By accessing the 66 low-earth-orbit (LEO) satellites in the Iridium network, users can achieve global communications coverage *(see figure)* in addition to the ARC-210 radio's standard capabilities.

The addition provides a significant improvement in the radio's capabilities with little or no downside: "The smart mount will be a low risk and cost-effective way to bring the added benefits of Iridium to the ARC-210 system, delivering reliable communications no matter where the mission is," says Troy Brunk, vice president and general manager, Communication, Navigation and Electronic Warfare Solutions for Rockwell Collins.

"Adding Iridium SATCOM to the ARC-210 leverages the Defense Information Systems Agency (DISA) secure gateway as well as the diverse and resilient Iridium NEXT constellation," says Ken Flowers, vice president of Government Solutions for Iridium. "Integration requires no modifications to the existing onboard radio and will enable reliable voice, data, and position location information anywhere on the planet." The smart mount, which was recently demonstrated to U.S. DoD representatives, extends the radio's basic line-of-sight (LOS) range to full global capabilities, using Iridium's satellites. ■

A smart mount adds satellite-based beyond line-of-sight (LOS) communications capabilities to ARC-210 VHF/UHF military radios. *(Courtesy of Rockwell Collins)*

Woven Webbings Hold Electronic Devices in Place

SPECIALIZED WOVEN fabrics can help wrap together numerous systems and circuits in aerospace and aviation applications, and long-time fabric developer Bally Ribbon Mills *(www.ballyribbon.com)* has developed a line of woven webbings especially for these types of applications. The fabrics include narrow two-dimensional (2D) and three-dimensional (3D) thermoset and thermoplastic fabrics as used in parachutes, flight suits, safety components, and air slides. The woven webbings, which are used in the International Space Station, can meet specific strength requirements for structure components in space and aviation systems.

Compared to materials based on steel and aluminum, these strong, lightweight webbings help reduce material costs and increase system safety levels. While the durable narrow woven fabrics are often fabricated into standard products, custom engineered products can be developed or special manufacturing processes modified to meet specific user requirements.

Advanced fabrics such as these allow for the integration of sensors and other electronic devices into the framework of commercial and military aircraft. *(Courtesy of Balley Ribbon Mills)*

The narrow woven fabrics, tapes, and webbing *(see figure)*, measuring 12 in. wide or less, are typically used in parachutes and many other commercial, military, and aviation applications. Advanced designs are developed based on enhanced weaving technologies and materials woven from high-performance fibers, such as Kevlar, Vectran, and Zylon. Woven 2D and 3D thermoset and thermoplastic polymer composite structures can be formed into net-shape structures by means of a multidimensional continuous weaving method.

The most recently developed fabrics include 2D and 3D Thermoplastic Composite Materials (TPCM) and narrow woven "E-WEBBINGS." TPCM fabric has been developed to provide localized reinforcement in molding/forming processes and offers excellent strength and shear resistance. The E-WEBBINGS materials were developed nominally for Internet of Things (IoT) sensors and devices targeted for commercial, personal, and military aircraft. The materials are constructed in such a way that allows for the integration of IoT sensors and other electronic devices into the fabrics. ■

Curtiss-Wright to Acquire Dresser-Rand Business

CURTISS-WRIGHT CORP. announced its intention to acquire the assets of the Dresser-Rand Government Business, a leading supplier of high-speed rotating components and equipment used in many U.S. Navy aircraft and sea vessels. Dresser-Rand is a business unit of Siemens Government Technologies, a wholly owned U.S. subsidiary of Siemens AG (located in Germany). The transaction will take place for $212.5 million in cash. The acquired unit will operate as part of the power segment of Curtiss-Wright *(www.curtisswright.com)*.

"The acquisition of Dresser-Rand's government business portfolio significantly expands our shipset content and increases our footprint on new U.S. Navy Nuclear vessels, establishes a prominent Curtiss-Wright presence at U.S. Navy shipyards, and provides an opportunity to grow our existing U.S. Navy aftermarket business," says David C. Adams, Chairman and CEO of Curtiss-Wright Corp. Dresser-Rand designs and produces high-speed rotating components and systems, including reciprocating compressors, steam turbines, and steam system valves. The hardware supports Nimitz-class and Ford-class aircraft carriers, Virginia-class and Columbia-class submarines, and most major U.S. Navy shipbuilding programs. ■

JACK BROWNE | Technical Contributor

Discovering ADCs and DACs for Defense Electronics Systems

As data converters gain more speed and bandwidth, it presents designers with new opportunities to take fresh looks at applications like radar and communications.

DEFENSE ELECTRONIC systems rely on both analog and digital signals and components. And often, in the middle of those systems, highly integrated converters are used to ease the coexistence of analog and digital signals. In spite of the sophistication of their signal-processing chores, analog-to-digital converters (ADCs) and digital-to-analog converters (DACs) are often taken for granted.

1. Analog-to-digital and digital to analog converters (ADCs and DACs) are complex ICs usually housed in multipin packages. *(Courtesy of Analog Devices)*

But finding the best ADCs and DACs for an application requires some familiarity with how they work and how performance is described in terms of key parameters. Fortunately, these components are available from a wide range of vendors in many shapes and sizes to serve defense electronics systems, from secure communications systems to surveillance and radar platforms.

An ADC uses sampling to make instantaneous measurements of an analog input signal over its voltage range, converting those measurements into digital words with resolution equal to the converter's number of bits. The sampling rate takes place at the frequency (or multiple of that frequency) of the clock oscillator used for timing the ADC. A DAC essentially does the opposite, converting digital input code into analog output signals.

The precision and stability of the clock oscillator are important factors in achieving accurate ADC and DAC performance. Both types of converters appear similar, as integrated circuits (ICs) typically supplied in miniature multipin housings *(Fig. 1)*.

ADCs and DACs have a number of performance parameters in common that allow comparisons of different units, including frequency range/bandwidth, sampling rate, and bit resolution. How well each type of component performs the task for which it is designed depends on how well it maintains the accuracy and integrity of the signals it must process throughout the signal/data-conversion processes. In any system, that accuracy will also be impacted by associated components in the signal chain, such as amplifiers and filters on either side of the converter.

For an ADC, its bandwidth is the frequency range of signals that can be measured at its input port. Wider bandwidths allow the capture of higher-frequency signals, although bandwidth is also usually synonymous with cost—ADC costs increase with wider bandwidths and higher frequencies. An ADC designed for use at audio frequencies, such as 20 Hz to 20 kHz, may be low in cost, depending upon other performance parameters, such as bit resolution, but it is also limited in bandwidth. Even in the audio range, a bandwidth of 100 kHz or more may be preferred to include the digitization of higher-order harmonic frequencies.

ADC frequency/bandwidth requirements for defense electronics systems must be carefully considered, so that enough of the input signal can pass from analog form to digital form. These systems range from surveillance and EW systems, where the nature of the signals to be processed may be relatively unknown, to communications systems that may employ advanced forms of frequency- and phase-based modulation schemes.

SAMPLES SIMPLIFIED

The minimum sampling rate for an ADC is usually determined by the frequency and bandwidth of the signals to be digitized and the number of channels to be digitized. Nyquist theory states that at least two samples are needed to represent the simplest waveforms, so the minimum sampling rate is at least two times the bandwidth of a signal of interest. More samples (a higher sampling rate) bring greater precision by means of a practice known as oversampling (exceeding the Nyquist frequency).

For example, when capturing enough samples on a continuous-wave (CW) signal to provide 90-deg. resolution, four samples per cycle would be needed to capture samples at 90, 180, 270, and 360 deg. per signal cycle. Pulses or more irregular signal waveforms may require more samples per cycle. While it may be true that a defense electronics system's ADCs will never be accused of capturing too many samples, too few samples per cycle of a signal frequency can result in aliasing errors and an inability to accurately reconstruct that signal into analog form.

The number of ADC samples per signal cycle depends on the allowable average error tolerance, the method of reconstruction of the waveform, and the end use of the sampled data. The actual error of discrete data samples will be impacted by the throughput error of the data acquisition and conversion system, along with any errors contributed by the system's computer or other digital-signal-processing devices. Increasing the number of samples per cycle for an ADC, or applying different forms of filtering in the system (including at the output of the DAC), can improve the accuracy of the sampled data.

Larger amounts of sampled data deliver increased accuracy when returning the data to analog form through a DAC, although with tradeoffs at the system level. Larger amounts of data require larger memory capacities and potentially slower computer processing speeds, typically resulting in larger size, weight, and power (SWaP) in a system. The faster sampling rates required to generate more data usually translate into higher levels of power consumption.

The number of ADC bits determines the resolution of the data-acquisition system. The number of bits defines the number of digital codes used to represent the original analog waveform. For example, an 8-b ADC uses 256 increments to represent the original analog waveform. A 10-b converter uses 1024 digital codes, while a 12-b converter uses 4096 digital codes.

All ADCs suffer some amount of aperture error, which refers to the amplitude and time errors of the sampled data points for a waveform due to the uncertainty of dynamic data changes during the sampling process. Using high-speed ADCs with fast sampling rates is one way to minimize aperture errors, and fast ADC data-conversion speeds are needed for sampling higher-frequency signals.

The least-significant bit (LSB) of the digital code used in the sampling process also plays a part in determining ADC accuracy, since the digital code produced by an ADC will have an inherent quantization error of ±0.5LSB. That means the analog voltage represented by the digital codes may actually be somewhere between adjacent digital codes. High-performance ADCs can control aperture error to less than ±0.5LSB.

CHANGING DEFENSE APPROACHES

Recent trends in ADCs and DACs for commercial and military applications have included wider bandwidths and faster sampling rates. This has allowed system designers to reevaluate their approaches to a particular platform.

Within communications and EW radios, for example, signal sampling has traditionally taken place at the radio's intermediate-frequency (IF) stage. Moreover, the availability of ADCs with limited bandwidths and sampling rates may have required the use of numerous different frequency-mixer IF stages to downconvert received signals within the input range of an ADC. But as ADCs (and DACs at the output of the receiver) gain in bandwidth and sampling rate, sampling can take place at higher IF, or in some cases, by direct sampling of RF signals.

Multiple suppliers offer ADCs and DACs with bandwidths in excess of 1 GHz qualified for use across the military operating-temperature range of −55 to +125°C. As an example, Texas Instruments *(www.ti.com)*, which acquired National Semiconductor and its considerable ADC/DAC portfolio, offers system designers its model ADC14155 ADC with 14-b resolution, sampling rates to 155 Msamples/s, and typical full-power bandwidth of 1.1 GHz for IF sampling. It is supplied in a 48-lead, thermally enhanced ceramic package and can be installed on an evaluation board *(Fig. 2)* for ease of testing. The company's WaveVision software provides computer control of the data converter.

At even higher frequencies and sampling rates, Texas Instruments' ADC12DJ3200 family of advanced CMOS ADCs enables direct conversion of RF/microwave input signals to 8 GHz and higher. For example, the 12-b model ADC12DJ3200 ADC can be used as a single- or dual-channel digitizer, with single-channel sampling rates to 6.4 Gsamples/s and dual-channel sampling

2. Evaluation boards can simplify the testing of high-speed ADCs like the 14-b model ADC14155, which operates at sampling rates to 155 Msamples/s and typical full-power bandwidth of 1.1 GHz for IF sampling. *(Courtesy of Texas Instruments)* rates to 3.2 Gsamples/s. With a full-power, 3-dB input bandwidth of 8 GHz and low noise floor for capturing low-level input signals, it is a candidate for receivers in applications from communications and EW to electronic intelligence (ELINT) and radar systems. It enables direct-sampling system designs at S- and C-band frequencies *(for more details on the ADC12DJ3200 ADC, see "High-Speed Converters Provide Direct Conversion at C-Band" at mwrf.com)*.

Analog Devices *(www.analog.com)*, with its advanced 28-nm silicon CMOS semiconductor technology, has also developed high-speed, high-resolution ADCs and DACs. These enable sampling and signal generation at higher frequencies in commercial wireless communications systems, such as fourth-generation (4G) Long Term Evolution (LTE) cellular communications systems and coming fifth-generation (5G) wireless networks, as well as high-performance military radar and communications systems. The highly integrated devices include the dual-channel AD9172, which is essentially two RF DACs on a chip *(Fig. 3)*. It is capable of 16-b resolution at sampling rates to 12.6 Gsamples/s for generation of high-resolution analog outputs to 8 GHz and beyond.

3. The AD9172 is essentially two DACs in one package, capable of 16-b resolution and sampling rates to 12.6 Gsamples/s. *(Courtesy of Analog Devices)*

Additional suppliers of high-speed ADCs and DACs for military applications include Cobham *(www.ams.aeroflex.com)*, DATEL *(www.datel.com)*, Mercury Systems *(www.mrcy.com)*, Microchip *(www.microchip.com)*, and Teledyne e2v *(www.e2v.com)*. Some, such as DATEL and Microchip, provide low-power packaged ICs at competitive prices.

Then there's Teledyne e2v, which sources its ADQ7DC, a complete ADC data-acquisition module with field-programmable gate array (FPGA) to simplify the chore of adding the digitizing function to a system. The module *(Fig. 4)* can be specified with one or two channels, 14-b resolution, and sampling rates to 10 Gsamples/s. The company also offers similarly compact modules with DACs for high-speed, low-latency signal generation to 7 GHz and as many as four signal channels per module. **de**

4. The model ADQ7DC is a complete ADC data-acquisition module with one or two channels, 14-b resolution, and sampling rates to 10 Gsamples/s. *(Courtesy of Teledyne e2v)*

JACK BROWNE | Technical Contributor

Arbitrary Waveform Generator Scales to 2 GHz

At frequencies reaching 2 GHz, this compact modular AWG can produce a variety of wideband output signals.

ARBITRARY WAVEFORM generators (AWGs), as the name suggests, offer the means of producing almost any type of signal waveform within the limits of their maximum sampling rate and bit resolution. The compact modular SDR14TX recently unveiled by Teledyne Signal Processing (SP) Devices *(www.spdevices.com)*, for example, is a dual-channel, 14-b AWG with a maximum sampling frequency to 2 Gsamples/s. It can create wideband dc-coupled signal waveforms in the first Nyquist frequency range to 1 GHz and direct synthesis of RF waveforms in the second Nyquist frequency range to 2 GHz.

The versatile AWG can be used in a wide range of commercial, industrial, and military systems, including LiDAR, radar, test systems, and wireless communications networks. Its 1 GB of onboard memory stores the code required to produce often-used signal waveforms.

The SDR14TX AWG, packed into a modular housing *(Figs. 1 and 2)*, includes a field-programmable gate array (FPGA) that is accessible to a user for programming. The dual-channel signal source operates at sampling frequencies to 2 GHz per channel with 14-b vertical resolution. The dual output enables transmission of two synchronized but independent waveforms.

There's also support for generation and transmission of complex in-phase/quadrature (I/Q) modulated signals for advanced communications applications. An advanced waveform sequencing engine enables flexible waveform generation, and the built-in zero generation feature makes it possible to generate "silent" output without wasting any memory.

Multiple units can be readily synchronized for multichannel applications—each AWG is packed with 1 GB of data memory for storing waveform data to simplify programming of multiple waveforms. Every SDR14TX comes with either PXIe or PCIe data interfaces for interconnection with external systems.

The 50-Ω ports of the AWG are matched to most high-frequency systems, with output voltages to 1 V p-p for single-ended outputs and 2 V p-p for differential outputs. Signal outputs achieve 3-dB bandwidths as wide as 1 GHz with power spectral density of −152 dBm/Hz for single-ended waveforms and −149 dBm/Hz for differential waveforms. The spurious-free dynamic range (SFDR) is 52 dBc for single-ended output signals and 63 dBc for differential output signals, with both levels measured at 100 MHz.

For complex signal generation, as required in many communications, radar, and electronic-warfare (EW) systems, modular AWG signal sources such as these are well-suited for programming and producing advanced waveforms as needed, without excessive power consumption. The AWG is designed for +12 V dc power and is rated for maximum power consumption of 40 W.

TELEDYNE SIGNAL Processing (SP) Devices Sweden AB, Teknikringen 6, SE-583 30 Linkoping, Sweden

1. The modular SDR14TX arbitrary waveform generator (AWG) operates at sampling rates to 2 Gsamples/s and synthesizes output signals in the first Nyquist zone to 1 GHz and in the second Nyquist zone to 2 GHz. *(Courtesy of Teledyne SP Devices)*

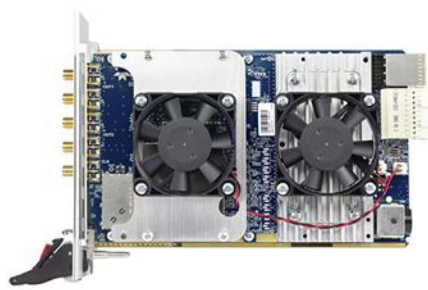

2. The compact, fan-cooled architecture of the SDR14TX AWG and its high sampling rates make it a candidate for signal generation in many different systems. *(Courtesy of Teledyne SP Devices)*

TEST CABLES up to 40 GHz!

Reliability You Can Trust... from $68.95 ea. (qty.1-9)

Why do 10,000 customers trust Mini-Circuits test cables? Because they simply don't fail! Our test cables have been performance qualified to 20,000 flexures* and come backed by our 6-month product guarantee**, so you can be confident you're getting rugged construction, reliability, and repeatable performance you can depend on. Whether you're performing production test, burn-in, over-temperature testing, hi-rel testing – you name it – chances are there's a Mini-Circuits test cable for your application in stock, ready for immediate shipment. Order some for your test setup at minicircuits.com today, and you'll quickly find that consistent long-term performance, less retesting and fewer false rejects really add up to bottom-line savings, test after test!

Model Family	Capabilities	Freq. (GHz)	Connectors†
KBL	Precision measurement, including phase, through 40 GHz	DC-40	2.92mm
CBL-75+	Precision 75Ω measurement for CATV and DOCSIS® 3.1	DC-18	N, F
CBL	All-purpose workhorse cables for highly-reliable, precision 50Ω measurement through 18 GHz	DC-18	SMA, N
APC	Crush resistant armored cable construction for production floors where heavy machinery is used	DC-18	N
ULC	Ultra-flexible construction, highly popular for lab and production test where tight bends are needed	DC-18	SMA, N
FLC	Flexible construction and wideband coverage for point to point radios, SatCom Systems through K-Band, and more!	DC-26	SMA, N
NEW! SLC	Super-flexible spaghetti cables with 0.047” diameter and 0.25” bend radius, ideal for enviromental test chambers.	DC-18	SMA
VNAC (M to F)	Precision VNA cables for test and measurement equipment through 40 GHz	DC-40	2.92mm

* All models except VNAC-2R1-K+

** Mini-Circuits will repair or replace your test cable at its option if the connector attachment fails within six months of shipment. This guarantee excludes cable or connector interface damage from misuse or abuse.

† Various connector options available upon request.

Contact apps@minicircuits.com to discuss your special requirements.

Mini-Circuits®

JACK BROWNE | Technical Contributor

Handling the Heat: Materials Make the Difference

Ever-smaller electronic systems with increasingly greater functionality depend on efficient thermal management to maintain performance and reliability.

THERMAL MANAGEMENT can be an important step in achieving a long operating lifetime for the circuits and devices in a defense electronics system. Active devices such as power transistors and laser diodes are never 100% efficient, which means some amount of power applied to these devices will be converted to heat. The lower the efficiency, the more heat is generated for a given amount of applied power.

To prevent damaging heat buildup around an active device, the heat must be dissipated into the surrounding environment or into the materials within a system. Different materials and structures can serve this purpose. However, with the current trend of designing greater functionality into smaller packages, DARPA and many other military organizations appear to be on a relentless quest for more effective heat-removing materials with outstanding thermal properties.

Part of the miniaturization push in military electronics involves increased use of active devices with high power densities, such as laser diodes and gallium-nitride-on-silicon-carbide (GaN-on-SiC) power transistors. While such devices are capable of high output power in terms of optical and electromagnetic (EM) signal energy, respectively, they are still less than 50% efficient. Therefore, a great deal of power-supply and input signal power will be converted to heat

Understanding the basic thermal properties of standard materials can ease the task of forming these thermal channels. For cooling purposes, one of the most essential material properties is thermal conductivity, or its capacity to conduct heat, which is measured in watts of power per meter per degree Kelvin (W/m-K). The inverse of thermal conductivity is thermal resistance. So, a material with good heat flow will have high thermal conductivity and low thermal resistance.

Copper is one of the more commonly used materials in electronic circuits with high thermal conductivity, about 400 W/m-K. Aluminum is another excellent thermal conductor, at about 235 W/m-K, often found in electronic circuits and systems. Of course, in electronic circuits, copper transmission lines (and thermal paths) are fabricated on dielectric substrate materials, such as polytetrafluoroethylene (PTFE) or various forms of ceramic materials that will have different values of thermal conductivity. The junction between different materials that must channel heat, such as copper lines on a ceramic substrate, is an area of concern not only for differences in the thermal conductivities of the materials, but in the way the materials respond to elevated temperatures.

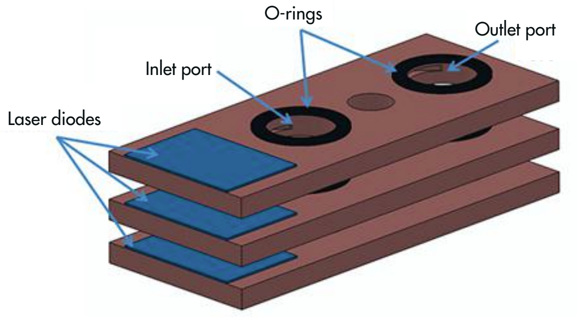

Microchannel coolers (MCCs) are structures with chambers for cooling liquids. Stacks of MCCs such as this can be used to cool multiple devices. *(Courtesy of Micro Cooling Concepts Inc., www.microcoolingconcepts.com)*

The coefficient of thermal expansion (CTE) is a key parameter that describes how much a material will increase in size as a function of temperature. For an effective thermal path, materials with high thermal conductivities are desired, as are materials with closely matched CTEs, to minimize stresses at the junctions of the materials when they expand with temperature.

Three-dimensional (3D) structures typically formed of thermally conductive metals or other materials are often used within circuits and systems to aid the flow of heat away from active devices. These structures include heatsinks, heatpipes, and miniature microchannel coolers (MCCs). MCCs *(see figure)* are structures that include channels for the flow of a cooling liquid, such as deionized water, to promote heat flow away from devices with high power density.

Military designers are faced with thermal-management challenges at all levels, from device through system, and the control of power and heat is essential for all branches as detailed by DARPA's Thermal Management Technologies (TMT) Program *(www.darpa.mil/program/thermal-management-technologies)*. It essentially seeks material advances, particularly on the nanostructure scale, to properly manage heat in present and future defense electronic systems. de

InGaP MMIC Mixer Converts 10 to 40 GHz

THE MDB-44H+ MMIC mixer leverages InGaP heterojunction-bipolar-transistor (HBT) semiconductor technology to cover a broadband frequency range. It can be used for frequency upconversion as well as downconversion, with an RF/LO frequency range of 10 to 40 GHz and an intermediate-frequency (IF) range of dc to 10 GHz. The Level 15 mixer works with a LO power level of +15 dBm. It achieves typical conversion loss of 8.0 dB when upconverting/downconverting signals from 10 to 20 GHz, 8.4 dB when translating signals from 20 to 30 GHz, and 8.9 dB when converting signals from 30 to 40 GHz. The typical 1-dB input compression point's power level is +10 dBm from 10 to 40 GHz with a typical input third-order intercept point (IP3) of +20 dBm from 10 to 20 GHz. The RoHS-compliant mixer is well-suited for commercial and military satellite and terrestrial communications radios and military radar systems. It is housed in a surface-mount MCLP package measuring just 3.0 × 3.0 × 0.89 mm.

MINI-CIRCUITS

P.O. Box 350166, Brooklyn, NY 11235-003; (718) 934-4500, www.minicircuits.com

180-deg. Hybrid Coupler Takes on Space to 26.5 GHz

THE MODEL 4010265SQ 180-deg. hybrid coupler is suitable for space applications from 1.0 to 26.5 GHz. It can be used for such functions as splitting and combining signals in amplifiers, switching circuits, and beamforming networks. The stripline 3-dB coupler has 3-dB insertion loss to 20 GHz and 3.6-dB or less loss to 26.5 GHz. It achieves better than 15-dB isolation between ports and is rated for 20 W average input power and 3 kW peak input power. The amplitude imbalance is controlled to ±1.0 dB to 20 GHz and within ±1.5 dB to 26.5 GHz. The phase imbalance is ±16 deg. across the frequency range. Maximum VSWR is 1.95:1. The coupler measures 4.04 × 1.35 × 0.52 in. with four female SMA connectors.

KRYTAR INC.

1288 Anvilwood Ave., Sunnyvale, CA 94089; (408) 734-5999, (877) 734-5999, e-mail: sales@krytar.com, www.krytar.com

GaN Amplifier Powers 9.0 to 9.9 GHz

THE BMPC9X89X8-8000 solid-state power amplifier (PA) builds upon GaN solid-state device technology to provide 8000 W pulsed output power across instantaneous bandwidths as wide as 500 MHz from 9.0 to 9.9 GHz for X-band radar applications. The Class AB PA provides 69-dB nominal power gain for pulse widths of 0.25 to 100 µs at duty cycles to 10% with better than 50 ns typical pulse rise/fall time. The amplifier features an internal ac power supply, female SMA connectors on the input and sample ports, and WR-112 or WR-90 rectangular waveguide flanges on the output ports. It holds harmonics to –60 dBc and phase noise to –100 dBc/Hz offset 100 Hz from the carrier. The PA, which is designed for 0 to +50ºC operating temperatures, includes an RJ-45 Ethernet control interface. It measures 19.00 × 12.25 × 24.00 in. and weighs 90 lbs.

COMTECH PST

105 Baylis Rd., Melville, NY 11747; (631) 777-8900, www.comtechpst.com

Up/Downconverter Takes On 2.7 GHz

THE CMX975 integrated-circuit (IC) frequency up/downconverter contains transmit and receive mixers, a low-noise amplifier (LNA), fractional-N and integer-N synthesizers for RF and IF functions, and voltage-controlled oscillators (VCOs). It an RF range of 1.0 to 2.7 GHz and an intermediate-frequency (IF) range of 10 to 500 MHz for use in L-band and S-band satellite communications (satcom) systems and military radios. The unit operates on a single +2.7- to +3.6-V dc supply, providing an 18-dB programmable gain range and 1.7-dB noise figure at 1.5 GHz. The operating temperature range is –40 to +85ºC.

CML MICROCIRCUITS LTD.

Oval Park, Langford, Maldon, Essex, CM9 6WG, England; +44 (0) 1621 875500, FAX: +44 (0) 1621 875600, E-mail: sales@cmlmicro.com, www.cmlmicro.com

Standard GaAs MMICs Can Qualify for Space

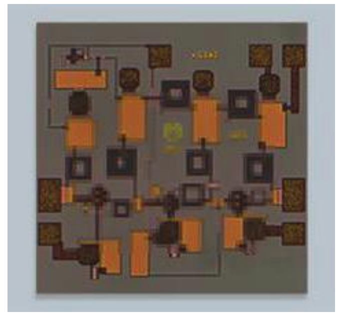

WHEN HIGH RELIABILITY for space-qualified system designs is essential, nearly 100% of a line of standard GaAs MMICs can be space-qualified per MIL-PRF-38534 Class K and MIL-PRF38535 Class S screening on die, hermetic packaged die, and hybrid assemblies. This type of screening includes visual inspection to MIL-STD-883 Method 2010B Class S, 100% element electrical RF test, and wafer lot qualification testing (per the requirements of MIL-PRF-38534 for MMIC devices). As an example of one of these parts, the CMD157 GaAs MMIC low-noise amplifier (LNA) is well-suited for wideband communications and electronic-warfare (EW) receivers, with more than 25-dB gain and only 1.5-dB noise figure. The 50-Ω matched device has a 1-dB compression point of +10 dBm.

CUSTOM MMIC

300 Apollo Dr., Chelmsford, MA 01824; (978) 467-4290, www.custommmic.com

Broadband LNA Quiets 8 to 18 GHz

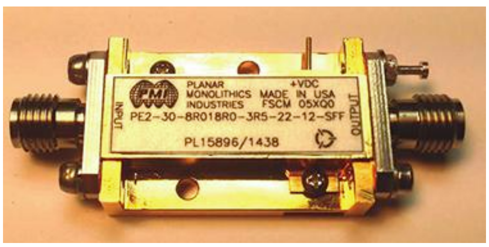

MODEL PE2-30-8R018RO-3R5-22-12-SFF—a broadband low-noise amplifier (LNA)—has a typical noise figure of 3.5 dB from 8 to 18 GHz. It also delivers 30-dB typical gain across that frequency range, with worst-case gain flatness of ±1.5 dB across the full operating frequency range. It provides+20 dBm output power at 1-dB compression while drawing no more than 325 mA current from a voltage supply of +12 to +15 V dc. The maximum input/output VSWR is 2.0:1. The amplifier comes with removable female SMA connectors in a standard PE2 housing.

PLANAR MONOLITHICS INDUSTRIES INC.

East Coast Operations, 7311-F Grove Rd., Frederick, MD 21704; (301) 662-5019, e-mail: sales@pmi-rf.com, www.pmi-rf.com.

Compact Amplifier Boosts 500 to 2800 MHz

THE TA1007 general-purpose amplifier provides 5 W output power from 500 to 2800 MHz and is well-equipped for wireless communications applications where small size and light weight are required. Based on GaAs technology, it delivers 39-dB typical gain and +37 dBm typical output power across its frequency range, with worst-case gain variation of 3 dB. The amplifier draws typical current of 1.9 A from a typical +12-V dc supply when operating in a 50-Ω system. The amplifier comes with high-speed on/off control as well as over-, under-, and reverse-voltage protection.

TRIAD RF SYSTEMS INC.

11 Harts Ln., Ste. 1, East Brunswick, NJ 08816; (855) 558-1001, e-mail: sales@triadrf.com, www.triadrf.com

Calibrated Sources Help Measure Noise

A LINE OF calibrated noise sources features 10 new models to provide the reference levels for noise measurements in frequency bands from 10 kHz to 18 GHz. The additions include excess-noise-ratio (ENR) levels from 15 to 30 dB with VSWRs as low as 1.25:1. The temperature coefficients are better than 0.01 dB/ºC and variations in output noise levels are held to less than 0.1 dB/%V. The noise sources feature 50-Ω hybrid circuit-board assemblies with packaged noise diodes and other discrete components tuned for optimum performance. The noise source assemblies are enclosed in rugged metal enclosures with SMA female connectors and, depending on the model, either solder pin or BNC female dc connector. All models are designed to meet MIL-STD-202F environmental requirements for humidity, shock, and vibration, and all models have EAR99 export classification.

FAIRVIEW MICROWAVE INC.

301 Leora Ln., Ste. 100, Lewisville, TX 75056; (800) 715-4396, (972) 649-6678, www.fairviewmicrowave.com

DC Blocking Dividers/Combiners Extend from 2 to 16 Ways

A SERIES OF DC blocking power dividers/combiners includes models in 2-, 3-, 4-, 6-, 8-, 12-, and 16-way configurations to serve a variety of signal combining and dividing requirements, such as receiver combining and antenna splitting in wireless communications networks. The dc blocking power dividers/combiners can be supplied with Type N, SMA, BNC, and TNC connectors covering frequencies from 0.8 to 2.2 GHz, with single broadband models covering 698 to 2700 MHz. The power dividers/combiners are made in the U.S. and come with a 36-month warranty.

MECA ELECTRONICS INC.

459 East Main St., Denville, NJ 07834; (866) 444-6322, (973) 625-0661, http://www.e-meca.com/power-divider-combiners/gps-dc-blocking-power-dividers

GaAs Schottky Doubler Extends to 80 GHz

THE MMD-3580L passive frequency doubler provides output signals from 35 to 80 GHz. The frequency doubler uses GaAs Schottky diodes fabricated with a GaAs MMIC process. It is available in the form of a bare die (model MMD-3580LCH) for wire-bonding and mounting on a PCB, as well as with coaxial connectors, like model MMD-3580LU-KW with 1-mm coaxial connectors. The doubler accepts input signals from 17.5 to 40 GHz input at maximum power levels of +7 to +11 dBm and operates with typical conversion loss of 12 dB. It can handle as much as +23 dBm power at any port and is designed for operating temperatures from –55 to +100ºC.

MARKI MICROWAVE INC.

215 Vineyard Ct., Morgan Hill, CA 95037; (408) 778-4200, www.markimicrowave.com

Low-Noise VCO Tunes 1,500 to 3,200 MHz

THE DCMO150318-5 is a compact, low-noise voltage-controlled oscillator (VCO) that tunes from 1,500 to 3,200 MHz with tuning voltages of +0.5 to +20.0 V dc. The surface-mountable VCO delivers +7 dBm output power when operating on a bias supply of +5 V dc and 30 mA. It has typical phase noise of –93 dBc/Hz offset 10 kHz from the carrier and –153 dBc/Hz offset 10 MHz from the carrier. Harmonics are typically –10 dBc. The oscillator, supplied in a miniature package measuring only 0.5 × 0.5 × 0.18 in., is well-suited for automated-assembly processes.

SYNERGY MICROWAVE CORP.

201 McLean Blvd., Paterson, NJ 07504; (973) 881-8800, www.synergymwave.com

Versatile SPDT Switch Handles 1 to 6000 MHz

THE BSW7221 single-pole, double-throw (SPDT) switch provides broadband signal control from 1 to 6000 MHz for both 50- and 75-Ω systems. It achieves 43-dB isolation across that wide frequency range, with low insertion loss of 0.49 dB. With switching speeds of 90 to 135 ns, the SPDT switch is well-suited for such applications as Wi-Fi, cable television (CATV), Internet of Things (IoT), and fifth-generation (5G) wireless communications networks. It is supplied in a six-lead UDFN package measuring 1.5 × 1.5 mm and operates on a single supply of +2.7 to +3.6 V dc.

BEREX INC.

3350 Scott Blvd., Ste. 6101, Santa Clara, CA 95054; (408) 452-5595, www.berex.com

Sector Antennas Span 2.2 to 5.0 GHz

RFMW LTD. now offers design and sales support for 4 × 4 MIMO/MANET sector antennas from Southwest Antennas, including the quad-polarized model 1009-036 (4.4 to 5.0 GHz) and dual-polarized model 1009-34 (2.2 to 2.5 GHz) antennas. Both antennas offer 12-dBi gain and handle 50 W RF power. Integral mounts offer 0 to 15 deg. of adjustable elevation downtilt in 2.5-deg. increments. The antennas incorporate Type N female connectors and are protected by a UV-stable Kydex radome. The antennas include hardware for mounting on 1- to 2-in.-diameter poles.

RFMW LTD., STOCKING DISTRIBUTOR FOR SOUTHWEST ANTENNAS

188 Martinvale Ln., San Jose, CA 95119; (408) 414-1450, e-mail: info@rfmw.com, www.rfmw.com

SIX TIPS FOR Developing Your Next Test System

RF/microwave test systems are each associated with specific circumstances, requirements, and challenges. Three universal factors come into play when defining any test system: performance, speed, and repeatability. Achieving the test system's required level of measurement integrity involves making tradeoffs between the three factors mentioned. In the application note "6 Hints for Enhancing Measurement Integrity in RF/Microwave Test Systems," Keysight Technologies discusses these tradeoffs and offers suggestions on how to address common problems.

The first hint that is presented is regarding the prioritization of performance, speed, and repeatability. The application note states that one or two of these will be the dominant factor that drives test requirements and equipment choices in most scenarios. Three tables are presented to show how each of the three factors mentioned affects the others.

Next, the importance of reviewing the nature and behavior of the device-under-test (DUT) is discussed. A typical automated test system performs the tasks of sourcing, measuring, and switching. Deciding which test instruments and cables to use depends on the electrical and mechanical attributes of the DUT. The application note emphasizes the need to avoid mismatches at connections, among other recommendations. Another point mentioned is the number and type of connectors for signals and power, as this has an impact on factors like the required size of switch matrices used in a test system and the complexity of system cabling.

Keysight Technologies, 1400 Fountaingrove Pky., Santa Rosa, CA 95403-1738; (800) 829-4444; www.keysight.com

Understanding, characterizing, and correcting RF signal paths are discussed next. The application note suggests that the calibration plane be as close as possible to the DUT. The next hint is about being aware of everything that is connected to an instrument, as everything between the instrument and the DUT can affect instrument performance and measurement repeatability. Three factors to take note of here are cables, switches, and signal conditioners.

The next topic concerns examining the operational attributes of switches. The operational attributes mentioned are device longevity, power requirements, and fail-safe operation. Lastly, the application note offers suggestions to accelerate measurement setup and execution time.

ENGINEERS RAISE THE BAR for Full-Screen Smartphones

FULL-SCREEN HANDSETS with edge-to-edge displays and screen aspect ratios of 18:9 are now being introduced by smartphone manufacturers. However, these features also come with their own set of RF-related challenges. Specifically, the space available for antennas is reduced, potentially causing problems like shorter battery life, connectivity issues, and lower data rates. In the white paper "Overcoming the RF Challenges of Full-Screen Smartphones," Qorvo explores the topic of enabling next-generation handset designs without sacrificing RF performance.

Smartphone manufacturers are transitioning to full-screen designs—i.e., displays that occupy nearly the entire face of the smartphone. Hence, less space is available for antennas, which must be located outside the area occupied by the screen. And with phones becoming narrower with the shift to 18:9 screen aspect ratios, antennas must be shorter. In addition, the number of antennas required in a smartphone is increasing, as more antennas are needed to deliver higher data rates using various approaches.

Reduced antenna area and length both can impact antenna performance. Specifically, reduced antenna area decreases antenna efficiency. Bandwidth is also reduced, making it more difficult to optimize efficiency at specific bands. The white paper notes the consequences of affected antenna performance, as potential problems include shorter battery life, poor connections, reduced operating range, and lower data rates.

Lower antenna efficiency and bandwidth affect key transmit (Tx) and receive (Rx) RF performance metrics like total radiated power (TRP) and Rx sensitivity. To compensate for these effects, increased performance is required throughout the Tx and Rx paths within the RF front end (RFFE). The white paper explains that integrated modules are important for achieving these performance improvements.

The white paper discusses approaches engineers can take to address full-screen design challenges. One of them is increasing TRP, which requires maximizing the performance of components in the Tx path. Such components include power amplifiers (PAs), filters, and antenna tuners. Increasing Rx sensitivity, which is another point mentioned, can be achieved by utilizing high-performance components like antenna-tuning solutions, low-loss filters and duplexers, and low-noise amplifiers (LNAs).

Qorvo Inc., 7628 Thorndike Rd., Greensboro, NC 27409; (336) 664-1233; www.qorvo.com

BARRY MANZ | Owner, Manz Communications Inc.

Over-the-Air TV Gets a Makeover

ATSC 3.0 isn't a tweak: It's a complete transformation that combines over-the-air content up to 4K UHD with streaming content from broadband, along with high-def audio, interactive features, and lots more.

The first Advanced Television Standards Committee (ATSC) standard for over-the-air (OTA) digital television broadcast (ATSC 1.0) was approved by the FCC in 1996. That was seven years after the World Wide Web was created, when only 0.04% of the world's population had internet access and cellular technology was in its second generation. It's obviously time for a change, and the new ATSC 3.0 provides just that—and then some. In fact, ATSC 3.0 is so much more advanced and comprehensive than its predecessor, it effectively makes OTA a true competitor to cable, fiber, satellite, and internet streaming for the first time.

With the vast majority of people receiving programming via cable, fiber, or subscription video-on-demand (SVOD) services like Netflix, Amazon, and Hulu, OTA probably seems archaic. However, the usage of OTA has actually increased about 4% per year in the last two years, mostly the result of cord-cutters supplementing their SVOD service with local content. The remainder of OTA users are mostly either people who cannot afford broadband or cable, are happy with what they get over the air, or simply don't watch TV. ATSC 3.0 should increase penetration even further, as it has some unique benefits.

Finalization of ATSC 3.0 effectively relegates ATSC 2.0 to telecom history—even Wikipedia devotes a paltry 73 words to the topic. The reason for the leapfrog from "1.0" to "3.0" is that even though ATSC 2.0 exists as a standard with full documentation, by the time it was finalized it was clear to the ATSC that additional capabilities would be required to keep OTA relevant in the future. Most of the features within ATSC 2.0 were "ported over" to ATSC 3.0, which is more comprehensive, requiring 20 standards and more than 1,000 pages of documentation.

ATSC 3.0 should serve the broadcast industry for a very long time, as it includes features previously available only via cable, fiber, or internet streaming, as well as some that aren't available from any other source. To provide such features, while also allowing the standard to accommodate enhancements in the future, ATSC 3.0 (unlike ATSC 2.0) is not backward-compatible with current ATSC 1.0 tuners.

To receive OTA channels, consumers will need new TVs, dedicated streaming boxes, external tuners, or a new type of appliance called a home gateway. The need to replace existing equipment was a major concern as the standard was being developed. Thus, last November, the FCC ordered broadcasters choosing to begin voluntary ATSC 3.0 transmission to simulcast ATSC 1.0 signals so that OTA viewers could retain service. The ATSC 1.0 simulcasts must offer similar programming to ATSC 3.0 channels for five years.

Based on the current pace of ATSC 3.0 rollouts, ATSC 3.0-enabled equipment, from TVs to home gateways and other ATSC 3.0 enablers, will be available a lot sooner than five years. In fact, at the Consumer Electronics Show (CES) in January—where with much fanfare the "ribbon cutting" for ATSC 3.0 formally took place—ATSC 3.0-capable TVs were announced by almost every manufacturer.

The drive to accelerate the pace was driven primarily by the South Korean government and its major manufacturers. LG Electronics introduced the world's first ATSC 3.0-capable 4K TV for the Korean market early last year with Samsung following shortly thereafter. The service is already available in Seoul and some other areas of the country from its leading terrestrial broadcasters, and the entire country should be covered by 2021. The 2018 Winter Olympics in PyeongChang showcased the country's accomplishments, as multiple events were broadcast OTA in 4K.

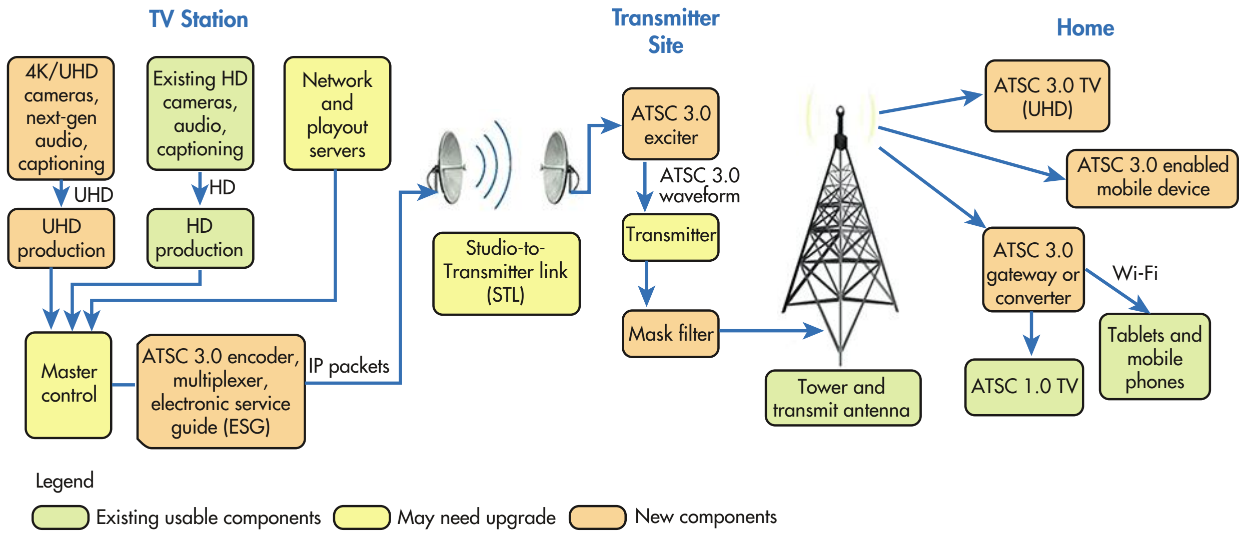

1. The ATSC 3.0 broadcast system as envisioned by the NAB shows the ability to use some existing broadcast equipment along with the new equipment that will be required. *(Source: NAB)*

In the U.S., the ATSC 3.0 rollout will take longer. However, it probably will not take as long as projected, as it is not the complete paradigm shift that 2009's analog-to-digital transition was. Sinclair Broadcast Group, the largest TV station operator in the U.S., and Korea's SK Telecom have signed a pact to build an ATSC 3.0 platform before this July.

The platform, called NG TV platform (for next generation), will deliver 4K content, customized IP-based interactive services, personalized and location-based advertising, fixed and mobile broadcast service, and emergency alerting. Sinclair's deployments and others should help speed the release of 4K content, which is currently mostly the domain of Blu-ray players, satellite providers DIRECTV and Dish, as well as Netflix, Amazon, and Comcast.

WHAT'S INSIDE ATSC 3.0

ATSC 3.0 is an IP-based technology that combines OTA signals (i.e., received from an antenna) with supplementary content delivered via broadband, thereby making it a hybrid system *(Fig. 1)*. The result is a combination of the interactive capabilities of streaming with the low cost of "one-to-many" OTA broadcast and the high image and audio quality of cable or satellite TV.

The ability to integrate internet-delivered content with that from OTA paves the way for finely-targeted advertising and two-way interactive services, as well as authenticated, tiered broadcast services. ATSC 3.0 supports legacy SD video resolutions up to 720 × 480, interlaced HD video resolutions up to 1,920 × 1,080, and progressive-scan video with resolution up to 3,840 × 2,160 and frame rates up to 120 fps, as well as digital watermarking of the audio signal and video signal.

In addition, ATSC 3.0 enables the long-awaited overhaul of the Emergency Alert System (EAS) via an Advanced Warning and Response Network (AWARN). Rather than a simple alert, it can deliver photos, surveillance video, storm tracks, evacuation routes, shelter instructions, hospital wait times, power outage locations, and other information. It can also "wake up" devices that are not powered on to deliver alerts.

Although TVs will soon be ATSC 3.0-compatible, the home gateway is also appealing. It performs multiple functions, combining OTA and internet-delivered content and sending it to a Wi-Fi router to stream devices throughout the home. As indoor reception is projected to be much better than with ATSC 1.0, many areas won't require an outdoor antenna. Instead, the antenna will be part of the home gateway. Greater signal strength is achieved by adaptable frequency capability that lets signals travel further and penetrate deeper into buildings and other RF-constrained places.

LG Electronics has been showing such a device called an "ATSC 3.0 Smart Antenna" at CES for the last three years *(Fig. 2)*. The module employs an electronically-steerable directional antenna and is very small, allowing it to be placed almost anywhere in a home. It integrates an ATSC 3.0 tuner-demodulator system-on-a-chip (SoC) and ATSC 1.0 analog tuner for backward compatibility. The National Association of Broadcasters (NAB) has developed its own gateway architecture through its PILOT initiative that has similar capabilities.

Although TVs will soon be ATSC 3.0-compatible, the home gateway is also appealing. It performs multiple functions, combining OTA and internet-delivered content and sending it to a Wi-Fi router to stream devices throughout the home. As indoor reception is projected to be much better than with ATSC 1.0, many areas won't require an outdoor antenna.

2. The LG Electronics ATSC 3.0 Smart Antenna combines the ability to receive OTA broadcast using an electronically-steerable antenna with an Ethernet interface to broadband to provide over-the-top content. An ATSC 1.0 tuner allows for backward compatibility. The combined signals are connected to a Wi-Fi router for distribution throughout a home. *(Source: LG Electronics)*

3. ATSC 3.0 enhances the concept of a digital dashboard by delivering audio, 4K video, text alerts, and other features to vehicle infotainment systems. *(Source: NAB)*

KEY TECHNOLOGIES

When the ATSC 1.0 standard was developed, it was based on the analog TV formula in which every channel was allocated 6 MHz of spectrum. This was enough bandwidth to deliver digital video at 19.39 Mb/s and to accommodate two HDTV and three SDTV channels. Now, in this same 6-MHz channel, ATSC 3.0 uses a more spectrally-efficient H.265 HEVC, (High Efficiency Video Coding) video compression technique rather than MPEG-2 used in ATSC 1.0. This makes it possible to transmit more video content with less data—it delivers 4K video in half the bandwidth of ATSC 1.0.

ATSC 3.0 also has better audio compression via Dolby AC-4 rather than the current Dolby AC-3 and supports viewing on ATSC-3.0-capable mobile devices as well as enhanced video capabilities from 3D to high dynamic range (HDR), high frame rate (HFR), and wide color gamut (WCG) technology currently available only via wired and satellite solutions. ATSC 3.0's mobile television support is enabled by its more robust signals, and the broadcast and automotive industries are working with developers to create an alternative to cellular-based delivery of everything from telematics and infotainment to diagnostics and emergency alerting *(Fig. 3)*.

COMING SOON(ER)

ATSC, NAB, and the broadcast industry have been working on upgrading the current standard for years. More than 12,000 patents have been issued to U.S., Korean, Japanese, and European companies. Although full deployment of ATSC 3.0 in the U.S. is still several years away, consumers considering upgrading to a 4K TV might be wise to delay that decision, as the benefits of ATSC 3.0 seem to be worth waiting for. It's likely that smartphones will incorporate it in the next two years, as well as vehicles. In short, OTA might seem as archaic as "rabbit ears," but the new standard not only rejuvenates it, but makes it both a complement to existing delivery systems and a new competitor as well. mw

IMS Plenary Session Speaker (Monday, 11 June 2018):

"The Hitchhiker's Guide To the Healthcare Galaxy: The Actions That Changed the Healthcare Landscape in America From 2017-2027"

Stephen K. Klasko, MD, MBA, President and CEO, Thomas Jefferson University and Jefferson Health

IMS Closing Session Speaker (Thursday, 14 June 2018):

"Extreme Platforms for Extreme Functionality"

Nader Engheta, PhD, H. Nedwill Ramsey Professor at the University of Pennsylvania

RFIC Plenary Session Speakers (Sunday, 10 June 2018):

"Compact Silicon Integrated mmWave Circuits: From Skepticism to 5G and Beyond"

Zachary J. Lemnios, Vice President, Science, Technology & Government Programs, IBM T.J. Watson Research Center

"The Road Ahead for Autonomous Cars – What's in for RFIC"

Lars Reger, Automotive Chief Technology Officer (CTO), Business Unit Automotive, NXP Semiconductors

IMBioC Opening Session Speaker (Thursday, 14 June 2018):

"Renal Denervation for Uncontrolled Hypertension: Complexity After Symplicity"

Dr. Nicholas J. Ruggiero II, MD

IMBioC Closing Session Speaker (Friday, 15 June 2018):

"Is There a Fundamental Law of Health and Disease?"

Dr. Chung-Kang Peng, Director of the Center for Dynamical Biomarkers at Beth Israel Deaconess Medical Center / Harvard Medical School (BIDMC/HMS)

EARLY BIRD REGISTRATION ENDS
14 MAY 2018

FOR MORE INFORMATION, VISIT WWW.IMS2018.ORG

PENNSYLVANIA CONVENTION CENTER • PHILADELPHIA, PENNSYLVANIA, USA

Exhibition Dates: 12–14 June 2018 • Symposium Dates: 10–15 June 2018

IEEE

Follow us on:

#IMS2018

MTT-S

JOHN DUNN | EM Technologist, AWR Group, NI
www.awrcorp.com

Dive into EM/Circuit Co-Simulation of a T/R Front-End Module and Actively-Scanned Array, Part 1

This article, part 1 of a two-part series, investigates the challenges associated with multi-technology circuit and EM simulation while also explaining how design software can address these challenges.

5G is poised to bring more integrated and sophisticated antenna and circuit modules to the modern defense and commercial electronics markets. For example, *Fig. 1* shows the type of antenna module that is now being prototyped by manufacturers like IBM and Ericsson.[1] This 28-GHz 5G antenna module is a 2.8 × 2.8 in, 8 × 8 patch array with 64-dual polarized elements and four monolithic microwave integrated circuits (MMICs) using a silicon-germanium (SiGe) process.

Other proposals in the design community use a combination of silicon and gallium-arsenide (GaAs)/gallium-nitride (GaN) technologies. The advantages of these types of modules are lower cost, smaller size, integration of multiple technologies, and ease of deployment.

This article, part 1 of a two-part series, examines today's multi-technology circuit and electromagnetic (EM) simulation challenges and the software tools that are needed to support the successful design of 5G products. Part 2 presents examples that illustrate the use of multi-technology in an EM simulation and EM/circuit co-simulation of an actively-scanned antenna array. Advanced technologies, such as parameterized 3D cells, shape pre-processing and simplification, 3D EM extraction, and in-situ measurements, are described.

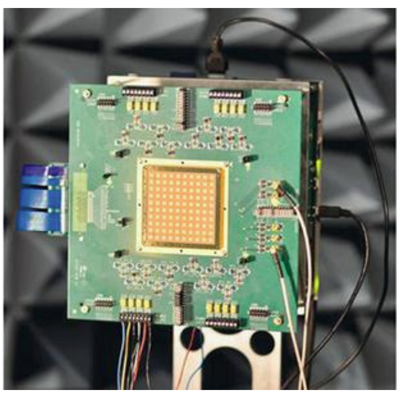

1. Shown is a 2.8-×-2.8 in. 28-GHz 5G antenna module with integration of multiple technologies.

MULTI-TECHNOLOGY CIRCUIT AND EM SIMULATION CHALLENGES

Designers of 5G products need RF/microwave software tools that enable them to work with multiple technologies integrated into one module, such as the dual-band transmit/receive (T/R) prototype module shown in *Fig. 2*. This wireless local area network (WLAN) module incorporates many different technologies integrated together, such as a GaAs power amplifier (PA), a SiGe PA (because much of the control electronics will be silicon), various surface-mount components, bulk-acoustic-wave (BAW)/surface-acoustic-wave (SAW) filters (very popular for mobile technology), and low-temperature co-fired ceramic (LTCC)/printed-circuit-board (PCB) technology with integrated passives. To support this type of design, the software design environment must overcome two big challenges.

DIFFERENT PHYSICAL TECHNOLOGIES

5G designers will need to use several different physical technologies (such as GaN, GaAs, ceramic, and silicon for the chips), as well as various board and module technologies (for example, low-loss organic materials for the boards and ceramics for the modules). The EM simulator must support these multiple technologies (commonly called multi-technologies) by being able to use multiple libraries or process design kits (PDKs).

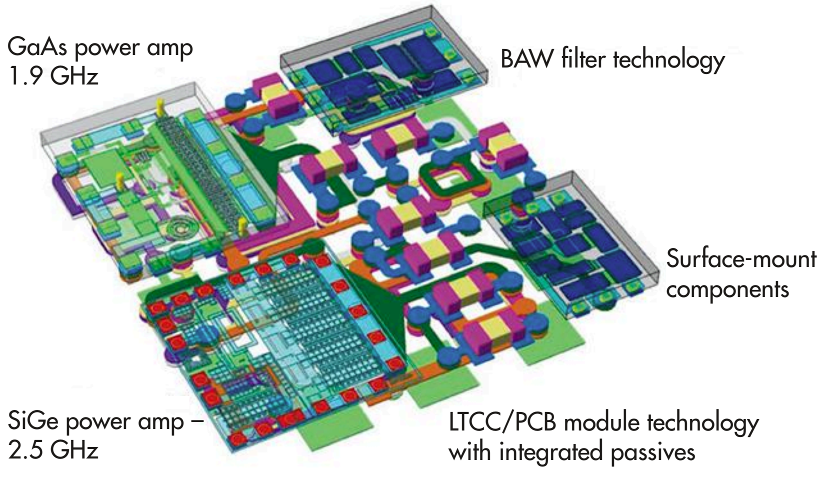

2. This figure illustrates a T/R dual-band WLAN module with many integrated technologies, which will connect to an antenna array.

These different technologies will exist in the same EM simulation if the geometry is a transition region between a chip and a module. The simulation environment must therefore support co-existence of libraries in the same project.

DIFFERENT EM AND CIRCUIT SIMULATORS

Different EM and circuit simulators will also be required, depending on the specific geometry and desired information. The software needs to support time-domain, frequency-domain, and more complex modulation-domain circuit simulators. In the time domain, SPICE-like simulators for SPICE-based models, silicon chips, and interconnect lumped parasitic nets will be needed.

Frequency domain (harmonic balance) will be needed for RF simulation of PAs and filters. Multi-technology designs will require a modulation domain for complex coding schemes, such as LTE, in which the carrier is deeply modulated and not periodic. Using simply SPICE or harmonic balance will not be sufficient, and designers are now moving towards more sophisticated hybrid simulation methods that the software will need to support.

Different EM simulation technologies are required, depending on the geometry being simulated. Planar EM simulators have higher capacity and speed for traditional planar-type layouts on PCBs and chips. For example, planar distributed filters, PA distribution manifolds, and interconnects on the board or chip are usually simulated with planar EM simulators. 3D simulators are required for transition regions between different technologies—for example, between a board and ball-grid array (BGA) module, or a module and a chip using bond wires.

MULTI-TECHNOLOGY DESIGN IN EM

EM is one of the bigger challenges in multi-technology design, mainly because more than one manufacturing technology is being used. For example, transitions between a chip on a board or a module and a chip involve multiple technologies. This requires two or more libraries (commonly called PDKs) for the various board, module, and chip technologies being used. Each library has a different stackup, artwork cells, and design rule checks (DRCs).

Using multiple libraries for different EM simulators also has complications because the stackup information can be different; material properties and ports and boundaries can be treated in different ways; and there are different simulation settings, such as solver accuracy and frequency ranges for each simulator. Drawing and layout creation is also a problem, since 3D and planar layouts typically have differences in their construction.

NI AWR Design Environment software offers a unique EM Socket tech-

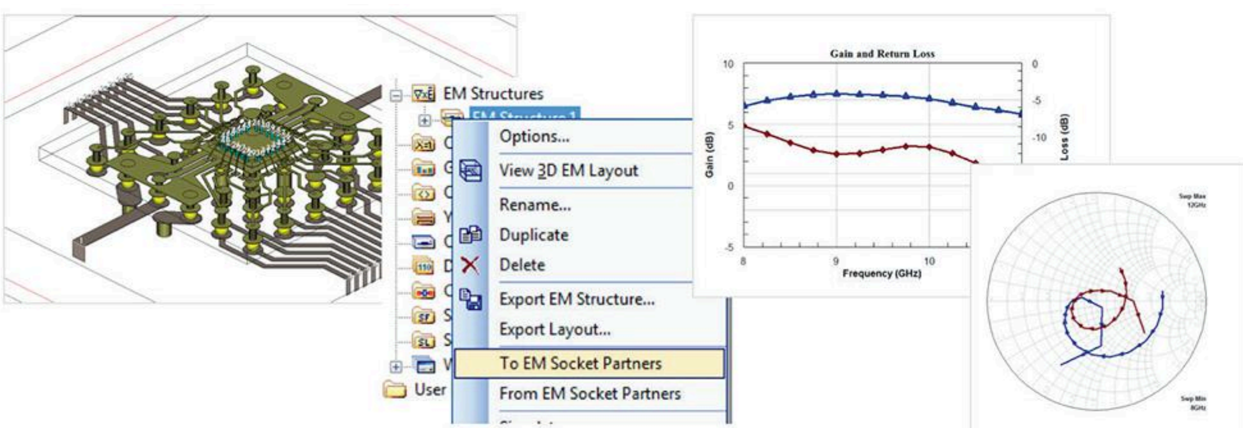

3. EM Socket allows users to take advantage of third-party EM tools. Shown here is AWR Connected for HFSS.

nology that provides one unified environment for controlling multiple EM simulators. These simulators include AXIEM planar and Analyst 3D finite-element method software, as well as third-party EM tools. *Figure 3* illustrates the AWR Connected for ANSYS HFSS that integrates HFSS with NI AWR software. Most of the layout is created in the AXIEM planar EM simulator shown on the left. HFSS is then selected as the EM simulator (middle). The resulting HFSS dataset is imported back into Microwave Office circuit design software to tune, optimize, perform yield analysis, and verify results *(right)*.

NI AWR Design Environment addresses the issue of using of both a 3D and a planar simulator in the same design by assuming chips, boards, and modules are essentially planar layouts with 3D "islands." While designers cannot draw 3D arbitrary shapes in a planar environment, they can import 3D shapes from a library of pre-drawn standard cells such as BGAs, bond wires, SMA connectors, and more.

A full 3D editor interfaces with the design environment if needed. Library (PDK) support for multiple technologies in NI AWR Design Environment is available for both the Microwave Office circuit simulator, where models from the different PDKs are used, and the EM simulators, where the artwork cells, materials, and stackup properties of the various PDKs are available.

4. Shown is a multi-technology layout of a MMIC in a QFN package on a Duroid PCB. Three technologies are employed.

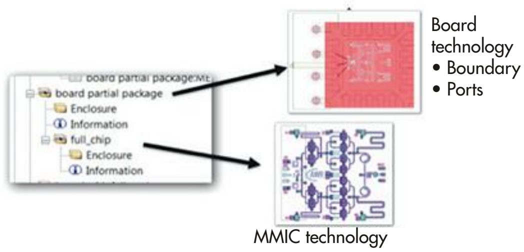

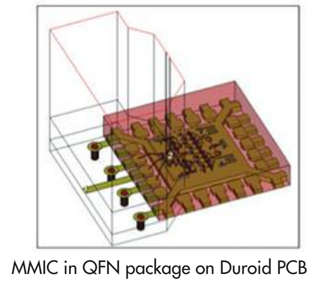

HIERARCHY TECHNOLOGY

Hierarchy technology is available within Microwave Office to enable and organize the use of multiple PDKs *(Fig. 4)*. Designers can use different technologies at the same time by assigning a technology to each layout cell. Different layouts/technologies can then be embedded within one another as cells and sub cells. Ports and boundaries are added at the highest level of hierarchy. The final layout is then flattened into a single layout and sent to the EM simulator. Clearly, a 3D EM simulator such as Analyst makes the most sense for multi-technology layouts.

CONCLUSION

Complex 5G and radar infrastructure requires the integration of antennas and circuitry. The challenge for EDA software is to support multiple technologies that require different circuit and EM simulators. Hierarchy at both the circuit simulation and EM level can be used to control multi-technology designs. Part 2 of this article will discuss EM/circuit co-simulation for antenna and circuit interactions, which can be modeled with in-situ simulation. mw

REFERENCES

1. *http://www.microwavejournal.com/articles/27830-ibm-and-ericsson-announce-5g-mmwave-phase-array-antenna-module*

Note: A video from EDI CON 2017 demonstrating EM/circuit co-simulation within NI AWR Design Environment is available for viewing at: *https://www.youtube.com/watch?v=F_48_RXQrvM&feature=youtu.be*

100W* POWER AMPLIFIERS

Now! 700 to 6000 MHz

Mini-Circuits' rugged, rack mount HPAs are perfect for your high power test applications such as EMI, reliability testing, and stress testing. Combined with our high-power, wideband splitters, they can be used to drive up to 80 test channels at once, saving you test time and cost in high-throughput test applications like burn-in, where parallel processing of many DUTs is a requirement. Now with two models spanning 700 to 6000 MHz with continuous 100W power across the band, you have a high-power workhorse for even more applications at a fraction of the cost of competitive products! They're available off the shelf, so place your order on minicircuits.com today for delivery as soon as tomorrow!

* @ Psat
** for HPA-272+; HPA-100W-63+ under test

FEATURES

- High Gain, up to 58 dB
- Excellent Flatness, ±2.0 dB or better
- High Reverse Isolation, 89 dB or better
- Operates on AC Line Power: 85-264V
- Internal Cooling
- Built-In Over-Temperature Protection
- Immunity to Open and Short Loads
- Life Test Qualified for 10,000 hrs at 100W Output**

Mini-Circuits®

www.minicircuits.com P.O. Box 350166, Brooklyn, NY 11235-0003 (718) 934-4500 sales@minicircuits.com

568 RevOrig

JACK BROWNE | Technical Contributor

Plug-In Sensor Measures Peak and Average Power to 8 GHz

With both Ethernet and USB ports, this peak power sensor and its easy-to-use software can transform a personal computer into a versatile measurement instrument with 8-GHz range.

The PWR-8P-RC smart power sensor has Ethernet and USB ports for connection to a PC running MS Windows-based software. Measurements of peak and average power levels for pulse-modulated and CW signals are possible from –60 to +20 dBm ranging from 10 MHz to 8 GHz.

RF/microwave power measurements at one time suggested the need for a power meter and separate power sensor built for the frequency and power measurement ranges of interest. But with the PWR-8P-RC smart power sensor from Mini-Circuits, a PC, and Microsoft Windows-based measurement software downloadable from the Mini-Circuits website, a compact power-measurement instrument can be assembled with frequency range of 10 MHz to 8 GHz. The instrument would also have power measurement range of –60 to +20 dBm for both pulse-modulated and continuous-wave (CW) peak and average power levels.

The smart power sensor includes both Ethernet (RJ45 receptacle) and USB interfaces for connection to a PC. It includes trigger in and out ports for synchronization with external test equipment, and provides a video output (dc to 10 MHz) for use with systems requiring an automatic-level-control (ALC) connection. The PWR-8P-RC *(see figure)* is well-suited for profiling CW signals, remote power monitoring of communications signals, and measurement of short pulsed waveforms, such as radar pulses. Under USB control, the power sensor's current consumption is typically 400 mA, while under Ethernet control, current consumption is typically 540 mA.

The smart power sensor is capable of measuring pulses typically as short as 5 μs with duty cycles down to 0.001%. Combined with its easy-to-use software, the power sensor can capture the power levels of a wide range of input signals, and then graphically depict CW power levels and an assortment of pulsed signal parameters, including peak power, rise and fall times, crest factor, and pulse width.

The PWR-8P-RC is able to measure power for signal events across a capture period of 0.01 to 2.5 ms, applying a sampling rate of 2 μs. For reduced sampling rates, it can extend the capture period to as long as 1000 ms. The sensor offers a maximum pulse profiling bandwidth of 100 kHz.

The smart power sensor can be used for measurements at operating temperatures from 0 to +50°C. It provides measurement resolution of 0.01 dB and exhibits a worst-case VSWR of 1.25:1 and typical VSWR of 1.15:1. It offers excellent measurement accuracy across its frequency and power measurement ranges. At room temperature (+25°C), across its full power measurement and frequency ranges, the typical measurement accuracy is ±0.10 dB.

For the extended operating temperature range of 0 to +50°C, when measuring the lowest power levels (–55 to –50 dBm), the typical power measurement accuracy across the full frequency range is ±0.35 dB or better. For that same temperature range, when measuring power levels from –50 to 0 dBm across the full frequency range, the power measurement accuracy is typically ±0.15 dB or better. For measurements of the highest power levels (0 to +20 dBm) across all frequencies at operating temperatures of 0 to +50°C, the typical power measurement accuracy is ±0.10 dB.

Full software for the power sensor can be downloaded from the Mini-Circuits website, including the Windows-based graphical user interface (GUI) with its extensive pulse-profiling features and a full application programming interface (API) with instructions for Windows and Linux 32- and 64-b environments. The power sensor includes a 6.8-ft.-long USB cable and female Type N to male SMA adapter as accessories. The smart power sensor measures 4.85 × 2.50 × 1.20 in. (123.1 × 63.5 × 30.5 mm) with a Type N connector. P&A: $1,895.00; stock. mw

MINI-CIRCUITS, P. O. Box 35166, Brooklyn, NY 11235-0003; (718) 934-4500, www.minicircuits.com.

Interview

CHRIS DeMARTINO | Technology Editor

Can S-SIX Technology Make Full-Duplex Communication a Reality?

In this Q&A, Sriram Vishwanath, co-founder of GenXComm, talks about the self-interference cancellation technology his company has developed and the benefits it offers.

Can you tell us about simultaneous self-interference cancellation (S-SIX) technology?

S-SIX is designed to enable wideband (around 1 GHz), low noise figure, tunable self-interference cancellation in both the analog and digital domains. It has traditionally been very difficult to achieve such wide bandwidths, tunability, and low noise figures for analog/RF systems. S-SIX is uniquely capable of achieving this, thus allowing for the design of good interference-cancellation systems.

Interference-cancellation systems that do not possess these characteristics may remove interference, but in doing so, introduce considerable noise. This can drastically impact the link budget, causing the system performance to be poor. Moreover, without wideband tunability, a new component would be required for any changes, giving the system no agility and reconfigurability. S-SIX offers it all in one: a solution that works across bands, with a noise figure that does not impact the link budget while eliminating interference.

What are some of the benefits of this technology? Furthermore, what applications will it enable?

The most obvious benefit of S-SIX is full-duplex communication, but there are many other benefits. By cancelling interference in a wideband manner, the solution is also a tunable filter that can eliminate interference in adjacent and/or overlapping bands. This results in multi-channel/multi-band radios that can operate in adjacent bands (without a guard band) simultaneously, without leakage into one another.

It also results in much better range extenders, mesh networks, and other ways in which radios can operate in two or more bands simultaneously. Further, it results in radios that can coexist on a multi-RAT platform. This includes LTE and Wi-Fi coexistence, as well as LAA/Wi-Fi coexistence.

GenXComm *(www.genxcomm.com)* has already publicly demonstrated its technology. Can you talk about what you found?

We found a genuine interest in full duplex across market segments and communities. The notion that we waste half the spectrum and can use it using S-SIX is immediately obvious across these segments. In one public demonstration, we turned our cancellation off and on, and the rapid change in performance made the impact of full duplex much more real to the audience. These demonstrations also help dispel some misconceptions about S-SIX: that it is only good for full duplex—and even then, [that] it just works in a lab environment. Self-interference cancellation does much more than full duplex (as listed in the question above), and it does work robustly indoors and outdoors.

The company recently announced the initial closing of a $9 million Series A investment round. Can you tell us more about that, as well as what we can expect to hear in the future?

The company recently closed a total $9 million in Series A ($7 million first close and a $2 million second close). We raised our Series A with a focus on delivering products to make our motto "Life without Interference" a reality across market segments. We are actively hiring—please spread the word!

We are planning to announce new partnerships and demonstrate our next-generation product in 2018. This is going to be an exciting, action-packed year for GenXComm. mw

MICHAEL SCHEFTER | Chief Scientist, Norsat International
www.norsat.com

What Makes Ka-band Systems Tick?

Ka-band satellites have arrived after more than two decades of trials, testing, and small commercial attempts. Their designs still bring up some important issues, though.

Although Ka-band satellites have been around for more than 20 years, many early versions did not have commercial services. However, over the last few years, more commercial Ka-band satellites have been launched into space with powerful narrow beams that provide huge throughputs. *Table 1* depicts the commercial Ku and Ka frequency bands.

Currently, Ka-band equipment is more expensive due to the high cost of Ka-band microwave power components and the higher accuracies required for waveguides, antennas, and antenna superstructures. Volume manufacturing has started to reduce this cost, making some low-power systems more affordable.

However, Ka-band does present some challenges, many of which can be mitigated by new high throughput satellites (HTSs) or with the proper design of the ground equipment. This article will look at the system impact of channel properties, including propagation and rain degradation.

TABLE 1: SUMMARY OF KA AND KU UPLINK AND DOWNLINK FREQUENCIES

	Ku-band	Ka-band
Earth to space (uplink)	13.75 – 14.5 GHz	29 – 30 GHz or 29.5 - 30 GHz
Space to earth (downlink)	10.7 – 12.75 GHz usually in 500 or 750-MHz bands	17.2 – 20.2 GHz in 1-GHz bands
Polarization	Linear orthogonal	Circular orthogonal

SATELLITE LINK DESIGN

Simply due to physics, Ku- and Ka-band systems perform differently in terms of propagation loss, rain attenuation, increased noise during rain, low-noise-block-downcoverter (LNB) noise figure (NF), and antenna gains. Some of these differences cancel each other out, while others are mitigated with satellite design, earth station design, and/or link parameters.

The actual satellite design is beyond the control of most satellite-communication link designs. The design of a satellite-communication link is based on a link budget. The link budget defines the transmit effective isotropic radiated power (EIRP) and receive gain-to-noise-temperature (G/T) required to close a link, given design parameters such as availability, data rates, modulation, coding, antenna sizes, block-upconverter (BUC) power, and LNB performance. These parameters affect cost, service-level agreements (SLAs), throughput, and bandwidth requirements, among others. Tradeoffs can be made with various parameters to tailor a solution for a given application.

The following sections present a comparative link budget for discussion. Several properties of the link budget are discussed relative to system performance, including propagation loss, rain attenuation, and the increase in noise due to rain.

COMPARATIVE LINK BUDGET

One comparison of Ku- and Ka-band system performance is provided in *Table 2*, which offers a pseudo real-world example of Ku- and Ka-band link budgets. This link budget is representative of an inbound transmission in which a 1-meter antenna transmits toward a large hub. In this example, the satellite has both Ku- and Ka-band spot beams. These satellite parameters are representative; changes to these parameters can greatly influence system performance. In this example, the overall link availability is 99.5%. The transmit and receive earth stations are co-located in an International Telecommunications Union Rain Region K. The link budgets were prepared using the Satmaster Software.[1]

Typically, link budgets assume that only one of the uplink or downlink links are affected by rain. The worst case is usually assumed. In the example link budget in Table 2, the overall $E_b/(N_o+I_o)$ is based on an uplink affected by rain, while the rain degradations on the downlink are included for further discussion.

TABLE 2: COMPARISON OF KU AND KA LINK BUDGETS				
	Ku-Band 1 m to Hub Inbound		Ka-Band 1 m to Hub Inbound	
	Clear sky	Rain	Clear sky	Rain
Uplink				
Transmit EIRP	46.18 dBW	49.65 dBW	46.22 dBW	56.20 dBW
Free space loss	207.45	207.45 dB	213.49 dB	213.49 dB
Atmospheric absorption	0.22 dB	0.38 dB	0.38 dB	0.80 dB
Scintillation	0.00 dB	0.49 dB	0.00 dB	0.37 dB
Cloud	0.00 dB	1.15 dB	0.00 dB	2.68 dB
Rain	0.00 dB	2.71 dB	0.00 dB	8.06 dB
Total degradation	0.22 dB	4.27 dB	0.38 dB	11.54 dB
Satellite G/T	6 dB/K		13 dB/K	
$E_b/(N_0+I_0)$	6.75 dB	6.79 dB	6.71 dB	6.82 dB
Downlink				
Satellite EIRP	52 dBW		64 dBW	
Free space loss	205.93 dB	205.93 dB	209.91 dB	209.91 dB
Atmospheric absorption	0.18 dB	0.28 dB	0.34 dB	0.77 dB
Scintillation	0.00 dB	0.39 dB	0.00 dB	0.23 dB
Cloud	0.00 dB	0.81 dB	0.00 dB	1.22 dB
Rain	0.00 dB	1.74 dB	0.00 dB	3.71 dB
Total degradation	0.18 dB	2.86 dB	0.34 dB	5.71 dB
Noise increase due to precipitation	0.00 dB	2.90 dB	0.00 dB	2.96 dB
Receive G/T	31.00 dB	28.10 dB	33.58 dB	30.63 dB
$E_b/(N_0+I_0)$	6.87 dB	8.46 dB	6.92 dB	15.18 dB
Overall				
$E_b/(N_0+I_0)$	3.80 dB	3.80 dB	3.80 dB	3.80 dB

PROPAGATION LOSSES

A geostationary satellite is located about 36,000 kilometers above the equator, creating a huge propagation loss from the earth station to the satellite. For the earth-to-space link, the propagation loss is about 6 dB worse for Ka-band than for Ku-band. For the space-to-earth link, the propagation loss is about 4 dB worse.

Free-space loss is proportional to the square of the signal wavelength. Antenna gain is also proportional to the square of the signal wavelength. Thus, all other parameters being equal, the increased gain of the transmit and receive earth antennas at Ka-band compensates for this increased free-space loss. In the link-budget example in Table 2, the antenna efficiencies are not the same; Ka-band is assumed to be slightly less efficient as is typical in practice.

Since the gain of the antenna at Ka-band is higher than at Ku-band, smaller antennas are often used. Requirements for a smaller antenna can be the result of application-related size constraints (i.e., COTM applications), portability requirements, or simply cost. For transmitting, a Ka-band antenna, which is half the diameter of a Ku-band antenna, will provide about the same gain as the Ku-band antenna. For receiving, a Ka-band antenna that is about 65% of the size of a Ku-band antenna will deliver similar gain as the Ku-band antenna.

SIGNAL DEGRADATION DUE TO RAIN

Over the years, there have been many studies on rain degradation at Ka-band. Simply put, signal degradation due to rain is much more pronounced at Ka-band than at Ku-band for a given link availability requirement, elevation angle of antenna, and rain region.

In Table 2, the link budget for each of the uplinks and downlinks were specified to have a link availability of 99.75%; the rain region for both transmit and receive earth stations was Rain Region K. The signal degradation would be less in drier environments and in applications where the link availability can be reduced. Conversely, rain degradation will increase in wetter environments, or in cases where the link availability requirement is higher.

On the receive side, the system performance is determined by the G/T, which includes the receive antenna gain (G) and the system noise temperature (T). The system noise temperature includes contributions from antenna noise temperature and the LNB noise temperature or NF.

In Table 2, the signal degradation in the Ku-band uplink due to rain is about 4.3 dB. For Ka-band, the uplink signal degradation is about 11.5 dB. For Ku-band, the downlink signal degradation due to rain is about 2.9 dB; for Ka-band, it is about 5.7 dB.

As noted earlier, overall performance is usually based on the worst-case scenario of uplink or downlink degradation. This is because it is assumed that it will not be raining at both the uplink and downlink sites at the same time. Of course, in the above example, it would be raining at both the uplink and downlink sites, as they are co-located. The link budget was calculated using only the worst-case link, which in this case, is the uplink.

INCREASE IN NOISE DUE TO RAIN

In addition to signal attenuation due to rain-related phenomena, the noise seen at the receive antenna increases during rain events. In Table 2, we see the noise increase by almost 3 dB for both Ku- and Ka-band. The atmospheric noise temperature due to rain is independent of frequency and is proportional to the signal attenuation.[2] The effect of the rise in noise temperature on link performance is a degraded G/T. The link performance is degraded not only by the attenuation of the received signal, but also due to increased noise temperature.

Note that in the link budget, it was assumed that only the uplink was affected by rain. Therefore, overall $E_b/(N_o+I_o)$ does not include this increase in noise.

EIRP PERFORMANCE

The transmit EIRP calculated in the link budget is the EIRP required to close the link based on the satellite performance and the design parameters of link availability, coding and modulation, and receive antenna. EIRP is calculated as the BUC transmit power in dBW plus the antenna gain in dBi. Using smaller antennas mean using larger BUCs for the same EIRP. Small antennas with large BUCs may exceed the regulatory off-axis EIRP requirements.

The required system EIRP varies considerably between clear sky and rain fade. In Table 2, the difference between the EIRP required for clear sky and rain fade is about 3.5 dB for a Ku-band system and 10 dB for a Ka-band system. This means for a given antenna size, the BUC power for clear sky is less than half of that required for rain conditions.

For the Ka-band system, the BUC power required at clear sky is about one-tenth of that required for a faded condition. Designing for faded conditions would require a much larger BUC. For example, in Table 2, an 8-W BUC is required for the Ka-band faded condition. In contrast, the same link performance can be achieved in clear sky with less than 1 W. A drawback of using a larger BUC is that without uplink power control (ULPC), the link may use a larger percentage of the satellite transponder power than the percentage of transponder bandwidth. Thus, the user would need to pay for this power-equivalent bandwidth, resulting in increasing operating costs.

RECEIVE G/T

On the receive side, the system performance is determined by the G/T, which includes the receive antenna gain (G) and the system noise temperature (T). The system noise temperature includes contributions from antenna noise temperature and the LNB noise temperature or NF. A "good" Ku-band LNB has a NF of about 0.7 dB. For Ka-band, it would need to have a NF of about 1.3 dB to be considered "good." Typical LNB NFs at Ku-band are 0.7 to 0.8. At Ka-band, they are typically 1.3 to 1.6 dB.

For the same size antenna, antenna noise temperature is higher at Ka-band. The additional gain of the antenna means G/T for the same size antenna is usually better than the Ku-band antenna despite the higher NF and antenna noise. *Table 3* compares the clear sky G/T between Ku- and Ka-band systems.

TABLE 3: COMPARISON OF CLEAR SKY G/T FOR KU- AND KA-BAND

	Ku-Band	Ka-Band
1-m antenna receive gain	40.1 dBi	44.1 dBi
Tant (at 20-deg. elevation)	46 K	80 K
LNB NF	0.7 dB	1.3 dB
G/T	19.6 dB/K	20.8 dB/K

The Ka-band G/T in clear sky is 1.2 dB better. This result implies that if the Ku- and Ka-band signal at the receive antenna are the same, the Ka-band system $E_b/(N_o+I_o)$ would be 1.2 dB better. This margin could be used to increase throughput by almost 33% at the expense of bandwidth. More throughput in the same bandwidth could also be

6-GHz Absorptive SPDT Switch Has USB, I2C, and SPI Control

Mini-Circuits' model U2C-1SP2T-63VH is a high-isolation absorptive single-pole, double-throw (SPDT) switch with USB, I^2C, and SPI control interfaces. It features high port-to-port isolation and low insertion loss from 10 to 6000 MHz and is well suited for large-volume, production testing. As many as 30 units can be connected in serial under SPI control, while as many as 8 units can be connected under I^2C parallel control. The 50-Ω component hot switches input levels to 2 W and has typical switching speed of 700 ns. Insertion loss ranges from 3.2 dB at 700 MHz to 5.0 dB at 6000 MHz. Typical isolation between ports is 110 dB from 10 through 5000 MHz and 105 dB from 5000 to 6000 MHz. The RoHS-compliant SPDT switch measures 3.0 × 2.0 × 0.47 in. with SMA female connectors. A user-friendly GUI for Windows and programming support can be downloaded free of charge from the Mini-Circuits' website.

75-Ω Power Splitter/Combiner Goes 16 Ways to 2700 MHz

Mini-Circuits' model ZB16PD-272-75F+ is a 16-way, 0-deg. 75-Ω power splitter/combiner for use from 695 to 2700 MHz, in such applications as cable-television (CATV) and WiMAX systems. It handles as much as 5 W input power as a splitter and features low insertion loss of typically 1.2 dB or less across the full frequency band and high isolation of typically 24 dB from 695 to 2450 MHz and 20 dB from 2450 to 2700 MHz. The full-band phase unbalance is typically 5 deg. while the typical amplitude unbalance is 0.5 dB across the full frequency range. The RoHS-compliant power splitter/combiner is supplied with F-type connectors and has an operating temperature range of -55 to +100°C.

Coaxial Amplifier Combines Low Noise, Flat Gain from 0.1 to 20 GHz

Mini-Circuits' model ZVA-213UWX+ is an ultrawideband amplifier in a coaxial package with wide dynamic range from 0.1 to 20.0 GHz. It has typical gain of 14 dB from 0.1 to 18.0 GHz and 13 dB from 18 to 20 GHz, with typical noise figure of 3.5 dB from 0.1 to 6.0 GHz, 2.5 dB from 6.0 to 12.0 GHz, 2.7 dB from 12.0 to 18.0 GHz, and 3.4 dB from 18.0 to 20.0 GHz. The typical output power at 1-dB compression ranges from +16 dBm from 0.1 to 6.0 GHz to +13 dBm from 18 to 20 GHz, while the typical output third-order intercept point (IP3) ranges from +29.5 dBm for 0.1 to 6.0 GHz to +26 dBm for 18.0 to 20.0 GHz. The RoHS-compliant, 50-Ω amplifier is well suited for C-band satcom, S-band radar, WLAN, and Wi-Fi systems. It measures 1.30 × 0.98 × 0.56 in. (33.02 × 24.89 × 29.46 mm) with 2.92-mm coaxial connectors.

Rugged Amplifier Drives 100 W from 2.5 to 6.0 GHz

Mini-Circuits' model ZHL-100W-63+ Class AB high-power amplifier delivers 100 W saturated output power from 2.5 to 6.0 GHz for communications, radar, and other broadband applications. It provides 58-dB typical gain over that frequency range with ±2 dB typical gain flatness. The rugged amplifier has built-in self-protection against overheating and reverse polarity and can even deliver as much as 50 W output power while surviving short- and open-circuit conditions at the output port. It draws typical supply current of 8 A from a 30-V DC supply. The compact, RoHS-compliant power amplifier measures 6.0 x 9.1 x 1.2 in. with SMA connectors and is available with optional heat sink and fan attachment for cooling.

Coaxial Low-Noise Amplifier Quiets 0.5 to 8.0 GHz

Mini-Circuits' model ZX60-83LN12+ is a broadband low-noise amplifier (LNA) in a coaxial package for applications from 0.5 to 8.0 GHz. It features typical noise figure of 1.6 dB at 0.5 GHz, 1.4 dB at 2.0 GHz, 1.5 dB at 4.0 GHz, and 2.3 dB at 8.0 GHz, with typical gain of 22.1 dB at 0.5 GHz, 22.1 dB at 2.0 GHz, 21.5 dB at 4.0 GHz, and 18.0 dB at 8.0 GHz. The output power at 1-dB compression is typically +12.8 dBm at 0.5 GHz, +20.7 dBm at 2.0 GHz, +18.3 dBm at 4.0 GHz, and +17.2 dBm at 8.0 GHz. The output third-order intercept point (OIP3) is typically +31.5 dBm at 0.5 GHz, +35.2 dBm at 2.0 GHz, +31.0 dBm at 4.0 GHz, and +28.5 dBm at 8.0 GHz. The RoHS-compliant amplifier includes SMA connectors in a housing measuring 0.74 × 0.75 × 0.46 in. (18.80 × 19.05 × 11.68 mm). It typically draws 77 mA from a +12-V DC supply.

Hand-Formable Interconnect Cables Fit Tight Spots to 40 GHz

Mini-Circuits' model 086-3KM+ hand-formable coaxial cables are HandFlex™ cables in 3-in. lengths with 2.92-mm male connectors for use from DC to 40 GHz. They are hand formable with a 6-mm minimum bend radius for tight-fitting installations. The 50-Ω cables feature low-loss (0.6 dB at 40 GHz) and can handle high power levels: 61 W power at 1 GHz and 7 W power at 40 GHz. The cables consist of gold-plated beryllium-copper center conductors, tin-soaked copper braid outer shield, and low-loss PTFE dielectric material. The cables, which are excellent for military and aerospace systems and as replacements for custom-bent 0.086-in.-diameter semi rigid cables, are suitable for operating temperatures from -55 to +85°C.

Ka-band systems can provide high throughput using smaller terminals, but they suffer from rain degradations much more than that experienced by Ku-band systems. For the same size antennas, the additional gain at Ka-band mitigates the additional free-space loss.

achieved by employing a more efficient modulation/coding scheme in the system design. Conversely, the designer may use less bandwidth with a more efficient modulation/coding scheme and maintain the same throughput, thus decreasing the operating costs.

As discussed, a decrease in antenna size to approximately 65 cm for the Ka-band system would provide about the same receive gain, but would reduce the system G/T. *Table 4* compares the G/T for a one-meter Ku-band antenna and a 65-cm Ka-band antenna.

TABLE 4: COMPARISON OF G/T FOR 1-M KU AND 65-CM KA ANTENNAS

	Ku-Band (1 m)	Ka-Band (65 cm)
Antenna gain	40.1 dBi	40.3 dBi
Tant (at 20-deg. elevation)	46 K	80 K
LNB NF	0.7 dB	1.3 dB
G/T	19.6 dB/K	16.7 dB/K

For a typical inbound link, the G/T of the receive earth station is not usually a problem and does not limit the link budget. However, on the outbound, systems are often receive-limited, meaning that the receive antenna G/T limits the performance of the link. Receive G/T can be improved with larger antennas, reducing losses between the antenna and LNB, and to some extent by utilizing LNBs with better NF. While it is difficult to reduce the LNB NF below 0.7 dB for Ku-band and 1.3 dB for Ka-band, screening of LNBs can be used to improve NFs.

The receive G/T limitations can also be overcome with additional transmit EIRP. However, the added transmit power may require additional satellite power, thus making the whole link more expensive. That's because the space segment cost will be based on the power-equivalent bandwidth rather than the occupied bandwidth.

WHAT DOES THIS MEAN?

Ka-band systems can provide high throughput using smaller terminals, but they suffer from rain degradations much more than that experienced by Ku-band systems. For the same size antennas, the additional gain at Ka-band mitigates the additional free-space loss. Modern HTS satellites offer high G/T and EIRP that eases the EIRP and G/T requirements at the earth stations. However, designing a system to meet a given link availability means the system must be designed for this worst case, resulting in additional cost or size relative to clear-sky conditions, especially for Ka-band.

If the link quality and SLA can vary, degradations due to rain can be lessened by:

1. Adaptive modulation and coding
2. Reduced throughput
3. Reduced bit-error-rate (BER) performance (more errors)

Each of these techniques either lowers the transmitted information rate or increases bandwidth, or otherwise reduces link availability.

Large hub earth stations can help on the inbound by eliminating any receive limitations. Increasing earth-station size, resulting in higher G/T, has diminishing returns in terms of link-budget performance.

ULPC will mitigate transponder power used during clear skies and should reduce operating costs. ULPC does not mitigate the requirement to size the transmit antenna/BUC to meet the faded conditions.

CONCLUSION

Ka-band systems present challenges in terms of link budgets. For antennas of the same size, the increased gain of the earth-station antenna for Ka-band compensates for the additional propagation losses.

In clear sky, Ka-band systems generally outperform Ku-band systems, at least in terms of requiring less EIRP for the same bandwidth. This is mostly due to the increased performance of Ka-band satellites. However, rain fades for Ka-band must be mitigated with more transmit power or some form of adaptive coding/modulation that reduces the data rates but increases the coding gain. mw

REFERENCES

1. Satmaster Pro Mk9.1a.
2. JPL D-32584, "Atmospheric Noise Temperature Induced by Clouds and Other Weather Phenomena at SHF Band (1-45 GHz)," Christian Ho, Stephen Slobin, Kelly Gritton, Jet Propulsion Laboratories, 11 August 2005.

SPDT Fail-Safe Switches Control DC to 26.5 GHz

THE MSP2TA SERIES of rugged, reliable absorptive fail-safe switches operate for 10 million switching cycles or more, guaranteed, and as many as 100 million switching cycles if properly maintained. Models are available for dc to 18 GHz and as wide as dc to 26.5 GHz with low loss and high isolation. The make-before-break, RoHS-compliant, single-pole, double-throw (SPDT) 50-Ω switches operate on +24 V dc, handling input power levels to 20 W. Typical insertion loss is 0.1 dB from dc to 1 GHz, 0.25 dB or better from 1 to 12 GHz, and 0.54 dB or better from 12 to 26.5 GHz. Typical isolation is 85 dB from dc to 1 GHz, 70 dB or better from 1 to 12 GHz, and 55 dB or better from 12 to 26.5 GHz. Typical VSWR is 1.20:1 from dc to 12 GHz and 1.25:1 from 12 to 26.5 GHz, with switching speed of 20 ms across operating temperatures of –15 to +45°C. The smallest version, the MSP2TA-26XL+ component module, measures 2.00 × 2.25 × 0.50 in. (50.80 × 57.15 × 12.70 mm), while larger models MSP2TA-26-PM+ and MSP2TA-26-BM+ are available for panel- and base-mount applications.

MINI-CIRCUITS, P. O. Box 350166, Brooklyn, NY11235-003; (718) 934-4500, *www.mini-circuits.com*

Low-Loss Bondply Builds Multilayer PCBs

THE RO4460G2 BONDPLY material exhibits a dielectric constant (Dk) of 6.15 for use in attaching circuit laminate layers in multilayer circuit constructions. When multiple layers of high-performance laminates are needed for high-frequency analog or high-speed digital designs, RO44060G2 material provides reliable, long-term attachment of layers with minimal loss or irregularity between other circuit materials, such as coefficient of thermal expansion (CTE). The availability of RO4460G2 bondply provides circuit designers with a 0.004-in. (0.101-mm) bonding layer that complements the company's RO4360G2 low-loss, glass-reinforced 6.15 Dk copper-clad thermoset laminates.

ROGERS CORP., Advanced Connectivity Solutions, 100 S. Roosevelt Ave., Chandler, AZ 85226; (480) 961-1382; *www.rogerscorp.com*

LDMOS Amplifier Drives 20 to 500 MHz

THE BHED2758-500 LDMOS power amplifier (PA) provides 500 W typical CW output power from 20 to 500 MHz with 57-dB nominal power gain. The PA, which provides a dynamic range of 10.5 dB in seven steps and incorporates AM/FM/SSB modulation control, can deliver high output power into high-VSWR antenna loads for testing. Designed for operating temperatures from 0 to +50°C and altitudes to 10,000 ft., the LDMOS PA controls spurious noise levels to –60 dBc or less, with typical second harmonics of –25 dBc and typical third harmonics of –20 dBc. It is equipped with an Ethernet/RS-422 control interface, weighs 120 lbs., and fits a 7U-high 19-in.-wide rack-mount enclosure. It includes Type N female input connectors, SC female output connectors, internal built-in-test (BIT) functionality, and an internal ac power supply.

COMTECH PST, 105 Baylis Rd., Melville, NY 11747; (631) 777-8900, *www.comtechpst.com*

Synthesizer Slashes Phase Noise to 4 GHz

THE KFSW200400-100 frequency synthesizer employs patented REL-PRO technology to achieve low noise levels from 2 to 4 GHz. The RoHS-compliant signal source works with a 10-MHz reference to provide at least –3 dBm output power across the frequency range in 1-MHz tuning steps with 10-ms typical settling time. The 50-Ω frequency synthesizer exhibits –110 dBc/Hz phase noise offset 100 kHz from the carrier, with –10 dBc typical harmonic noise and –80 dBc typical spurious noise. The signal source includes a 3.3-V CMOS lock detect indicator. It measures 2.750 × 1.750 × 1.000 in. with female SMC connectors and is designed for operating temperatures from –40 to +85°C.

SYNERGY MICROWAVE CORP., 201 McLean Blvd., Paterson, NJ 07505; (973) 881-8800; *www.synergymwave.com*

Coaxial Attenuator Spans 18 to 40 GHz

THE MODEL SKA-1834033535-KFKF-A1-M GAAS MMIC attenuator provides an attenuation range of 0 to 35 dB across a broad frequency range of 18 to 40 GHz. It operates on standard control voltages of 0 to –3 V dc, but can work with control voltages to –5 V dc. The coaxial attenuator comes with female K connectors on the input and output signal ports, and a female SMA connector on the control port.

SAGE MILLIMETER INC., 3043 Kashiwa St., Torrance, CA 90505; (424) 757-0168, *www.sagemillimeter.com*

This index is provided as an additional service by the publisher, who assumes no responsibility for errors or omissions.

Subscription Assistance and Information:
(ISSN 0745-2993)
Microwaves & RF is published monthly. Microwaves & RF is sent free to individuals actively engaged in high-frequency electronics engineering. In addition, paid subscriptions are available. Subscription rates for U.S. are $95 for 1 year ($120 in Canada, $150 for International). Published by Informa Media Inc., 9800 Metcalf Ave., Overland Park, KS 66212-2216. Periodicals Postage Paid at Kansas City, MO and additional mailing offices. POSTMASTER: Send change of address to Microwaves & RF PO Box 2100, Skokie, IL 60076-7800. For paid subscription information, please contact Microwaves & RF at PO Box 2100, Skokie IL 60076-7800. Canada Post Publications Mail agreement No. 40612608. Canada return address: IMEX Global Solutions PO Box 25542, London ON N6C 6B2.